Summer 2017

# Confidence-based model validation for reliability assessment and its integration with reliability-based design optimization

Min-Yeong Moon
*University of Iowa*



Follow this and additional works at: https://ir.uiowa.edu/etd
Part of the Mechanical Engineering Commons

CONFIDENCE-BASED MODEL VALIDATION FOR RELIABILITY ASSESSMENT AND ITS INTEGRATION WITH RELIABILITY-BASED DESIGN OPTIMIZATION

by

Min-Yeong Moon

A thesis submitted in partial fulfillment
of the requirements for the Doctor of
Philosophy degree in Mechanical Engineering
in the Graduate College of
The University of Iowa

August 2017

Thesis Supervisor: Professor Kyung K. Choi

Graduate College
The University of Iowa
Iowa City, Iowa

CERTIFICATE OF APPROVAL

PH.D. THESIS

This is to certify that the Ph.D. thesis of

Min-Yeong Moon

has been approved by the Examining Committee for the thesis requirement for the Doctor of Philosophy degree in Mechanical Engineering at the August 2017 graduation.

Thesis Committee: ______________________________
Kyung K. Choi, Thesis Supervisor

______________________________
Jia Lu

______________________________
Hiroyuki Sugiyama

______________________________
Shaoping Xiao

______________________________
David A. Lamb

ACKNOWLEDGMENTS

First I would like to thank my advisor Professor Kyung. K Choi for his continuous support and academic guidance throughout my Ph.D. studies. I appreciate all his effort and education in my Ph.D. program. The knowledge, skills, and technical writing that I have developed under his guidance will continue to benefit me throughout my future career. I also thank Professors Jia Lu, Hiroyuki Sugiyama, Shaoping Xiao, and Dr. David A. Lamb for their invaluable advices on this research as my thesis committee. I would also like to express my sincere thanks for all the help and encouragements from my senior colleagues, Dr. Hyunkyoo Cho and Dr. Nicholas Gaul.

I also would like to acknowledge the technical and financial support of the Automotive Research Center (ARC) in accordance with Cooperative Agreement W56HZV-04-2-0001 U.S. Army Tank Automotive Research, Development and Engineering Center (TARDEC). This support is greatly appreciated.

ABSTRACT

Conventional reliability analysis methods assume that a simulation model is able to represent the real physics accurately. However, this assumption may not always hold as the simulation model could be biased due to simplifications and idealizations. Simulation models are approximate mathematical representations of real-world systems and thus cannot exactly imitate the real-world systems. The accuracy of a simulation model is especially critical when it is used for the reliability calculation. Therefore, a simulation model should be validated using prototype testing results for reliability analysis. However, in practical engineering situation, experimental output data for the purpose of model validation is limited due to the significant cost of a large number of physical testing. Thus, the model validation needs to be carried out to account for the uncertainty induced by insufficient experimental output data as well as the inherent variability existing in the physical system and hence in the experimental test results. Therefore, in this study, a confidence-based model validation method that captures the variability and the uncertainty, and that corrects model bias at a user-specified target confidence level, has been developed. Reliability assessment using the confidence-based model validation can provide conservative estimation of the reliability of a system with confidence when only insufficient experimental output data are available.

Without confidence-based model validation, the designed product obtained using the conventional reliability-based design optimization (RBDO) optimum could either not satisfy the target reliability or be overly conservative. Therefore, simulation model validation is necessary to obtain a reliable optimum product using the RBDO process. In this study, the developed confidence-based model validation is integrated in the RBDO process to provide truly confident RBDO optimum design. The developed confidence-based model validation will provide a conservative RBDO optimum design at the target confidence level. However, it is challenging to obtain steady convergence in the RBDO

process with confidence-based model validation because the feasible domain changes as the design moves (*i.e.*, a moving-target problem). To resolve this issue, a practical optimization procedure, which terminates the RBDO process once the target reliability is satisfied, is proposed. In addition, the efficiency is achieved by carrying out deterministic design optimization (DDO) and RBDO without model validation, followed by RBDO with the confidence-based model validation. Numerical examples are presented to demonstrate that the proposed RBDO approach obtains a conservative and practical optimum design that satisfies the target reliability of designed product given a limited number of experimental output data.

Thus far, while the simulation model might be biased, it is assumed that we have correct distribution models for input variables and parameters. However, in real practical applications, only limited numbers of test data are available (parameter uncertainty) for modeling input distributions of material properties, manufacturing tolerances, operational loads, etc. Also, as before, only a limited number of output test data is used. Therefore, a reliability needs to be estimated by considering parameter uncertainty as well as biased simulation model. Computational methods and a process are developed to obtain confidence-based reliability assessment. The insufficient input and output test data induce uncertainties in input distribution models and output distributions, respectively. These uncertainties, which arise from lack of knowledge – the insufficient test data, are different from the inherent input distributions and corresponding output variabilities, which are natural randomness of the physical system.

# PUBLIC ABSTRACT

An engineering system has inherent variabilities induced by manufacturing processes, operating conditions, etc. To deal with these variabilities, the reliability, which is defined as the probability of success of required performance under the specified condition during the design life, is measured. In order to carry out reliability analysis for an engineering system, engineers often use simulation models that can predict the behavior of real-physics with less time and cost. However, the simulation models are simplifications of real-world systems because they involve various idealizations and assumptions. In other words, a simulation model could be biased and thus may not accurately represent the real-world system. Accordingly, accurate reliability cannot be obtained using the biased simulation model. Therefore, the simulation model should be validated using prototype testing results for reliability analysis. However, in practical engineering applications, experimental output data for the purpose of model validation is limited due to the significant cost of product testing. Therefore, model validation for reliability analysis needs to account for the uncertainty induced by insufficient experimental output data. For this reason, in this study, a confidence-based model validation method that captures the uncertainty and corrects model bias has been developed to obtain a validated simulation model. The validated simulation model obtained from the confidence-based model validation will provide conservative estimation of the reliability of system with confidence even with insufficient experimental output data.

Furthermore, simulation model validation is necessary to obtain a reliable optimal product design that satisfies all requirements and specifications set by designers. Therefore, the developed confidence-based model validation is integrated with the reliability-based design optimization (RBDO) process to obtain truly reliable and optimal product design that satisfies target reliability when it is manufactured. The developed model validation helps RBDO to obtain a conservative RBDO optimum design at the target

confidence level for insufficient experimental output data. The RBDO with model validation may require experimental output data at a number of different design points during the optimization process. Thus, in this study, a practical optimization procedure is proposed, which reduces the number of prototype testing required. We demonstrate that the proposed RBDO approach obtains a conservative and efficient optimum design that truly satisfies the target reliability even using a limited number of experimental output data.

Thus far, it is assumed that we have correct distribution models for input variables and parameters. However, in real practical applications, true input distribution models, which require a large number of input test data, may not be obtainable (*i.e.*, parameter uncertainty). Therefore, the reliability needs to be estimated by considering parameter uncertainty, insufficient output test data, as well as biased simulation model. An advanced confidence-based reliability assessment method is developed, which combines both uncertainties due to limited number of input/output data and the biased model, and estimates confidence-based reliability at the user-specified target confidence level. The proposed confidence-based reliability assessment method can estimate the reliability of complex mechanical system with appropriate conservativeness, using limited numbers of input and output test data; and simulation model.

TABLE OF CONTENTS

LIST OF TABLES

LIST OF FIGURES

LIST OF ABBREVIATIONS AND SYMBOLS

| | |
|---|---|
| AKDE | Adaptive KDE |
| $B_i(\mathbf{x};\mathbf{v})$, $B_i(\mathbf{x};\, CL^{Target})$ | Model Bias Correction and Confidence-Based Model bias at $CL^{Target}$ for $i^{th}$ Performance Measure, $G_i(\mathbf{x})$ |
| $B_i(\mathbf{x})$ | Unknown Model Bias for $i^{th}$ Performance Measure, $G_i(\mathbf{x})$ |
| $C(u,\upsilon;\theta)$ | Copula Density Function |
| CDF | Cumulative Distribution Function |
| CCDF | Complementary CDF |
| $CL^{Target}$ | Target Confidence Level |
| CAE | Computer-Aided Engineering |
| CVM | Complex Variable Method |
| DDO | Deterministic Design Optimization |
| DKG | Dynamic Kriging |
| DRM | Dimension Reduction Method |
| $d_i$, $\mathbf{d}$ | $i^{th}$ Design Variable and Design Variable vector |
| $\mathbf{d}^{L}$, $\mathbf{d}^{U}$ | Lower and Upper Design Bounds |
| FDM | Finite Difference Method |
| FORM | First-Order Reliability Method |

| | |
|---|---|
| $f\left(p_F \mid h_0, \mathbf{y}^e\right)$ | Conditional PDF of Probability of Failure |
| $F_{p_F}\left(p_F \mid \mathbf{y}^e\right)$ | CDF of Probability of Failure |
| $F_{Re}\left(Re \mid \mathbf{x}^e, \mathbf{y}^e\right)$ | CDF of Reliability |
| $f_{\mathbf{x}}\left(\mathbf{x};\mathbf{d}\right)$ | Input Joint PDF of **x** |
| $G_i(\mathbf{x}), G_i^{true}(\mathbf{x})$ | (Biased) Simulation Output and True Output of $i^{th}$ Performance Measure |
| $g(\mathbf{x};\mathbf{v})$ | Validated Simulation Output, $g(\mathbf{x};\mathbf{v}) = G(\mathbf{x}) + B(\mathbf{x};\mathbf{v})$ |
| $H(\mathbf{v})$ | Hellinger Similarity |
| $h\left(y_i^e; h_0\right)$ | Variable Bandwidth |
| $h_0$, $h_0^{(i)}$ | Fixed (Reference) Bandwidth and $i^{th}$ Realization of $h_0$ in MCMC Sampling |
| KDE | Kernel Density Estimation |
| $K\left(\bullet\right)$ | Kernel |
| $L\left(\mathbf{y}^e \middle| h_0\right)$ | Likelihood Function |
| $\mathbf{v}$ | Optimization Variable Vector (Mean and Standard Deviation of Model Bias) |
| $M$ | Number of MCS Samples in Sampling-Based Bayesian Analysis (Single Level Bayesian Model) |
| MCMC | Markov Chain Monte Carlo |

| | |
|---|---|
| MCS | Monte Carlo Simulation |
| MPP | Most Probable Point |
| *NC* | Number of Constraints |
| *NDV* | Number of Design Variables |
| *NRV* | Number of Input Random Variables |
| *nMCS* | Number of MCS Samples in Sampling-Based Reliability Calculation |
| $nMCS_h$ | Number of MCS Samples in the Hierarchical Bayesian Model |
| *ne* | Number of Experimental Output Data |
| *nd* | Number of Input Test Data |
| $n_p$ | Prior Sample Size |
| PDF | Probability Density Function |
| $P(h_0)$, $P\left(h_0 \mid \mathbf{y}^e\right)$ | Prior Distribution and Posterior Distribution for $h_0$ |
| $P\left(h_0 \mid \zeta, \boldsymbol{\psi}, \mathbf{x}^e\right)$ | Prior Distribution for $h_0$ in Hierarchical Bayesian Analysis |
| $P\left(\zeta, \boldsymbol{\psi} \middle| \mathbf{x}^e\right)$ | Probability of Input Distribution Model (Hyper Prior in Hierarchical Bayesian Model) |
| $P_F$ | Probability of Failure |
| $p_F\left(h_0 \mid \mathbf{y}^e\right)$ | Probability of Failure Evaluated Given $h_0$ |
| $P_F^{confidence}(CL^{Target})$ | Confidence-Based Probability of Failure at $CL^{Target}$ |

| | |
|---|---|
| $P_{F_i}^{Target}$ | Target Probability of Failure for $i^{th}$ RBDO Constraint |
| $p(g(\mathbf{x};\mathbf{v}))$ | Validated Simulation Output PDF |
| $q(g;CL^{Target})$ | Confidence-Based Target Output PDF |
| RBDO | Reliability-Based Design Optimization |
| *Re* | Reliability |
| $\sigma_s$, $IQR_s$ | Standard Deviation and Interquartile Range of Simulation Output PDF |
| $\sigma_s^{random}\left(\zeta,\boldsymbol{\psi},\mathbf{x}^e\right)$ | Randomly Selected Standard Deviation of Simulation Output PDF with Sample Size of *ne* |
| SORM | Second-Order Reliability Method |
| $\tau$ | Kendall's Tau of Correlated Random Variables |
| $\theta$ | Correlation Coefficient for Copula |
| V&V | Verification and Validation |
| $x_i$, $\mathbf{x}$, $\mathbf{x}^{(k)}$ | $i^{th}$ Input Random Variable, Input Random Variable Vector and $k^{th}$ Realization of $\mathbf{x}$ in MCS Samples |
| $\mathbf{x}_i^e$, $\mathbf{x}^e$ | $i^{th}$ Input Data and Input Data Vector |
| $y_i^e$, $\mathbf{y}^e$ | $i^{th}$ Experimental Output Data and Experimental Output Data Vector |
| $\bar{\Omega}_{F_i}$ | Modified Failure Domain with Model Bias for $i^{th}$ RBDO Constraint, $\bar{\Omega}_{F_i} \equiv \left\{\mathbf{x}: G_i\left(\mathbf{x}\right) + B_i\left(\mathbf{x};CL^{Target}\right) > 0\right\}$ |

| | |
|---|---|
| $\boldsymbol{\psi}$ | Input Distribution Parameter Vector |
| $\zeta$ | Input Distribution Type |

# CHAPTER 1

# INTRODUCTION

This research presents a new model validation methodology that can be used for confidence-based reliability assessment and reliability-based design optimization (RBDO). The developed model validation method is integrated into the RBDO process to obtain a reliable and optimized design that satisfies target reliability when manufactured. The developed confidence-based model validation deals with practical prototype testing when only a small number testing is available due to the significant cost of physical testing. The developed confidence-based reliability assessment accounts for insufficient input data due to limited number of input testing as well as small number of experimental output data due to expensive cost of full-scale prototype testing.

For the simulation model validation, the proposed confidence-based model validation takes into consideration the uncertainty induced by a limited number of experimental output data. This uncertainty induces uncertain predicted output probability density function (PDF). In other words, there are many candidates of predicted output PDF that could represent the limited number of experimental output data. Accordingly, a reliability (probability of failure) of the system, which is calculated based on the predicted output PDF, becomes uncertain. To handle the uncertainty induced by insufficient data, a confidence-based target output distribution that estimates the probability of failure conservatively, needs to be obtained. To do that, the uncertainty distribution of the probability of failure is quantified using Bayesian analysis. Then, a confidence-based probability of failure that satisfies the user-specified target confidence level on the uncertainty distribution is selected. The confidence-based target output distribution is the candidate distribution which produces the confidence-based probability of failure. After that, model validation optimization, which corrects model bias, is carried out to match the current biased simulation output PDF to the confidence-based target output distribution. Then, confidence-based model validation can be used for conservative reliability assessment, which is integrated in the RBDO process to obtain a conservative RBDO design. Accordingly, the designer can have confidence that the RBDO design obtained using confidence-model validation would satisfy the target probability of failure with certain probability level – target confidence level.

In Section 1.1, background information for a better understanding of the proposed study is provided. In particular, it describes the type and source of uncertainty in Section 1.1.1, RBDO in Section 1.1.2, and model verification and validation in Section 1.1.3. Section 1.2 introduces the objective of the proposed study, and the organization of the thesis is provided in Section 1.3.

## 1.1 Background and Motivation

### 1.1.1 Type and Source of Uncertainties

Uncertainties in computer simulation can be classified into two major types (Klir & Folger, 1988; Oberkampf, Helton & Sentz, 2001; Oberkampf & Roy, 2010). Aleatory uncertainty is the uncertainty due to inherent randomness, which is also referred to as stochastic uncertainty, variability and inherent uncertainty. The fundamental nature of aleatory uncertainty is randomness. For discrete variables, the randomness is parameterized by the probability of each possible value. For continuous variables, the mathematical representation of the randomness is a probability distribution. Epistemic uncertainty, the second type, is the uncertainty due to lack of knowledge, which is also referred to as reducible uncertainty and knowledge uncertainty. Its fundamental source is incomplete information or knowledge of any type that is related to the system of interest or its simulation. For example, lack of knowledge can include a modeling issue for the physical system and experimental output data used for model validation. It is common to refer to epistemic uncertainty simply as *uncertainty* and aleatory uncertainty as *variability*. In this study, we clearly distinguish between variability (*i.e.*, aleatory uncertainty) and uncertainty (*i.e.*, epistemic uncertainty). As the fundamental nature of each is different, different approaches are required to consider and characterize each.

Various sources of variabilities and uncertainties can occur in computational analysis and simulation modeling. Kennedy and O'Hagan (2001) have identified where they come from. The first source is parametric variability which is the randomness of the input variable. The thickness of a steel plate that can vary randomly within a tolerance could be an example. It might not be exactly designed and constructed due to manufacturing error. This inherent variability in the engineering system is taken care of by calculating the reliability of the system in RBDO constraints, which will be explained in detail in Section 1.1.2. Another source is parameter uncertainty, which comes from input variables whose exact values (or probabilistic distribution) are unknown. The parameter uncertainty can occur in two situations. First, we may not be able to carry out complete coupon testing to identify probability distribution of input parameter such as friction coefficient or other physical/material properties. In this case, an unknown input parameter for which only the reference value or the manufacturer's guess is available is defined as a calibration parameter. Thus statistical properties such as mean and standard deviation of the calibration parameter become uncertain. Second, we may be able to carry out a coupon test to identify certain parameters even though testing cannot be done many times. Then the uncertainty from lack of input test data needs to be considered.

The other source can be structural uncertainty (model bias or discrepancy) that is the fundamental inability of simulation to reproduce the real physical behavior because of simplification and idealization. Furthermore, there is numerical uncertainty which is a numerical error in the implementation of the computer simulation. However, simulation is often assumed to be numerical error-free. Another source is experimental uncertainty (or observation error) which is an error in measuring the experimental responses. This can possibly be noticed by repeating measurements many times. Among those various uncertainties, (1) parameter uncertainty, (2) input variability resulting in output variability, and (3) model bias are considered in this study. In addition, there exists the uncertainty that comes from insufficient experimental (output) data, which is taken into consideration in the developed method.

### 1.1.2 Reliability-Based Design Optimization

Deterministic design assumes that all design variables, parameters and system variables are deterministic values. In other words, there is no variability in design variables and parameters. However, engineering systems have variabilities due to manufacturing imperfections (*e.g.*, dimension and material properties) and natural environmental change (*e.g.*, wave load and wind speed). Moreover, these variabilities propagate the performance measure, which results in output variability. Thus, deterministic design optimization (DDO) methods are not usually suitable for the engineering design process because they do not account for inherent variability in input and the resulting output variability. As a result, the DDO optimum designs are not reliable (typically only 50% reliable). To capture the input and output variability in the design process, RBDO should be used to obtain an optimal design that satisfies the desired reliability level (*i.e.*, the target probability of failure) under the variabilities. The input variability is embodied using an input joint PDF, and the output variability resulting from the input variability is obtained using the input joint PDF and simulation model. To capture the output variability, the safety of the system is measured using the probability of failure that is the probabilistic constraint in the RBDO formulation.

Methodologies to evaluate the reliability of a system in RBDO can be categorized two ways: sensitivity-based reliability analysis using most-probable point (MPP), and sampling-based reliability analysis. In the sensitivity-based reliability analysis, there have been various approaches such as the first-order reliability method (FORM)

(Chiralaksanakul & Mahadevan, 2005; Haldar & Mahadevan, 2000; Hasofer & Lind, 1974; Tu, Choi & Park, 1999, 2001), the second-order reliability method (SORM) (Haldar & Mahadevan, 2000; Hohenbichler & Rackwitz, 1988) and the dimension reduction method (DRM) (Lee, Choi, Du & Gorsich, 2008; Lee, Choi & Gorsich, 2010; Rahman & Wei, 2006, 2008). All sensitivity-based approaches do require the sensitivities of the performance functions to search MPP. FORM and SORM compute the probability of failure by approximating the performance function using the first- and second-order Taylor series expansion at the MPP, respectively. The DRM represents a multi-dimensional function using the sum of one-dimensional functions. Even though sensitivity-based reliability analysis is very popular, it may not be applicable for some engineering applications where sensitivity information is not available due to implicit, highly nonlinear and complicated performance function.

On the other hand, sampling-based reliability analysis is useful for many applications where the sensitivity of a performance function cannot be easily obtained (Lee, Choi & Zhao, 2011a; Lee, Choi, Noh, Zhao & Gorsich, 2011b). In the sampling-based approach, reliability is usually calculated using Monte Carlo simulation (MCS) (Rubinstein & Kroese, 1981). MCS uses a very large number (*e.g.*, one million) of samples. Thus, direct use of MCS requires a huge number of computer-aided engineering (CAE) simulations, such as Finite Element Analysis (FEA). That leads to an extremely expensive computational cost. To resolve this issue, surrogate models are used, which can reduce computational time by using a small number of CAE analyses (Shi, Yang & Zhu, 2012; Song, Choi & Lamb, 2013a; Song, Choi, Lee, Zhao & Lamb, 2013b; Zhao, 2011; Zhao, Choi & Lee, 2011). If accurate surrogate models are available, the probability of failure and its sensitivity can be accurately obtained using MCS, and the prediction using surrogate models does not involves the approximation of constraints. In this study, the sampling-based method using surrogate models has been used to evaluate reliability and sensitivity for RBDO.

### 1.1.3 Model Verification and Validation

Usually product development and design require a number of hardware prototypes and tests of the designed product. For this reason, computer simulation plays an increasingly important role in various engineering design projects with the rapid increase of computational power. A simulation model predicts the response of a system and is used to design the product with reduced time and costs. However, an accurate simulation model is not easy to obtain because the simulation model is an approximate imitation of real systems, including idealizations and simplifications. As a consequence, confidence of the simulation model needs to be verified and validated using rigorous hardware testing. The verified and validated simulation model will be able to describe the experimental outcomes of the physical system.

Various communities have recognized the importance of model verification and validation (V&V) procedure in simulation modeling, and have published their own definitions of V&V. In conformity with the Institute of Electrical and Electronic Engineering (IEEE) (IEEE, 1984, 1990), verification is defined as "The process of evaluating the products of a software development phase to provide assurance that they meet the requirements defined for them by the previous phase." Validation, on the other hand, is defined as "the process of testing a computer program and evaluating the results to ensure compliance with specific requirements." It is clear that the IEEE focuses on V&V of computer program or software. On the other hand, the definitions of V&V provided by the US department of Defense (DoD), the American Institute of Aeronautics and Astronautics (AIAA) and the American Society of Mechanical Engineers (ASME) communities are more related to a model that is supposed to depict a physical system (AIAA, 1998; ASME, 2006; DoD, 1994). Verification is defined by the ASME Committee as "the process of determining that a computational model accurately represents the underlying mathematical model and its solution." The definition of verification defined by DoD and AIAA is also very similar to the one defined by the

ASME. In addition, the definition of validation accepted by DoD, AIAA and ASME is "the process of determining the degree to which a model is an accurate representation of the real world from the perspective of the intended uses of the model." It is noted that the definition of validation by DoD, AIAA and ASME is an emphasis on measuring the accuracy of a model.

Figure 1.1 shows traditional model verification and validation activities. In this study, it is assumed that model verification can be successfully completed because it can be easily done by refining the model and correcting the computer code. We have more concern about model validation, which is difficult as it incorporates experiments that cannot be done many times. Usually actual prototyping and testing are very expensive; thus, only a limited number of experimental output data can be used for the purpose of model validation. As for the activity of model validation, there are several aspects that different researchers address. The first aspect is assessing the accuracy of a simulation model by comparing it with a set of experimental output data. In some literatures, model accuracy has been quantitatively estimated using a validation metric (Chen, Xiong, Tsui & Wang, 2006; Ferson, Oberkampf & Ginzburg, 2008; Oberkampf & Barone, 2006). The second aspect is quantifying the uncertainties (*i.e.*, model bias and calibration parameter, as explained in Section 1.1.1) in the simulation model to improve its predictive capability.

These works are useful for model analysts. However, from the design engineer's point of view, they do not offer enough because they do not consider the reliability of the designed product. The validated simulation model may not guarantee an accurate prediction unless a large number of tests are provided for the validation. Because the accuracy of the simulation model is very important when we evaluate the reliability of the system. This study is particularly focused on developing a new model validation framework that can be applied for reliability assessment and reliability-based design optimization with insufficient experimental output data. The developed method does not seek to find an accurate model by directly matching a simulation model and experimental output data. Since experimental output data is lacking, we cannot even measure a correct accuracy between simulation model and the data. Thus, the confidence concept is introduced in developed model validation without looking for accurate simulation model. Developed model validation conservatively estimates a probability of failure so that a user can have confidence that the designed product using a validated simulation model would be reliable.

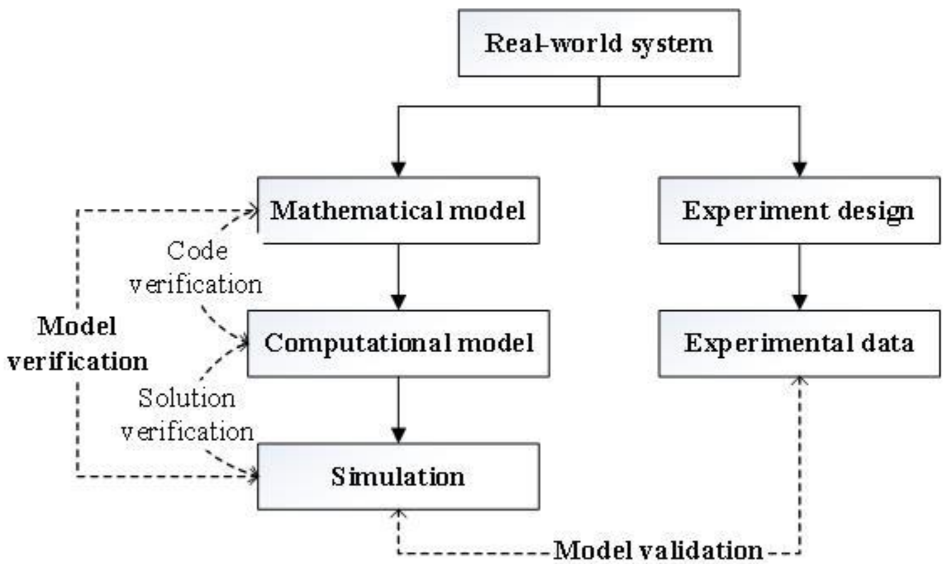


Figure 1.1 Role of Conventional Model Verification and Valdation

## 1.2 Objective of Proposed Study

The main goal of this thesis is to develop a methodology of confidence-based reliability assessment of the design by incorporating model validation using insufficient experimental output data. The RBDO method uses a simulation model without incorporating prototype test results to obtain an RBDO optimum design. Accordingly, a product designed using the conventional RBDO methods may not be reliable or overly-designed. The developed confidence-based model validation has to be integrated with the RBDO process in order to provide a reliable product design.

Specific research objectives are:

1. To develop a new model validation method that can be used for reliability analysis by taking account the uncertainty induced by insufficient experimental output data. The new model validation has several novel features. First, the model validation proposed in this study is concerned with the insufficient experimental output data. Hence, the new model validation method handles the uncertainty due to insufficient test data, as well as output variabilities caused by input variabilities. Due to the uncertainty, the predicted output PDF and probability of failure become uncertain quantities. Using a sampling-based Bayesian approach, the uncertainty distribution of the probability of failure, which contains the uncertainty induced by the insufficient test data, can be quantified.

   Second, the proposed method enables the user to control confidence level (*i.e.*, conservativeness) in estimating reliability. In the presence of the uncertainty, we cannot determine predicted output PDF with certainty. For this reason, we need to find a conservatively predicted output PDF – a target output PDF – to which the simulation model will be matched. Accordingly, the validated simulation model can have a confidence that estimated probability of failure would be larger than the true probability of failure. At the same time, the target output PDF should not be overly conservative to obtain a cost-effective optimum design. To do that, a confidence-based target output PDF and probability of failure are selected at a user-specified target confidence level. By controlling the target confidence level, users can control the confidence level of estimated reliability.

2. To develop a new RBDO method using confidence-based model validation that can provide truly reliable and conservative RBDO optimum design even with a limited number of experimental output data. When the model validation is carried out during a design optimization process, the feasible domain (*i.e.*, solution space) changes as model bias is corrected at the changed design point. This results in a moving-target problem, which can cause difficulty in convergence in the optimization iteration. As a result, the RBDO optimum design may not be easily obtained. For this reason, a practical RBDO procedure using confidence-based model validation is proposed in this study. The proposed RBDO method requires experimental output data only at a few design configurations. Hence, the proposed RBDO can provide a conservative, reliable and yet cost-effective design without requiring a large number of different prototype (design) tests.
3. To develop a new reliability assessment methodology that can provide conservative reliability estimation with appropriate confidence level for practical engineering applications. As explained earlier, a large number of prototype testing is not viable. For the same reason, only a limited number of coupon or element testing is carried out. Hence, accurate input distribution model is not available since there exists the uncertainty induced by insufficient number of input data. Therefore, the developed reliability assessment should account for insufficient input data due to a limited number of coupon or element testing as well as insufficient experimental output data. The proposed method can provide conservative reliability estimation by providing appropriate confidence level.

## 1.3 Organization of Thesis

Chapter 2 presents literature survey of conservative RBDO approach under the uncertainty and model validation approach used for design optimization, which are the motivation for the proposed method. In addition, the limitations of previous works are described.

Chapter 3 reviews conventional RBDO approach which does not use model validation, and specifically focuses on how to perform sampling-based reliability analysis and RBDO which are used in this study.

Chapter 4 proposes a new confidence-based model validation method that enables a conservative assessment of the reliability of an engineering system for a practical experimental situation. To deal with a practical situation, the uncertainty induced by insufficient experimental output data is considered. First, the uncertainty distribution of the probability of failure is quantified using sampling-based Bayesian analysis. Second, the confidence-based target output PDF and probability of failure are obtained at the user-specified target confidence level. Third, model validation optimization is carried out for model bias correction to obtain a validated simulation model (*i.e.*, simulation output PDF). Finally, sampling-based reliability analysis is performed using the validated simulation output PDF, which yields the conservative estimation of reliability for insufficient experimental output data.

Chapter 5 demonstrates performance of the proposed confidence-based model validation method using various numerical tests. The developed method is applied to a highly nonlinear two-dimensional mathematical example. First, the target confidence level is verified by carrying out repeated validation tests with different sets of experimental output data. Second, the convergence of the proposed validation method is shown with increasing the data size. Third, a case study is carried out for different types of biased simulation model.

Chapter 6 presents reliability-based design optimization using confidence-based model validation. The challenge of RBDO with model validation is identified. To resolve that, a practical RBDO procedure using confidence-based model validation is proposed and is tested using the 2-D mathematical example.

Chapter 7 presents confidence-based reliability assessment for industry practical situation, which handles insufficient input data, as well as insufficient experimental output data that is considered in Chapter 4. In the presence of the limited number of input data, true input distribution model cannot be obtained. First, the uncertainty quantification of input model is carried out. Second, the uncertainty induced by limited number of input data is combined with the uncertainty due to limited number of output data. To do that, a hierarchal Bayesian model is formulated to quantify the uncertainty distribution of reliability. After that, confidence-based reliability is selected at the target confidence level in similar way as described in Chapter 4.

Chapter 8 presents the conclusions of the study and future works to be carried out to enhance the proposed methods.

# CHAPTER 2

# LITERATURE SURVEY

## 2.1 Conservative RBDO Approaches under Uncertainty

Conventional reliability analysis and RBDO methods require (1) an accurate input probabilistic model (*i.e.*, input joint PDF) and (2) an accurate simulation model. However, both the accurate input joint PDF and the accurate simulation model cannot be achieved in real engineering applications. The accurate input joint PDF can be obtained only when enough coupon or element tests are available; the accurate simulation model is not achievable because the simulation model is merely a mathematical approximation of physical behavior (the second issue will be discussed in Section 3.3.2). However, due to expensive cost, only a limited number of input data is available in real problems. In the presence of the uncertainty due to the limited number of input data, the conservative design can be achieved by estimating a probability of failure that is larger than the true value. Picheny, Kim, and Haftka (2010) addressed the danger of underestimating the probability of failure due to the limited number of data; they developed a conservative estimation of probability of failure using a bootstrap method assuming the input distribution type is known. In this context, there have been many research efforts to achieve conservative RBDO design in compensation for the limited input data. Gunawan and Papalambros (2006) used beta distribution to model the distribution of reliability and carried out multi-objective RBDO that maximizes the overall confidence level of the reliability while minimizing cost. Youn and Wang (2008) sought the worst case from the distribution of reliability, which is the beta distribution, and defined the worst case as the target reliability for RBDO. Their work has been followed by Choi, An, and Won (2010). Reliability-based design optimization with an input statistical model with standard deviation and correlation coefficient that are adjusted using confidence level of them has been proposed; it fully covers the target reliability region for RBDO (Noh, Choi, Lee, Gorsich & Lamb, 2011a; Noh, Choi, Lee, Gorsich & Lamb, 2011b). Cho et al. (2016) used a confidence level of probability of failure as a probabilistic constraint for conservative RBDO. However, the aforementioned methods consider insufficient input data, not the experimental (output) data, and assume the simulation model is accurate – no model bias. Thus, the methods are not valid for the case of a biased simulation model. Therefore, physical experiments should be incorporated to validate the simulation model. Hence, this thesis deals with experimental (output) data to validate a simulation model for RBDO.

## 2.2 Model Validation Approaches

There have been various research efforts to quantify the uncertainties involves in simulation model (explained in Section 1.1.1) to improve the prediction capability of the simulation model. Some works consider either parameter uncertainty (Drignei, Mourelatos, Kokkolaras, Pandey & Koscik, 2012a; Drignei, Mourelatos, Pandey & Kokkolaras, 2012b; Loeppky, Bingham & Welch, 2006; Xiong, Chen, Tsui & Apley, 2009; Youn, Jung, Xi, Kim & Lee, 2011) or model bias (Jiang, Chen, Fu & Yang, 2013; Pan, Xi & Yang, 2016; Xi, Fu & Yang, 2013) to correct the simulation model. Firstly, aforementioned parameter calibration adjusts either the parameter for a deterministic problem or the statistical properties of the parameter under the variability to match the simulation model to experimental output data. Secondly, model bias is approximated inside of the entire design space and is added to simulation model to capture the discrepancy between the simulation model and the experimental output data. Though there have been attempts to consider both the parameter uncertainty and the model bias, it is not easy to distinguish the effect of each of them on the output (Arendt, Apley & Chen, 2012a; Arendt, Apley, Chen, Lamb & Gorsich, 2012b; Higdon, Nakhleh, Gattiker & Williams, 2008). As for design application, parameter calibration has been simultaneously performed within the local domain in the DDO procedure. Experimental output data is required at every design iteration to adjust calibration parameters (Drignei et al., 2012a; Drignei et al., 2012b). However, deterministic design is not useful from the view point of a reliable product.

This thesis addresses the important research topic of developing model validation for the RBDO process, which can reduce error in designing a reliable product. There has been limited research on model validation for RBDO (Jiang et al., 2013; Pan et al., 2016). The model bias has been approximated over the entire design space, and then the simulation model with model bias correction has been used for the RBDO process. However, this method requires experimental output data over the entire design space to estimate model bias. In other words, it requires product testing at a large number of design configurations; therefore, it is not practical. Moreover, the RBDO optimum designs may not satisfy the target probability of failure because the true probability of failure cannot be accurately evaluated unless sufficiently large number of experimental output data is provided at each design configuration. Thus, they are not appropriate for RBDO with a limited number of experimental output data.

Furthermore, even though we have the accurate input distribution model, we do not know the exact input variable values that correspond to the experimental output data; only the mean value of the input is known. This thesis handles this situation, which is associated more often with real practical applications. This differs from the case that conventional model validation approaches deal with.

# CHAPTER 3
# CONVENTIONAL RELIABILITY-BASED DESIGN OPTIMIZATION USING SAMPLING-BASED RELIABILITY ANALYSIS

This chapter describes how to carry out RBDO using sampling-based reliability analysis. As explained in Section 1.1.2, sampling-based reliability analysis is useful for engineering applications in which accurate sensitivities of performance function are not available. Therefore, this thesis uses sampling-based RBDO. Because existing sampling-based RBDO methods assume that simulation is accurate and do not incorporate it with experimental output data, it is referred to as conventional RBDO.

## 3.1 Conventional RBDO Formulation

This section explains the conventional RBDO approach which does not perform a model validation. The mathematical formulation of a conventional RBDO problem is expressed as

$$\begin{aligned} &\text{minimize} \quad \text{Cost}(\mathbf{d}) \\ &\text{subject to} \quad P_{F_i}(\mathbf{d}) = P\left[G_i(\mathbf{x}) > 0\right] \le P_{F_i}^{Target},\ i = 1,\cdots,NC\ , \\ &\qquad\qquad \mathbf{d}^L \le \mathbf{d} \le \mathbf{d}^U,\quad \mathbf{d} \in \mathbb{R}^{NDV} \text{ and } \mathbf{x} \in \mathbb{R}^{NRV} \end{aligned} \tag{3-1}$$

where $\mathbf{d} = \mu(\mathbf{x}^{NDV})$ is the design variable vector, which is the mean value of the *NDV*-dimensional random variable vector $\mathbf{x}^{NDV}=[x_1, x_2,\ldots, x_{NDV}]^T$, $\mathbf{x}$ is the *NRV*-dimensional random input variable vector, $G_i(\mathbf{x})$ is the performance function (obtained using simulation model) for $i^{\text{th}}$ probabilistic constraint $P_{F_i}(\mathbf{d})$, $P_{F_i}^{Target}$ is the target probability of failure for the $i^{\text{th}}$ probabilistic constraint, and *NC*, *NDV* and *NRV* are the number of probabilistic constraints, design variables, and input random variables, respectively. It is noted that $G_i(\mathbf{x})$ can be evaluated using CAE simulation (simulation output) because analytical expression of $G_i(\mathbf{x})$ is usually unknown. Thus, in conventional RBDO, $G_i(\mathbf{x})$ may not be accurate because CAE simulation involves idealizations and assumptions. In other words, a simulation model could underestimate or overestimate the true probability of failure. Accordingly, the conventional RBDO optimum may lead to unreliable design or overly conservative design. This issue will be discussed and a new model validation for RBDO will be proposed in Chapters 4, 5 and 6.

## 3.2 Sampling-Based RBDO

This section explains sampling-based RBDO. In sampling-based RBDO, the probabilistic constraint is calculated using MCS and its responses evaluated using surrogate models, which will be explained in Section 3.2.1. Furthermore, the sensitivity of the performance function is not required to evaluate the sensitivity of the probabilistic constraint. The sensitivity calculation of the probabilistic constraint is described in Section 3.2.2.

### 3.2.1 Sampling-Based Reliability Analysis

A probability of failure, denoted by $P_F$, is defined using a multi-dimensional integral as

$$P_F \equiv P\left[\mathbf{x} \in \Omega_F\right] = \int_{\Omega_F} f_{\mathbf{x}}\left(\mathbf{x}\right) d\mathbf{x} = \int_{\mathbb{R}^{NRV}} I_{\Omega_F}\left(\mathbf{x}\right) f_{\mathbf{x}}\left(\mathbf{x}\right) d\mathbf{x}, \quad (3\text{-}2)$$

where $\mathbf{x} = [x_1, x_2, \ldots, x_{NRV}]^T$ is a random input variable vector, $f_{\mathbf{x}}(\mathbf{x})$ is an input joint PDF, and $\Omega_F$ is the failure domain that is defined by $\Omega_F \equiv \left\{\mathbf{x} : G\left(\mathbf{x}\right) > 0\right\}$. $I_{\Omega_F(\mathbf{x})}$ is the indicator function which is defined as

$$I_{\Omega_F}(\mathbf{x}) \equiv \begin{cases} 1 & \mathbf{x} \in \Omega_F \\ 0 & otherwise \end{cases}. \tag{3-3}$$

In most engineering applications, Eq. (3-2) cannot be analytically evaluated because performance measure $G(\mathbf{x})$ is usually nonlinear and the input joint PDF does not follow Gaussian. To tackle this issue, sampling-based reliability analysis, which calculates the probability of failure using MCS and the surrogate models, can be used. Thus, to compute the probability of failure in Eq. (3-2), MCS samples, generated at a given design and following the input joint PDF, need to be evaluated by simulation output responses $G(\mathbf{x})$. However, direct use of MCS requires a huge number of CAE simulations to evaluate reliability, which leads to expensive computational cost. To resolve this issue, surrogate models need to be implemented for the calculation of the probability of failure. In this study, the dynamic kriging (DKG) method (Song et al., 2013a; Zhao et al., 2011), which is one of the most accurate surrogate model methods (Sen, Davis, Jacobs & Udaykumar, 2015; Volpi et al., 2015), has been used. Then the probability of failure in Eq. (3-2) can be approximated using MCS method as

$$P_F \equiv P\left[\mathbf{x} \in \Omega_F\right] \cong \frac{1}{nMCS} \sum_{k=1}^{nMCS} I_{\Omega_F}\left(\mathbf{x}^{(k)}\right), \tag{3-4}$$

where $nMCS$ is the number of MCS samples, and $\mathbf{x}^{(k)}$ is the $k^{\text{th}}$ realization of $\mathbf{x}$.

### 3.2.2 Stochastic Sensitivity Analysis

Consider the derivative of a probabilistic response $h(\boldsymbol{\mu})$, such as a probability of failure or statistical moments with respect to $\mu_i$. For the sensitivity analysis, the following four regularity conditions are required (Rahman, 2009; Rubinstein & Shapiro, 1993).

1. Input Joint PDF $f_{\mathbf{x}}(\mathbf{x};\boldsymbol{\mu})$ is continuous.
2. The mean $\mu_i \in \mathrm{M}_i \subset \mathbb{R}$, $i = 1,\ldots,N$, where $\mathrm{M}_i$ is an open interval on $\mathbb{R}$.
3. The partial derivative $\partial f_{\mathbf{x}}(\mathbf{x};\boldsymbol{\mu})/\partial\mu_i$ exists and is finite for all $\mathbf{x}$ and $\mu_i$. In addition, $h(\boldsymbol{\mu})$ is a differential function of $\boldsymbol{\mu}$.
4. There exists a Lebesgue integrable dominating function r($\mathbf{x}$) such that

$$\left| h(\mathbf{x}) \frac{f_{\mathbf{x}}(\mathbf{x};\boldsymbol{\mu})}{\mu_i} \right| \le r(\mathbf{x}) \tag{3-5}$$

for all $\boldsymbol{\mu}$.

When the above four conditions are satisfied, the partial derivative of probability of failure in Eq. (3-2) with respect to $\mu_i$ can be calculated as (Lee et al., 2011a; Lee et al., 2011b)

$$\begin{aligned}
\frac{\partial P_F(\boldsymbol{\mu})}{\partial \mu_i} &= \frac{\partial}{\partial \mu_i} \int_{\mathbb{R}^{NRV}} I_{\Omega_F}(\mathbf{x})\, f_{\mathbf{X}}(\mathbf{x};\boldsymbol{\mu})\, d\mathbf{x} \\
&= \int_{\mathbb{R}^{NRV}} I_{\Omega_F}(\mathbf{x}) \frac{\partial f_{\mathbf{X}}(\mathbf{x};\boldsymbol{\mu})}{\partial \mu_i} d\mathbf{x} \\
&= \int_{\mathbb{R}^{NRV}} I_{\Omega_F}(\mathbf{x}) \frac{\partial \ln f_{\mathbf{X}}(\mathbf{x};\boldsymbol{\mu})}{\partial \mu_i} f_{\mathbf{X}}(\mathbf{x};\boldsymbol{\mu})\, d\mathbf{x} \\
&= E\left[ I_{\Omega_F}(\mathbf{x}) \frac{\partial \ln f_{\mathbf{X}}(\mathbf{x};\boldsymbol{\mu})}{\partial \mu_i} \right]
\end{aligned}, \tag{3-6}$$

where $E[\bullet]$ represents the expectation operator. Here, the partial derivative of the log function of the joint PDF with respect to $\mu_i$ is the first-order score function and is denoted as

$$s_{\mu_i}^{(1)}(\mathbf{x};\boldsymbol{\mu}) = \frac{\partial \ln f_{\mathbf{X}}(\mathbf{x};\boldsymbol{\mu})}{\partial \mu_i}. \qquad (3\text{-}7)$$

Thus, the design sensitivity of the probability of failure using the score function does not include the gradients of the performance function, that is, the simulation model. Instead, the first-order score function in Eq. (3-7) needs to be derived, which can be analytically performed assuming the input variable follows a standard distribution such as normal, log-normal, Gumbel, or Weibull. Table 3.1 shows those four marginal PDFs.

Table 3.1 Marginal PDF and Distribution Parameters

| Type | PDF, $f_{\mathbf{X}}(x)$ | Distribution parameters |
|---|---|---|
| Normal | $\frac{1}{\sqrt{2\pi}\sigma} e^{-0.5[(x-\mu)/\sigma]^2}, x \in (-\infty, \infty)$ | $\mu$ : mean<br>$\sigma$ : standard deviation |
| Log-normal | $\frac{1}{\sqrt{2\pi} x\bar{\sigma}} e^{-0.5[(\ln x-\bar{\mu})/\bar{\sigma}]^2}, x \in (0, \infty)$ | $\bar{\sigma}^2 = \ln\left[1+(\sigma/\mu)^2\right]$,<br>$\bar{\mu} = \ln(\mu) - 0.5\bar{\sigma}^2$ |
| Gumbel | $\alpha e^{-\alpha(x-\nu)-e^{-\alpha(x-\nu)}}, x \in (-\infty, \infty)$ | $\mu = \nu + \frac{0.577}{\alpha}, \sigma = \frac{\pi}{\sqrt{6}\alpha}$ |
| Weibull | $\frac{k}{\upsilon}\left(\frac{x}{\upsilon}\right)^{k-1} e^{-(x/\upsilon)^k}, x \in [0, \infty)$ | $\mu = \upsilon\Gamma\left(1+\frac{1}{k}\right)$,<br>$\sigma^2 = \upsilon^2\left[\left(1+\frac{2}{k}\right) - \Gamma^2\left(1+\frac{1}{k}\right)\right]$ |

The derivation of the first-order score function can be performed for two different cases – independent and correlated random input variables. For an independent random input variable, the first-order score function for $\mu_i$ can be derived as

$$s_{\mu_i}^{(1)}(\mathbf{x};\boldsymbol{\mu}) \equiv \frac{\partial \ln f_{\mathbf{X}}(\mathbf{x};\boldsymbol{\mu})}{\partial \mu_i} = \frac{\partial}{\partial \mu_i}\left(\prod_{i=1}^{NRV} f_{X_i}(x_i;\mu_i)\right) = \frac{\partial f_{X_i}(x_i;\mu_i)}{\partial \mu_i}, \tag{3-8}$$

where $f_{X_i}(x_i;\mu_i)$ is the marginal PDF corresponding to the $i^{\text{th}}$ input random variable. Table 3.2 summarizes the derivation of Eq. (3.8) for four commonly used marginal PDFs.

Table 3.2 First-Order Score Function for $\mu_i$ for Independent Random Variables

| Marginal distribution type | First-order score function, $s_{\mu_i}^{(1)}(\mathbf{x};\boldsymbol{\mu})$ |
|---|---|
| Normal | $\frac{x_i - \mu_i}{\sigma_i^2}$ |
| Log-normal | $-\frac{1}{\bar{\sigma}_i}\frac{\partial \bar{\sigma}_i}{\partial \mu_i} + \frac{1}{\bar{\sigma}_i^2}\left(\frac{\ln x - \bar{\mu}_i}{\bar{\sigma}_i}\right)\left[\bar{\sigma}_i \frac{\partial \bar{\mu}_i}{\partial \mu_i} + (\ln x - \bar{\mu}_i)\frac{\partial \bar{\sigma}_i}{\partial \mu_i}\right]$ |
| Gumbel | $\alpha_i - \alpha_i e^{-\alpha(x_i - \nu_i)}$ |
| Weibull | $\frac{1}{k_i}\frac{\partial k_i}{\partial \mu_i} - \frac{1}{\nu_i}\frac{\partial \nu_i}{\partial \mu_i} + \frac{\partial k_i}{\partial \mu_i}\ln\frac{x_i}{\nu_i} - \frac{(k_i - 1)}{\nu_i}\frac{\partial \nu_i}{\partial \mu_i} - \left(\frac{x_i}{\nu_i}\right)^{k_i}\left(\frac{\partial k_i}{\partial \mu_i}\ln\frac{x_i}{\nu_i} - \frac{k_i}{\nu_i}\frac{\partial \nu_i}{\partial \mu_i}\right)$ |

Source: Lee, I., Choi, K. K., Noh, Y., Zhao, L. & Gorsich, D. (2011b). Sampling-based stochastic sensitivity analysis using score functions for RBDO problems with correlated random variables. *Journal of Mechanical Design*, 133(2), 021003.

For bivariate correlated random input variables, $X_i$ and $X_j$, the joint PDF can be expressed as (Noh et al., 2011a; Noh et al., 2011b)

$$\begin{aligned} f_{\mathbf{X}}(\mathbf{x};\boldsymbol{\mu}) &= \frac{\partial C(u,\upsilon;\theta)}{\partial u \partial \upsilon} f_{X_i}(x_i;\mu_i) f_{X_j}(x_j;\mu_j) \\ &\equiv c(u,\upsilon;\theta) f_{X_i}(x_i;\mu_i) f_{X_j}(x_j;\mu_j) \end{aligned}, \tag{3-9}$$

where $C$ is a copula function, $u$ and $\upsilon$ are CDFs for $X_i$ and $X_j$, respectively, and $\theta$ is the correlation coefficient between $X_i$ and $X_j$. Table 3.3 lists commonly used copula functions.

Table 3.3 Commonly Used Copula Functions

| Copula type | $C(u,\upsilon;\theta)$ |
|---|---|
| Clayton | $\left(u^{-\theta}+\upsilon^{-\theta}-1\right)^{-1/\theta}$ |
| AMH | $\dfrac{u\upsilon}{1-\theta(1-u)(1-\upsilon)}$ |
| Frank | $-\dfrac{1}{\theta}\ln\left[1+\left(e^{-\theta u}-1\right)\left(e^{-\theta\upsilon}-1\right)/\left(e^{-\theta}-1\right)\right]$ |
| FGM | $u\upsilon+\theta u\upsilon(1-u)(1-\upsilon)$ |
| Gaussian | $\int_{-\infty}^{\Phi^{-1}(u)}\int_{-\infty}^{\Phi^{-1}(\upsilon)}\dfrac{1}{2\pi\sqrt{1-\theta^2}}\exp\left[\dfrac{2\theta sw-s^2-w^2}{2(1-\theta^2)}\right]dsdw$ |
| Independent | $u\upsilon$ |

In Eq. (3-9), the partial derivative of the copula function with respect to marginal CDFs $u$ and $\upsilon$ is called the copula density function, $c(u,\upsilon;\theta)$, which is derived in Table 3.3. Accordingly, the first-order score functions in Eq. (3-8) for a correlated bivariate input random variables can be derived as

$$s_{\mu_i}^{(1)}(\mathbf{x};\boldsymbol{\mu})\equiv\frac{\partial\ln f_{\mathbf{X}}(\mathbf{x};\boldsymbol{\mu})}{\partial\mu_i}=\frac{\partial\ln c(u,\upsilon;\theta)}{\partial\mu_i}+\frac{\partial f_{X_i}(x_i;\mu_i)}{\partial\mu_i}. \tag{3-10}$$

The derivative of the first term is shown in Table 3.4 and the second term of the right-hand side is identical to Eq. (3-8). In Table 3.4, $\Phi(\bullet)$ and $\phi(\bullet)$ indicates the standard normal CDF and PDF, respectively. The partial derivative of marginal CDF, $\partial u/\partial \mu_i$, used to calculate log-derivative of copular density function in Table 3.4 can be easily derived as shown in Table 3.5.

Table 3.4 Log-Derivative of Copula Density Function

| Copula type | $\dfrac{\partial \ln c(u,\upsilon;\theta)}{\partial \mu_i}$ |
|---|---|
| Clayton | $\left(-\dfrac{1+\theta}{u}+\dfrac{(2\theta+1)u^{-(1+\theta)}}{u^{-\theta}+\upsilon^{-\theta}-1}\right)\dfrac{\partial u}{\partial \mu_i}$ |
| AMH | $\left[\dfrac{-\theta^2(1-\upsilon)+\theta(\upsilon+1)}{1+\theta^2(1-u)(1-\upsilon)-\theta(2-u-\upsilon-u\upsilon)}-\dfrac{3\theta(1-\upsilon)}{1-\theta(1-u)(1-\upsilon)}\right]\dfrac{\partial u}{\partial \mu_i}$ |
| Frank | $\theta\left[\dfrac{2\left(e^{\theta(1+u)}-e^{\theta(u+\upsilon)}\right)}{e^{\theta}-e^{\theta(1+u)}-e^{\theta(1+\upsilon)}+e^{\theta(u+\upsilon)}}+1\right]\dfrac{\partial u}{\partial \mu_i}$ |
| FGM | $\left[\dfrac{2\theta(1-\upsilon)}{1-\theta(1-2u)(1-2\upsilon)}\right]\dfrac{\partial u}{\partial \mu_i}$ |
| Gaussian | $\left[\dfrac{\Phi^{-1}(u)}{\phi\left(\Phi^{-1}(u)\right)}+\dfrac{\theta\Phi^{-1}(\upsilon)-\Phi^{-1}(u)}{\phi\left(\Phi^{-1}(u)\right)\left(1-\theta^2\right)}\right]\dfrac{\partial u}{\partial \mu_i}$ |
| Independent | 0 |

Source: Lee, I., Choi, K. K., Noh, Y., Zhao, L. & Gorsich, D. (2011b). Sampling-based stochastic sensitivity analysis using score functions for RBDO problems with correlated random variables. *Journal of Mechanical Design*, 133(2), 021003.

Table 3.5 Partial Derivatives of Marginal CDF with Respect to $\mu_i$

| Marginal distribution type | Partial derivative of marginal CDF, $\dfrac{\partial u}{\partial \mu_i}$ |
|---|---|
| Normal | $-\dfrac{1}{\sigma_i}\phi\left(\dfrac{x-\mu_i}{\sigma_i}\right)$ |
| Log-normal | $-\dfrac{1}{\bar{\sigma}_i}\left(\dfrac{\partial \bar{\mu}_i}{\partial \mu_i}\bar{\sigma}_i + \dfrac{\partial \bar{\sigma}_i}{\partial \mu_i}(\ln x - \bar{\mu}_i)\right)\phi\left(\dfrac{\ln x - \bar{\mu}_i}{\bar{\sigma}_i}\right)$ |
| Gumbel | $-\alpha_i e^{-\alpha_i(x-\nu_i)-e^{-\alpha_i(x-\nu_i)}}$ |
| Weibull | $e^{-\left(\frac{x_i}{\nu_i}\right)^{k_i}}\left(\dfrac{x_i}{\nu_i}\right)^{k_i}\left(\dfrac{\partial k_i}{\partial \mu_i}\ln\dfrac{x_i}{\nu_i} - \dfrac{k_i}{\nu_i}\dfrac{\partial \nu_i}{\partial \mu_i}\right)$ |

Source: Lee, I., Choi, K. K., Noh, Y., Zhao, L. & Gorsich, D. (2011b). Sampling-based stochastic sensitivity analysis using score functions for RBDO problems with correlated random variables. *Journal of Mechanical Design*, 133(2), 021003.

It can be found that the first-order score function, which is used to compute the design sensitivity of the probability of failure, does not require the gradient of performance measure. As explained in Section 3.2.1, for the efficiency, the sampling-based RBDO uses surrogate models to evaluate the output response value. Once accurate surrogate models are available, the MCS can be applied to estimate the sensitivity of the probability of failure as well as the probability of failure. In that sense, the calculation of the design sensitivity of the probability of failure in Eq. (3-6) can be approximated using MCS as

$$\frac{\partial P_F}{\partial \mu_i} \cong \frac{1}{nMCS}\sum_{k=1}^{nMCS} I_{\Omega_F}\left(\mathbf{x}^{(k)}\right) s_{\mu_i}^{(1)}\left(\mathbf{x}^{(k)};\boldsymbol{\mu}\right), \qquad (3\text{-}11)$$

where *nMCS* is the number of MCS samples, and $\mathbf{x}^{(k)}$ is the $k^{\text{th}}$ realization of **x**. It can be seen that the first-order score function does not involve the sensitivity of surrogate models which is known to be inaccurate. Furthermore, the calculation of score function is not an approximation method such as the finite difference method (FDM) because it uses an analytical expression of the input PDF. However, there exists MCS error that depends on the target probability of failure and MCS sample size. The MCS error can be defined as (Haldar & Mahadevan, 2000)

$$\varepsilon\% = \sqrt{\frac{\left(1 - P_F^{Tar}\right)}{nMCS \times P_F^{Tar}}} \times 200\%, \tag{3-12}$$

where $P_{F_i}^{Target}$ is the target probability of failure. It is shown that the number of MCS samples should be increased to satisfy the desired accuracy level. In addition, the number of MCS samples should be very large to increase the accuracy when the target probability of failure is small (*e.g.*, 6-sigma design). In the following chapters, the sampling-based RBDO method using MCS applied to the very accurate DKG models described in this chapter will be used.

# CHAPTER 4

# PROPOSED CONFIDENCE-BASED MODEL VALIDATION FOR CONSERVATIVE RELIABILITY ASSESSMENT CONSIDERING LIMITED EXPERIMENTAL OUTPUT DATA

In this section, a new methodology of model validation for reliability assessment with insufficient experimental output data is proposed. The proposed model validation accounts for the uncertainty caused by insufficient experimental output data and includes two steps. In Step 1, using sampling-based Bayesian analysis, a target output PDF that conservatively estimates a probability of failure at a target confidence level is obtained. In Step 2, confidence-based model bias correction is carried out by matching the simulation output PDF to the target output PDF obtained in Step 1. The simulation model, which is validated using the developed method, may not predict true probability of failure; but it satisfies the target confidence level. Because the methodology provides the confidence of the simulation model (or the RBDO design when it is integrated in the RBDO process) with the target confidence level, it is referred to as confidence-based model validation.

In Section 4.1, the underlying philosophy of model validation for reliability analysis is explained. In this study, a target output PDF is introduced, to which simulation output PDF needs to be matched. Section 4.2 addresses the issue when only insufficient experimental output data is provided in real practical situations. Accordingly, new model validation method should account for the uncertainty induced by insufficient experimental output data. Furthermore, it is emphasized that this thesis handles the situation in which the exact input values that correspond to experimental output data are unknown. To handle this issue, the proposed confidence-based model validation selects a confidence-based target output PDF. Section 4.3 describes in detail the computational procedure to select a confidence-based target output PDF that estimates the probability of failure conservatively. The conservativeness is controlled by a user-specified target confidence level. Section 4.4 explains model validation optimization, which corrects model bias by matching simulation output PDF with confidence-based target output PDF. After that, a validated simulation output PDF that satisfies the target confidence level can be obtained. Note that the validated simulation model obtained using the developed method does not predict the true probability of failure but rather estimates the probability of failure conservatively with a certain probability – the target confidence level.

## 4.1 Philosophy of Model Validation for Reliability Analysis

The output variability, which is represented by the output PDF, is combination of the input variability and simulation. Modeling of an accurate output PDF can be achieved under two requirements: (1) correct input variability is known by the input joint PDF and (2) the simulation model has no bias. It is noted that, for the biased simulation model, the accurate output variability cannot be estimated even though the correct input variability is given. The output PDF has to be accurately identified to accurately estimate the reliability of system because an inaccurate output PDF would yield an underestimation or overestimation of the probability of failure. Hence, estimating an accurate output PDF is an essential task in reliability analysis. To do that, the simulation output PDF (the output PDF obtained using simulation model before model validation), not the deterministic output, needs to be validated against experimental output data that is a realization of real physics. At the same time, experimental output data needs to be treated as a random quantity since it involves manufacturing variability and systematic uncertainties in the experimental measurement. For this reason, in each experiment, not all physical conditions, such as the specimen and the measurement of response, can be exactly reproduced. This indicates that the true response value is random. Thus, the randomness of the experimental output data is represented by the true output PDF in this study. Accordingly, theoretically, the simulation output PDF needs to be matched with the true output PDF. However, the true output PDF is not available in practical applications because the model bias is unknown. Therefore, instead of using true output PDF, we have to predict a target output PDF, to which the simulation output PDF will be validated as shown in Figure 4.1. However, the selection of the target output PDF is not simple since there could be various possible predicted output PDFs that could represent the given experimental output data. The underlying idea of selecting an appropriate target output PDF will be explained in Section 4.2.

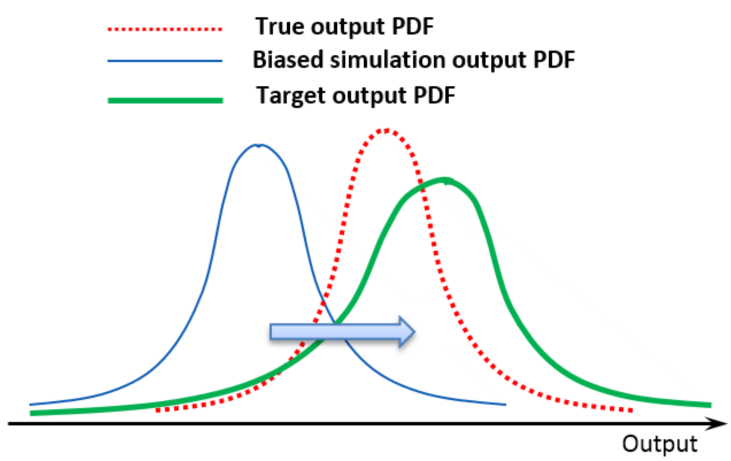


Figure 4.1 Illustration of Output PDFs

## 4.2 How to Handle an Insufficient Experimental Output Data in Proposed Model Validation

It is very difficult to characterize true model bias accurately. Obtaining accurate model bias exactly means obtaining true output PDF using enormous number of experiments. However, in real engineering problems, we cannot experiment with all uncertain quantities due to the expense of full-scale product testing, so only a limited number of experimental output data is available. Furthermore, this thesis handles the situation in which the exact input values that correspond to the experimental output data are unknown; only the mean value of the input is known. For example, in the collision test of the same five vehicles, we do not have the exact difference of the input variable value (*e.g.*, geometry dimension and material properties) between those five vehicles; only mean value of the input is known. The obtained experimental (output) results may correspond to a different combination of input variable values while their mean values are supposed to be the same. This assumption, which is more associated with real practical applications, differs from the situation that conventional validation approaches deal with. It is noted that we validate the simulation output PDF against the target output PDF, rather than using pointwise validation, because only experimental output data is given; the exact input values are unknown, as mentioned above.

In addition, there is the uncertainty induced by insufficient experimental output data. In the presence of the uncertainty due to insufficient experimental output data, a predicted output PDF becomes uncertain; there could be various possible predicted output PDFs as shown in Figure 4.2. Accordingly, an uncertainty also exists in the predicted probability of failure, which is calculated based on the predicted output PDF. Therefore, among the predicted output PDFs, one has to be selected as a target. To compensate for the uncertainty induced by the limited number of experimental output data, the system should predict the reliability conservatively so that the designed product is conservative. In this study, we suggest to conservatively estimate target output PDF that overestimates the true probability of failure of the system among many possible candidates of predicted output PDFs. In the meantime, conservativeness should be appropriate not to yield an overly conservative design. The proposed method enables engineers to specify the level of conservativeness, and the confidence concept needs to be introduced to control the conservativeness. A detailed numerical procedure to select the confidence-based target output PDF will be explained in Section 4.3.

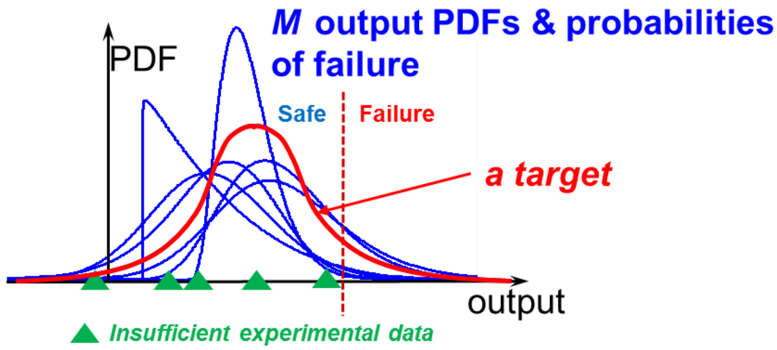


Figure 4.2 Uncertainty in Target Output PDF and Probability of Failure Due to Insufficient Experimental Output Data

## 4.3 Conservative Estimation of Target Output PDF and Probability of Failure Using Sampling-Based Bayesian Analysis

### 4.3.1 Bayesian Modeling of Output PDF

To model an output PDF, we have to carefully choose a distribution type. Because the output PDF is a combination of input PDF and nonlinear output response, the distribution type of output PDF may not be any standard parametric distribution. In that sense, a non-parametric method such as the Pearson system or Kernel Density Estimation (KDE) is useful when a standard parametric distribution type cannot properly describe data or when we want to avoid assumptions about the output PDF. We found that the Pearson system, which covers various types of parametric distributions, fails to describe highly skewed distributions (Pearson, 1916) while KDE can handle them. Therefore, KDE is chosen to predict output PDFs in this study. Consider an independent and identically distributed data $y_i$ sampled from unknown density $f$. The estimated density function in KDE is defined as

$$\tilde{f}(y) = \frac{1}{nh_0} \sum_{i=1}^{n} K\left( \frac{y - y_i}{h_0} \right), \qquad (4\text{-}1)$$

where $h_0$ is a smoothing parameter called the bandwidth and $K(\bullet)$ is a kernel. While a histogram places a discrete bin (box) at data points, KDE builds the kernel, which is a smooth and continuous function. The kernel is the non-negative integrable function that satisfies the following two requirements:

1. The integration over the entire real line should be one (*i.e.*, $\int_{-\infty}^{\infty} K(u)\,du = 1$)
2. $K(u) = K(-u)$ for all values of $u$.

In particular, the first requirement ensures that the result of KDE yields a PDF. Several types of kernel function that are commonly used are listed in Table 4.1. In Table 4.1, $I$ is the indicator function. As shown in Eq. (4-1), the advantage of the KDE is that there is only one unknown parameter, the bandwidth. If there exist many unknown parameters to be quantified, the uncertainty is easily overestimated, and the overestimation leads to an unnecessarily conservative output PDF. In KDE, because the bandwidth is the only unknown parameter, it has a strong influence on probability density; a large bandwidth leads to too smooth distribution, and a small bandwidth creates discontinuous distribution. Therefore, selecting an appropriate bandwidth is critical. The standard KDE in Eq. (4-1) uses a fixed bandwidth ($h_0$) assuming that the statistical properties of the underlying data are stationary. Consequently, the standard KDE tends to over-smooth the region where data is concentrated and to under-smooth the tail part of the distribution and the sparse data region. Adaptive kernel density estimation (AKDE), which has variable bandwidth can improve the standard KDE. For AKDE, Eq. (4-1) is modified as

$$\tilde{f}(y) = \frac{1}{nh(y_i)} \sum_{i=1}^{n} K\left(\frac{y - y_i}{h(y_i)}\right), \tag{4-2}$$

where $h(y_i)$ is the variable bandwidth that is narrower at high density region and wider at low density region.

Table 4.1 Types of Kernel Function

| Type | Kernel function, $K(u)$ |
|---|---|
| Uniform | $K(u) = \frac{1}{2} I_{[\lvert u\rvert \le 1]}$ |
| Triangular | $K(u) = (1 - \lvert u\rvert) I_{[\lvert u\rvert \le 1]}$ |
| Epanechinikov | $K(u) = \frac{3}{4}(1 - u^2) I_{[\lvert u\rvert \le 1]}$ |
| Gaussian | $K(u) = \frac{1}{\sqrt{2\pi}} \exp\left[-\frac{1}{2}u^2\right]$ |
| Biweight | $K(u) = \frac{15}{16}(1 - u^2)^2 I_{[\lvert u\rvert \le 1]}$ |
| Triweight | $K(u) = \frac{35}{32}(1 - u^2)^3 I_{[\lvert u\rvert \le 1]}$ |

In this study, AKDE is used to model output PDF using both experimental output data and simulation model. In AKDE, the uncertainty of the output PDF is reflected by the posterior distribution of the bandwidth, which is the multiplication of the likelihood function and the prior distribution of the bandwidth. The likelihood function only depends on experimental output data; the prior distribution is specified using the simulation output PDF. Detailed computational procedure will be explained. For the likelihood function, this paper uses a cross-validation likelihood function using Silverman's AKDE (Silverman, 1986), which is defined as

$$L\left(\mathbf{y}^e \middle| h_0\right) = \sum_{i=1}^{ne} \log \tilde{f}_{-i}\left(y_i^e; h_0\right), \tag{4-3}$$

where $ne$ is the number of experimental output data, $\mathbf{y}^e = [y_1^e, y_2^e, ..., y_{ne}^e]^T$ is the experimental output data vector, and $\tilde{f}_{-i}\left(y_i^e; h_0\right)$ is the leave-one-out estimator defined as

$$\tilde{f}_{-i}\left(y_i^e; h_0\right) = \left[\frac{1}{(ne-1)h\left(y_i^e; h_0\right)} \sum_{\substack{j=1 \\ j \neq i}}^{ne} K\left(\frac{y_i^e - y_j^e}{h\left(y_i^e; h_0\right)}\right)\right], \tag{4-4}$$

In Eq. (4-4), $h\left(y_i^e; h_0\right)$ is the variable bandwidth (Silverman, 1986) defined as

$$h\left(y_i^e; h_0\right) = h_0 \left(\frac{\lambda}{\tilde{f}\left(y_i^e; h_0\right)}\right)^{1/2} \text{ where } \lambda = \left[\prod_{i=1}^{ne} \tilde{f}\left(y_i^e; h_0\right)\right]^{\frac{1}{ne}}, \tag{4-5}$$

where $h_0$ is the fixed bandwidth, and $\tilde{f}\left(y_i^e; h_0\right)$ is the initial density estimation (pilot density) obtained using $h_0$. Once the fixed bandwidth $h_0$ is provided, the variable bandwidth $h\left(y_i^e;h_0\right)$ at each experimental output data point $y_i^e$ can be evaluated using Eq. (4-5). Therefore, we specify a prior distribution over the fixed bandwidth, denoted by $P(h_0)$, not the variable bandwidth, as defined below:

$$P\left(h_0\right) \sim \text{Gamma}\left(14, \frac{a}{14}\right), \text{ where } \; a = \left(\frac{4}{3n_p}\right)^{1/5} \min\left(\sigma_s, \frac{IQR_s}{1.34}\right). \tag{4-6}$$

Here, $\sigma_s$ and $IQR_s$ are the standard deviation and the interquartile range (*i.e.*, the difference between 75% and 25% quantile values) of the biased simulation output PDF, respectively. It is noted that the information of the biased simulation output PDF is used to construct the prior distribution. Even though the simulation model is inaccurate, it is the best information we have and can provide an informative prior in Eq. (4-6). In Eq. (4-6), $n_p$ is the prior sample size that indicates that we believe the information in the prior is equivalent to $n_p$ experimental output data. In this paper, $n_p$ is set to a small number 10 to represent lack of prior information. Prior sample size $n_p$ does not have a significant effect on the final result because $(4/3n_p)^{1/5}$ in Eq. (3-6) does not significantly vary depending on $n_p$. Thus, the number 10 could be applied for any problem dealing with an insufficient experimental output data. Because the bandwidth is a positive value, the gamma distribution can represent the prior well. The mean of $P(h_0)$ is $a$, which is the optimal bandwidth obtained from the simulation output PDF using Silverman's rule (Silverman, 1986). The distribution parameters 14 and $a$/14 in Eq. (4-6) have been selected such that the prior distribution of bandwidth covers the optimal bandwidth ($a$) for the extreme case in which $n_p$ is 1. The optimal bandwidth for the extreme case falls into the upper bound of the 95% confidence interval of prior distribution.

4.3.2 Quantification of Distribution of Probability of Failure

As stated earlier, with the presence of insufficient experimental output data, a predicted output PDF becomes uncertain. Accordingly, an uncertainty exists in the predicted probability of failure, which is calculated based on the predicted output PDF. To quantify uncertainty in the probability of failure, the distribution (specifically, marginal CDF) of probability of failure, which describes all possible probabilities of failure given insufficient experimental output data, is necessary. To obtain the distribution, the posterior distribution $P\left(h_0 \mid \mathbf{y}^e\right)$ for the fixed bandwidth is firstly formulated by the multiplication of the likelihood function of Eq. (4-3) and the prior distribution of Eq. (4-6) as

$$P\left(h_0 \mid \mathbf{y}^e\right) = L\left(\mathbf{y}^e \middle| h_0\right) P\left(h_0\right) \tag{4-7}$$

Once the fixed bandwidth $h_0$ is given, the variable bandwidth, which is the unknown parameter in constructing the output PDF, can be evaluated. Then, the predicted output PDF and the probability of failure are uniquely determined. As a result, the conditional PDF of the probability of failure ($p_F$), given the fixed bandwidth $h_0$ and the experimental output data $\mathbf{y}^e$, becomes the Dirac delta measure as

$$f\left(p_F \mid h_0, \mathbf{y}^e\right) = \delta\left[p_F - p_F\left(h_0 \mid \mathbf{y}^e\right)\right] = \begin{cases} +\infty & p_F = p_F\left(h_0 \mid \mathbf{y}^e\right) \\ 0 & p_F \neq p_F\left(h_0 \mid \mathbf{y}^e\right) \end{cases}, \tag{4-8}$$

where $p_F\left(h_0 \mid \mathbf{y}^e\right)$ is the obtained probability of failure when $h_0$ is given. The probability is the integration of Eq. (4-8). When $p_F$ equals $p_F\left(h_0 \mid \mathbf{y}^e\right)$, the probability becomes one, while the probability of getting any other values of $p_F$ is zero. The CDF of the probability of failure, $F_{p_F}\left(p_F \mid \mathbf{y}^e\right)$, can be formulated as

$$F_{p_F}\left(p_F \mid \mathbf{y}^e\right) = \int_0^{p_F} \int_{\Omega_{h_0}} f\left(p_F \mid h_0, \mathbf{y}^e\right) P\left(h_0 \mid \mathbf{y}^e\right) dh_0 dP_F \tag{4-9}$$

Meanwhile, the posterior distribution of $h_0$ in Eq. (4-9) cannot be analytically obtained so that the realization of the $h_0$ needs to be generated using the Markov Chain Monte Carlo (MCMC) sampler in accordance with $P\left(h_0 \mid \mathbf{y}^e\right)$. The Metropolis-Hasting algorithm has been used to obtain the random realization of $h_0$. Consequently, integration in Eq. (4-9) is numerically evaluated using MCS integration as

$$\begin{aligned} F_{p_F}\left(p_F \mid \mathbf{y}^e\right) &\cong \frac{1}{M} \int_0^{p_F} \sum_{i=1}^{M} \left[ f\left(p_F \mid h_0^{(i)}, \mathbf{y}^e\right) \right] dp_F \\ &= \frac{1}{M} \int_0^{p_F} \sum_{i=1}^{M} \delta\left[ p_F - p_F\left(h_0^{(i)} \mid \mathbf{y}^e\right) \right] dp_F = \frac{1}{M} \sum_{i=1}^{M} I_{\left[0, p_F\left(h_0^{(i)} \mid \mathbf{y}^e\right)\right]}\left(p_F\right) \end{aligned} \tag{4-10}$$

$$\text{where } I_{\left[0, p_F\left(h_0^{(i)} \mid \mathbf{y}^e\right)\right]}\left(p_F\right) = \begin{cases} 1 & \text{if } 0 \le p_F \le p_F\left(h_0^{(i)} \mid \mathbf{y}^e\right) \\ 0 & \text{if } p_F > p_F\left(h_0^{(i)} \mid \mathbf{y}^e\right) \end{cases},$$

$M$ is the number of MCS samples, and $h_0^{(i)}$ is the $i^{\text{th}}$ realization of $h_0$ after burn-in in MCMC sampling.

### 4.3.3 Selection of Confidence-Based Target Output PDF at Target Confidence Level

Using the CDF of the probability of failure, we can obtain the probability of failure at a specified percentile. A higher percentile indicates a more conservative estimation of the probability of failure. Therefore, the percentile is referred to as the confidence level. For example, the probability of failure at a 95% confidence level is higher than the one at an 80% confidence level as shown in Figure 4.3. Designers can choose a target confidence level, $CL^{Target}$, so that they can control the confidence level of the estimated probability of failure and so the confidence-based model validation. The probability of failure at the target confidence level, $p_F^{confidence}$ ($CL^{Target}$), is the confidence-based probability of failure, and the predicted output PDF, which produces the confidence-based probability of failure, is selected as the confidence-based target output PDF.

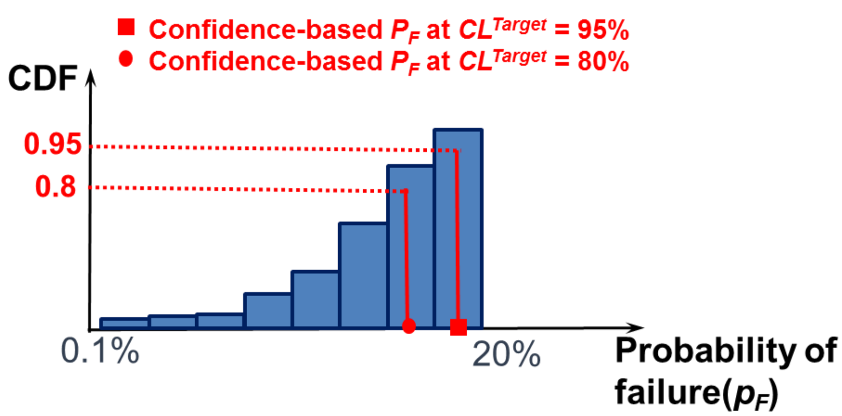


Figure 4.3 CDF of Probability of Failure

## 4.4 Model Validation Optimization for Confidence-Based Model Bias Correction

### 4.4.1 Formulation of Model Validation Optimization

Using the obtained confidence-based probability of failure and the target output PDF at $CL^{Target}$, the model bias can be estimated conservatively (Moon et al., 2015). Model bias correction is an optimization process to validate the biased simulation model. It is noted that the model validation optimization is not the design optimization. The objective is to minimize the distance between the simulation output PDF and the confidence-based target output PDF. The distance is measured by a similarity measure, denoted by validation measure. There exist various validation measures that can compare two distributions. The Kullback–Leibler divergence (K-L divergence) (Kullback & Leibler, 1951) is defined by

$$D_{KL}\left(M \| N\right) = \int_{-\infty}^{\infty} m\left(x\right) \log \frac{m\left(x\right)}{n\left(x\right)} dx, \tag{4-11}$$

where $m$ and $n$ denote the PDFs of $M$ and $N$. It is well known that the K-L divergence is non-negative but non-symmetric and unbounded. The CDF difference approach, which is defined as

$$\Delta\text{CDF} = \int_{-\infty}^{\infty} \left| F_M(x) - F_N(x) \right| dx, \tag{4-12}$$

where $F_M$ and $F_N$ are the CDFs of $M$ and $N$, is a symmetric measure but it requires heavy computational time. The Hellinger similarity (Nikulin, 2001) is a bounded and symmetric metric, which is defined by

$$H\left(M,N\right)=\frac{1}{2}\int_{-\infty}^{\infty}\left(\sqrt{m\left(x\right)}-\sqrt{n\left(x\right)}\right)^{2}dx=1-\int_{-\infty}^{\infty}\sqrt{m\left(x\right)n\left(x\right)}dx. \tag{4-13}$$

In the meantime, the Hellinger similarity can be expressed using the Bhattacharyya distance (*i.e.*, 1 − Bhattacharyya distance). In the Hellinger similarity, the maximum value (one) is achieved when two distributions do not have any overlap area; when two distributions are identical, the value goes to minimum (zero). In this study, the Hellinger similarity $H(\mathbf{v})$ in Eq. (4-14) is used as a validation measure to evaluate the distance between the simulation output PDF and the confidence-based target output PDF because it is symmetric, bounded and computationally efficient.

Using the Hellinger similarity, the model validation optimization is formulated to force the validated simulation output PDF to produce the confidence-based probability of failure that satisfies the target confidence level. The formulation of the model validation optimization can be expressed as

$$\begin{aligned}&\text{minimize} \quad H(\mathbf{v})=1-\int_{-\infty}^{\infty}\sqrt{p\left(g\left(\mathbf{x};\mathbf{v}\right)\right)q\left(g;CL^{Target}\right)}dg\\&\text{subject to} \quad p_F(\mathbf{v})=\mathrm{P}\left(g\left(\mathbf{x};\mathbf{v}\right)>0\right)=p_F^{confidence}\left(CL^{Target}\right)\ ,\\&\qquad\qquad \mathbf{v}^L\le\mathbf{v}\le\mathbf{v}^U,\quad \mathbf{v}\in\mathbb{R}^2 \ \text{and}\ \mathbf{x}\in\mathbb{R}^{NRV}\end{aligned} \tag{4-14}$$

where $\mathbf{x}$ is the input random variable vector, $\mathbf{v}$ is an optimization variable vector (not the design variable vector of RBDO), $q(g;CL^{Target})$ is the confidence-based target output PDF, $p_F^{confidence}(CL^{Target})$ is the confidence-based probability of failure and *NRV* is the number of input random variables. The elements of the optimization variable vector $\mathbf{v}$ are the statistical properties (*i.e.*, mean and standard deviation) of model bias function $B(\mathbf{x};\mathbf{v})$. The model bias function $B(\mathbf{x};\mathbf{v})$ has variability; hence, it follows a certain distribution at a given design due to the variability. Therefore, the mean and standard deviation ($\mathbf{v}$) of the model bias, not the deterministic value of model bias, have been adjusted in the model validation optimization. By minimizing the Hellinger similarity in Eq. (4-14), the validated simulation model – validated simulation output PDF – will be a distribution as similar to the target output PDF as possible. At the same time, by the constraint in Eq. (4-14), the validated simulation model will produce the confidence-based probability of failure.

The validated simulation model is defined as $g(\mathbf{x};\mathbf{v}) = G(\mathbf{x}) + B(\mathbf{x};\mathbf{v})$, where $G(\mathbf{x})$ is the biased simulation output. Accordingly, $p(g(\mathbf{x};\mathbf{v}))$ indicates the validated simulation output PDF with model bias correction. It is worth noting that the confidence-based target output PDF $q(g;CL^{Target})$ cannot be readily obtained as a function of the input random variable $\mathbf{x}$. Hence, $p_F^{confidence}$ $(CL^{Target})$ that corresponds to the $q(g;CL^{Target})$ cannot be used to calculate stochastic design sensitivity using the score function derived in Section 3.2.2 because $p_F^{confidencee}(CL^{Target})$ is not differentiable function of the RBDO design variable (*i.e.*, $\boldsymbol{\mu}$ defined in Section 3.1). On the other hand, the validated simulation output PDF $p(g(\mathbf{x};\mathbf{v}))$ is related to $\mathbf{x}$ that enables calculation of the stochastic sensitivity with respect to $\boldsymbol{\mu}$. For this reason, the model validation optimization is necessary to carry out stochastic sensitivity analysis in RBDO even though the target output PDF has been obtained from Bayesian analysis in Section 4.3.3. This is one of the reason that the simulation model is validated, not directly using the target output PDF in RBDO.

### 4.4.2 Validated Simulation Model

After carrying out the proposed model validation optimization in Section 4.4.1, validated simulation model (validation simulation output PDF) can be obtained with model bias correction. The proposed method seeks the confidence-based model bias by matching $g(\mathbf{x};\mathbf{v})$ to the confidence-based target output PDF $q(g;CL^{Target})$. Therefore, the model bias $B(\mathbf{x};\mathbf{v}_{opt})$ drawn at the optimum $\mathbf{v}_{opt}$ is conservative. As a result, the optimized model bias leads to the conservative evaluation of the probabilistic constraint in the RBDO process. Because the optimized model bias satisfies the target confidence level, it is denoted by confidence-based model bias, $B(\mathbf{x}; CL^{Target}) = B(\mathbf{x};\mathbf{v}_{opt})$. It is noted that the validated simulation model obtained using the confidence-based model bias is not intended to provide an accurate estimation of the true probability of failure, which is not possible in the presence of insufficient experimental output data. The confidence that the probability of failure estimated using the validated simulation model is larger than the true probability of failure is the same as the target confidence level, $CL^{Target}$, which we can control. Due to model bias correction, the failure domain defined in Section 3.2.1 needs to be updated. The failure domain for validated simulation model is defined by $\bar{\Omega}_F \equiv \left\{ \mathbf{x} : G(\mathbf{x}) + B\left(\mathbf{x}; CL^{Target}\right) > 0 \right\}$. Notice that the volume of failure domain for validated simulation model is increased by the confidence-based model bias term, $B(\mathbf{x}; CL^{Target})$. After simulation output MCS points are evaluated using DKG models, we need to update the output MCS point by adding confidence-based model bias for the conservative calculation of probability of failure at the target confidence level. Accordingly, the evaluation of probability of failure and stochastic sensitivity analysis using MCS need to be carried out on the modified failure domain as shown in Eq. (4-15) and Eq. (4-16), respectively.

$$P_F \equiv P\left[\mathbf{x} \in \bar{\Omega}_F\right] \cong \frac{1}{nMCS} \sum_{k=1}^{nMCS} I_{\bar{\Omega}_F}\left(\mathbf{x}^{(k)}\right), \tag{4-15}$$

$$\frac{\partial P_F}{\partial \mu_i} \cong \frac{1}{nMCS} \sum_{k=1}^{nMCS} I_{\bar{\Omega}_F}\left(\mathbf{x}^{(k)}\right) s_{\mu_i}^{(1)}\left(\mathbf{x}^{(k)}; \boldsymbol{\mu}\right). \tag{4-16}$$

where $nMCS$ is the number of MCS samples, and $\mathbf{x}^{(k)}$ is $k^{\text{th}}$ realization of $\mathbf{x}$.

### 4.4.3 Calculation of Sensitivity of Validation Measure

The model validation optimization in Eq. (4-14) requires sensitivity of Hellinger similarity with respect to **v** for its efficient and effective process. Hellinger similarity *H*(**v**) can be expressed by the function of validated simulation output PDF *p*(*g*(**x**;**v**)). Thus, to calculate the sensitivity of *H*(**v**), the sensitivity of the validated simulation output PDF *p*(*g*(**x**;**v**)) with respect to **v** is required. However, we cannot calculate an analytical expression of the validated simulation output PDF; and cannot derive the analytical sensitivity of the validated simulation output PDF. Hence, the sensitivity of Hellinger similarity should be calculated using an approximation method such as finite difference method (FDM). However, a certain amount of numerical error (MCS error) occurs in evaluating *H*(**v**) because MCS is used for the evaluation. Hence, an accurate sensitivity of *H*(**v**) using the conventional FDM cannot be obtained because the MCS error hinders finding the appropriate step size for the FDM. As the central FDM sensitivity of *H*(**v**) with respect to the *j*-th optimization variable $v_j$ is formulated as Eq. (4-17), it contains both truncation and round-off error inherently.

$$\left.\frac{\partial H}{\partial v_j}\right|_{FDM} \approx \frac{H\left(v_j+\Delta v_j\right)-H\left(v_j-\Delta v_j\right)}{2\Delta v_j}, \tag{4-17}$$

Hence, an appropriate finite difference step size $\Delta v_j$ is very difficult to obtain, so the FDM will suffer the numerical error. In this study, the complex variable method (CVM) has been used to improve the accuracy of the sensitivity (Martins, Sturdza & Alonso, 2003). The CVM is based on a Taylor series expansion that takes a perturbation along the imaginary axis as

$$H\left(\mathbf{v}_j+i\Delta\mathbf{v}_j\right)=H\left(\mathbf{v}_j\right)+i\Delta\mathbf{v}_j H'\left(\mathbf{v}_j\right)-\frac{\Delta\mathbf{v}_j^2 H''\left(\mathbf{v}_j\right)}{2!}+\ldots. \tag{4-18}$$

It is observed that the first-order derivative of $H(\mathbf{v})$ with respect to the $j$-th optimization variable $v_j$ can be obtained by isolating the imaginary part of Eq. (4-18) with a truncation error of order $\Delta v_j^2$ as

$$\left.\frac{\partial H}{\partial v_j}\right|_{CVM} = \frac{\operatorname{Im}\left[H\left(v_j + i\Delta v_j\right)\right]}{\Delta v_j} + \mathrm{O}\left(\Delta v_j^2\right), \tag{4-19}$$

where Im[·] is an imaginary part of a complex value. It is noted that the calculation of Eq. (4-19) does not subtract the response values, which avoids the round-off error. As a consequence, the truncation error can be minimized by using a sufficiently small step size. Thus, the sensitivity using CVM is stable and accurate even with small step size. One limitation of CVM is that performance measure analysis should be able to handle a complex variable. However, this limitation can be resolved by using a surrogate model for the performance measure.

# CHAPTER 5

# NUMERICAL TESTS TO DEMONSTRATE CONFIDENCE-BASED MODEL VALIDATION

In this chapter, the capability of the proposed confidence-based model validation is verified. In Section 5.1, a mathematical example for RBDO is described and conventional RBDO optimization without model validation is carried out to find the conventional RBDO optimum design. The simulation model used in this section underestimates the true probability of failure (*i.e.*, the non-conservative simulation model) so that the conventional RBDO optimum design does not satisfy the target probability of failure. Then, at this conventional RBDO optimum design, two numerical tests to verify the confidence-based model validation are performed for active constraints. First, it is demonstrated that the validated simulation model can satisfy the target confidence level. The second test is to check whether the validated simulation model converges to the true model as we use more experimental output data. In Section 5.2, different type of model bias is applied to the same mathematical example. The simulation model tested in this section overestimates the true probability of failure (*i.e.*, a conservative simulation model) so that the conventional RBDO design is already conservative. At this conservative conventional RBDO design, performance of the proposed confidence-based model validation will be discussed.

## 5.1 Numerical Verification of Confidence-Based Model Validation for RBDO

This section introduces a numerical example to demonstrate the effectiveness of the proposed confidence-based model validation method. Numerical tests to verify the confidence-based model validation will be carried out at the conventional RBDO optimum. Thus, in Section 5.1.1, conventional RBDO without model validation is firstly carried out, and the conventional RBDO optimum design is compared with the true RBDO optimum design to check whether it truly satisfies the target reliability in the presence of the model bias. In this section, a non-conservative simulation model is used as explained earlier. In Section 5.1.2, it is demonstrated that the validated simulation model can satisfy the target confidence level. In addition, it is verified that the validated simulation model converges to the true model as we use more experimental output data.

### 5.1.1 Example Description and Conventional RBDO

The following IOWA 2-D mathematical example is used:

$$\begin{aligned}&\text{minimize} \quad \text{Cost}(\mathbf{d}) = -\frac{(d_1+d_2-10)^2}{30} - \frac{(d_1-d_2+10)^2}{120}\\ &\text{subject to} \quad P\left[G_i(\mathbf{x})>0\right] \le P_{F_i}^{Target} = 2.275\%,\ i=1,2,3 \quad ,\\ &\qquad\qquad \mathbf{d}^L \le \mathbf{d} \le \mathbf{d}^U, \quad \mathbf{d}\in\mathbb{R}^2 \text{ and } \mathbf{x}\in\mathbb{R}^2\end{aligned} \tag{5-1}$$

where the biased simulation output $G_i(\mathbf{x})$ can be expressed by $G_i(\mathbf{x}) = G_i^{true}(\mathbf{x}) - B_i(\mathbf{x})$. Here, the unknown true output $G_i^{true}(\mathbf{x})$ is defined as

$$\begin{aligned}&G_1^{true}(\mathbf{x}) = 1 - \frac{x_1^2 x_2}{20}, \quad G_3^{true}(\mathbf{x}) = 1 - \frac{80}{x_1^2+8x_2+5}\\ &G_2^{true}(\mathbf{x}) = -1 + (0.9063x_1+0.4226x_2-6)^2 + (0.9063x_1+0.4226x_2-6)^3\\ &\qquad -0.6(0.9063x_1+0.4226x_2-6)^4 - (-0.4226x_1+0.9063x_2)\end{aligned} \tag{5-2}$$

In general, the biased simulation model obtained in the modeling process could (1) underestimate or (2) overestimate the true probability of failure. The former (non-conservative simulation model) leads to an unreliable RBDO optimum design, while the latter (conservative simulation model) leads to a conservative optimum design. The biased simulation model described in this section is a non-conservative simulation. The case of the conservative simulation model will be shown in Section 5.2. In this section, the unknown model bias $B_i(\mathbf{x})$ is defined as

$$\begin{aligned} &B_1(\mathbf{x}) = \frac{x_1}{25}, \quad B_2(\mathbf{x}) = \frac{x_2}{25} \\ &B_3(\mathbf{x}) = 0.15(-0.4226x_1 + 0.9063x_2)^2 \end{aligned} \quad . \tag{5-3}$$

Two input random variables $x_1$ and $x_2$ follow normal distribution as shown in Table 5.1, and they are correlated to each other with the Clayton copula (Kendall's tau, $\tau = 0.5$). The target probability of failure for all probabilistic constraints is 2.275%.

Table 5.1 Statistical Properties of Input Random Variables

| Input random variable | Distribution type | $\mathbf{d}^L$ | $\mathbf{d}^0$ | $\mathbf{d}^U$ | Standard deviation |
|---|---|---|---|---|---|
| $x_1$ | Normal | 0.0 | 5.0 | 10.0 | 0.3 |
| $x_2$ | Normal | 0.0 | 5.0 | 10.0 | 0.3 |

The limit states of the true output functions, $G^{true}(\mathbf{x}) = 0$, and the biased simulation output functions, $G_i(\mathbf{x}) = 0$, are drawn in Figure 5.1. It can be seen that the feasible domain by the biased model (surrounded by blue lines) is larger than the true feasible domain (surrounded by red lines) because the biased model is non-conservative compared to the true model. In this mathematical example, true output functions are treated as physical experiments, which are unknown.

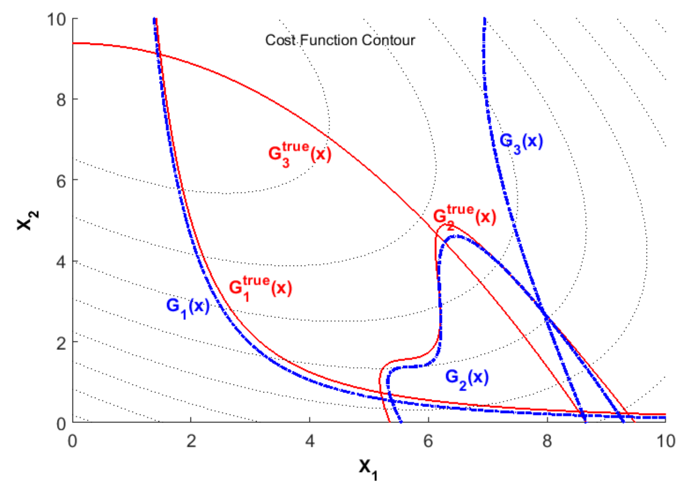


Figure 5.1 Contour of Cost Function and Limit States of Non-Conservative Simulation Output $G(\mathbf{x})$ and True Output $G^{true}(\mathbf{x})$

From the initial design $\mathbf{d}^0 = [5.0, 5.0]$, DDO has been carried out first for computational efficiency, and then the conventional RBDO has been launched at the DDO optimum design. During the conventional RBDO procedure, the model validation has not been carried out, which means no experimental output data is required. At the conventional RBDO optimum design, $\mathbf{d}^1 = [5.1050, 1.3947]$, the estimated probability of failure using the biased simulation model satisfies the target reliability as shown in Table 2. However, those values are not the true probability of failure due to the model bias. To check whether the conventional RBDO optimum design truly satisfies the target probability of failure, reliability analysis using the true output function in Eq. (5-2) has been carried out for active constraints as shown in Table 5.2. The true probability of failure is 5.550% for $G_1$ and 12.700% for $G_2$. Therefore, it can be seen that the conventional RBDO without incorporating model validation underestimates the true probability of failure and does not satisfy the target reliability level.

Table 5.2 True Reliability Analysis at Conventional RBDO Optimum

| Constraint | Estimated PF without model validation | True $P_F$ |
|---|---|---|
| $G_1$ | 2.285% | 5.550% |
| $G_2$ | 2.275% | 12.700% |

### 5.1.2 Repeated Tests of Confidence-Based Model Validation

The objective of the proposed confidence-based model validation is to obtain a conservative RBDO optimum design by evaluating the confidence-based probability of failure at the target confidence level. Therefore, it is necessary to check whether the probability of failure obtained using the validated simulation model truly satisfies the target confidence level. In theory, the confidence level is the probability that the true probability of failure is less than the confidence-based probability of failure. If the confidence level is 95%, the true probability of failure is smaller than its conservative estimation with 95% probability. In other words, the probability of underestimating the true probability of failure is 5%. However, this cannot be numerically demonstrated because the probability of the probability of failure is not known in advance, and therefore the confidence level is not directly interpretable to users. Practically, the 95% confidence level can be interpreted to mean that at least 95% of trials of the model validations with different sets of experimental output data conservatively estimate the true probability of failure.

To demonstrate whether the proposed method can satisfy the target confidence level, confidence-based model validation has been carried out 1000 times with 1000 independently drawn sets of experimental output data for two active constraints, $G_1$ and $G_2$ in Section 5.1.1. Each set contains ten experimental output data. Experimental output data has been randomly collected from the true output PDF. In these 1000 repeated tests, the target confidence level is set to 95%. Figure 5.2 shows the histogram of the confidence-based probabilities of failure obtained from 1000 repeated tests. For constraint $G_1$, among 1000 tests, 94.6% of the confidence-based probabilities of failure are larger than the true probability of failure (True $P_F$ = 5.550%) as shown in Figure 5.2. For constraint $G_2$, 98.1% of the tests evaluate larger confidence-based probabilities of failure than the true probability of failure (True $P_F$ = 12.700%). For both active constraints $G_1$ and $G_2$, the percentage is close to or larger than 95%. This highlights that the validated simulation model obtained using the confidence-based model validation satisfies the target confidence level of 95%. These repeated model validation tests have been carried out on a high-performance computing (HPC) system—Excalibur (30-50 nodes in parallel; each node has 32 cores and 128 GB memory)—at the U.S. Army Research Laboratory (ARL) as the test requires highly extensive computational time. One model validation test with ten experimental output data takes around 5-6 hours using 12 cores and 48 GB memory. Thus, in order to complete 1000 repeated tests, it would take around 250 days, which is not viable. Using the ARL HPC, 1000 repeated tests have been finished in 8 days.

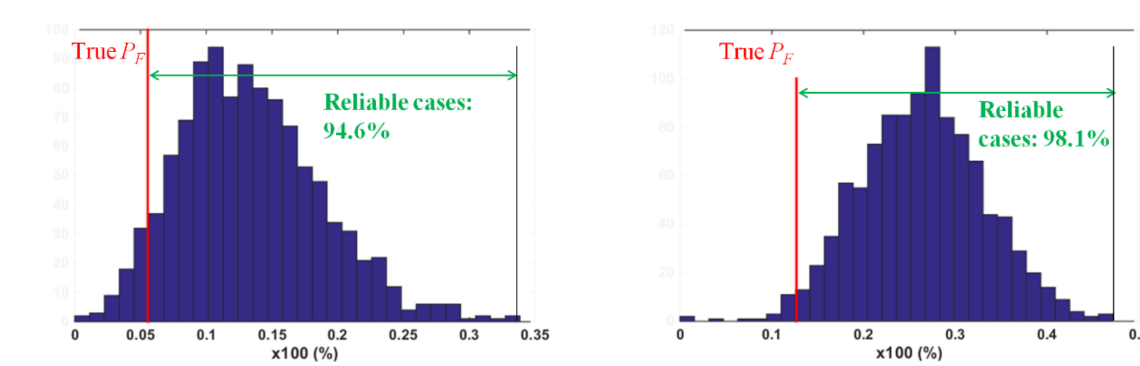


Figure 5.2 Histogram of Confidence-Based Probabilities of Failure for 1000 Tests (Left: Constraint $G_1$, Right: Constraint $G_2$)

In addition, it is important to note that in order to verify whether the proposed method satisfies the target confidence level, it required 1000s of runs with 1000 sets of experimental output data. This could not have been accomplished in a timely manner on desktop workstations. The ability to utilize the DOD High Performance Computing Modernization Program's Excalibur system, a 100,000 core, 3.7 PFLOP, Cray XC 40 at the ARL, was one of the keys to success for this research effort.

### 5.1.3 Convergence Study with the Increasing Number of Experimental Output Data

In this section, the number of experimental output data increases from five to 300. Five different cases (5, 10, 50, 100, and 300 data) are considered to investigate the effect of the size of experimental output data on the confidence-based model validation. For each case, ten different sets of data are randomly drawn from the true output PDF. The target confidence level is set to 95% for all cases. The confidence-based probability of failure for each case with each data set has been calculated; the mean and standard deviation of the confidence-based probability of failure have been obtained for each case. The summary of the convergence study is listed in Table 5.3.

Table 5.3 Convergence Behavior of Validated Simulation Model with Increasing Size of Experimental Output Data

| Data size | Mean of confidence-based probabilities of failure | | Standard deviation of confidence-based probabilities of failure | |
|---|---|---|---|---|
| | $G_1$ | $G_2$ | $G_1$ | $G_2$ |
| 5 | 11.903% | 29.520% | 5.550% | 6.891% |
| 10 | 15.159% | 22.521% | 5.882% | 6.258% |
| 50 | 11.915% | 20.750% | 3.065% | 4.177% |
| 100 | 9.493% | 19.811% | 2.450% | 2.094% |
| 300 | 7.479% | 15.868% | 0.916% | 1.409% |
| True | 5.550% | 12.700% | 0% | 0% |

It can be seen that the standard deviation of the confidence-based probability of failure is rather large for the cases of five and ten data. As the size of experimental output data increases, the standard deviation of the confidence-based probability of failure becomes smaller and converges to zero. In other words, the uncertainty induced by insufficient experimental output data vanishes as the size of experimental output data increases. Furthermore, the mean of confidence-based probability of failure is getting closer to the true probability of failure with increasing size of experimental output data. Therefore, it can be concluded that the validated simulation model obtained using the proposed confidence-based model validation converges to the true model by increasing the number of experimental output data. Moreover, we can see that the proposed method correctly reflects the amount of experimental output data.

## 5.2. Confidence-Based Model Validation Applied to Conservative Simulation Model

The previous section verified that the proposed confidence-based model validation using non-conservative simulation model can provide conservative reliability assessment. This section discusses the performance of the proposed model validation when it is applied to the conservative simulation model that overestimates the true probability of failure so that the conventional RBDO optimum design is already reliable. In this situation, two cases have been tested: (1) a small biased model and (2) a large biased model. For the conservative simulation model, $G(\mathbf{x})$ in Eq. (5-1) needs to be modified by adding positive bias to the true model. Table 5.4 shows conservative simulation output $G(\mathbf{x})$ for both the small and large biased models. In the table below, $G^{true}(\mathbf{x})$ is identical to Eq. (5-2).

Table 5.4 $G(\mathbf{x})$ for Conservative Simulation Model

| Amount of bias | Simulation output $G(\mathbf{x})$ |
|---|---|
| Small biased model | $G_1(\mathbf{x}) = G_1^{true}(\mathbf{x}) + \frac{x_1}{25},\ G_3(\mathbf{x}) = G_3^{true}(\mathbf{x}) + \frac{x_2}{25}$<br>$G_2(\mathbf{x}) = G_2^{true}(\mathbf{x}) + 0.15(-0.4226x_1 + 0.9063x_2)^2$ |
| Large biased model | $G_1(\mathbf{x}) = G_1^{true}(\mathbf{x}) + \frac{x_1}{4.18},\ G_3(\mathbf{x}) = G_3^{true}(\mathbf{x}) + \frac{x_2}{25}$<br>$G_2(\mathbf{x}) = G_2^{true}(\mathbf{x}) + 0.9(-0.4226x_1 + 0.9063x_2)^2$ |

Limit states of the biased simulation and true model for both cases (small and large bias) are graphically shown in Figure 5.3. Differing from the non-conservative simulation model discussed in Section 5.1, the feasible region for the simulation model is shrunken compared to the one for the true model. The expression of the cost function is identical to the one in Eq. (5-1). In the same manner as the conventional RBDO procedure in Section 5.1, conventional RBDO optimums using the conservative simulation model for both cases have been obtained; they are drawn in Figure 5.3.

Table 5.5 shows conventional RBDO optimum designs for both cases. At these conventional RBDO designs, estimated probabilities of failure using the biased simulation model satisfy the target probability of failure, 2.275%. On the other hand, the true probabilities of failure obtained using the true output function in Eq. (5-2) are smaller than the target probability of failure for both cases. Specifically, the large biased model significantly overestimates the true probability of failure as shown in Table 5.5. Accordingly, the conventional RBDO optimum using a large biased model provides a more conservative design than the one using a small biased model. It can be noted that the cost value at conventional RBDO optimum for both cases ($-1.8163$ for the small biased model and $-1.5892$ for the large biased model) have been increased compared to the true optimum cost value ($-1.8848$), as shown in Figure 5.3.

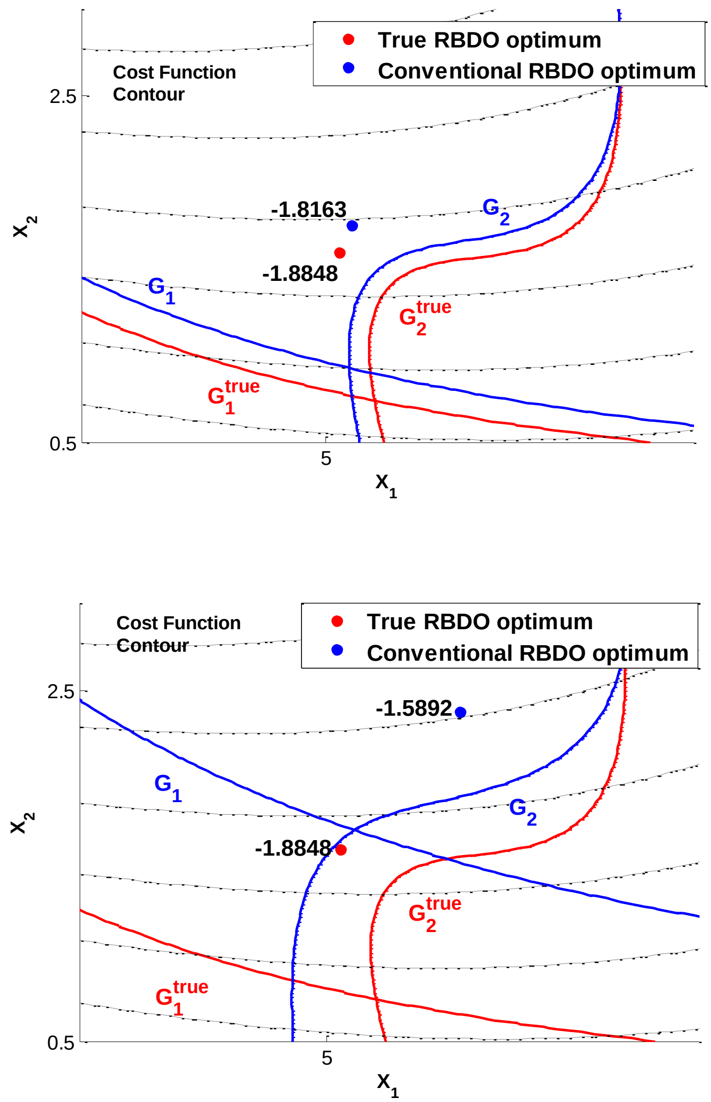


Figure 5.3 Contour of Cost function and Limit States for Conservative Simulation Output $G(\mathbf{x})$ and True Output $G(\mathbf{x})$ (Top: Small Biased Model, Bottom: Large Biased Model)

Table 5.5 Summary of Conventional RBDO for Conservative Simulation Model

| Amount of bias | Conventional RBDO optimum | | Estimated $P_F$ without model validation | | True $P_F$ | |
|---|---|---|---|---|---|---|
| | $d_1$ | $d_2$ | $G_1$ | $G_2$ | $G_1$ | $G_2$ |
| Small biased model | 5.1035 | 1.7491 | 2.277% | 2.275% | 0.803% | 0.571% |
| Large biased model | 5.5377 | 2.3745 | 2.279% | 2.282% | 0.001% | 1.376% |

At the conventional RBDO design listed in Table 5.5, the proposed confidence-based model validation is carried out to investigate how the proposed method can improve the original simulation model for different amounts of bias. In addition, it is questionable whether the proposed method can provide a less conservative simulation model when conservatively biased simulation model is given. The proposed model validation has been carried out for both active constraint $G_1$ and $G_2$ with different sizes of experimental output data (5 and 50) that are randomly drawn from the true output function in Eq. (5.2). The target confidence level is set to 95% for all tests. First, we would like to see the results for the small biased model. Figure 5.4 depicts the summary of output PDFs for the small biased model. It can be seen that the simulation output PDFs are located a little bit to the right side of the true output PDF which means more conservative simulation output PDFs than the true output PDF. After applying the proposed method, it is found that the confidence-based target output PDFs are located further to the right side of the simulation output PDF and are wider than the simulation output PDF. This indicates that the model validation optimization will force the validated simulation model to move away from the true model.

Table 5.6 shows the comparison between the result of the true reliability analysis and the confidence-based probability of failure using the proposed method for the small biased case. It can be seen that the validated simulation model overestimates more than the original simulation model so that it becomes a more conservative model. Specifically, the validated model with five experimental output data estimates a much larger probability of failure (*i.e.*, is more conservative) than the one with 50 experimental output data, as shown in Table 5.6. It is anticipated that the validated model using the proposed method would be less conservative than the original simulation model when enough experimental output data is available.

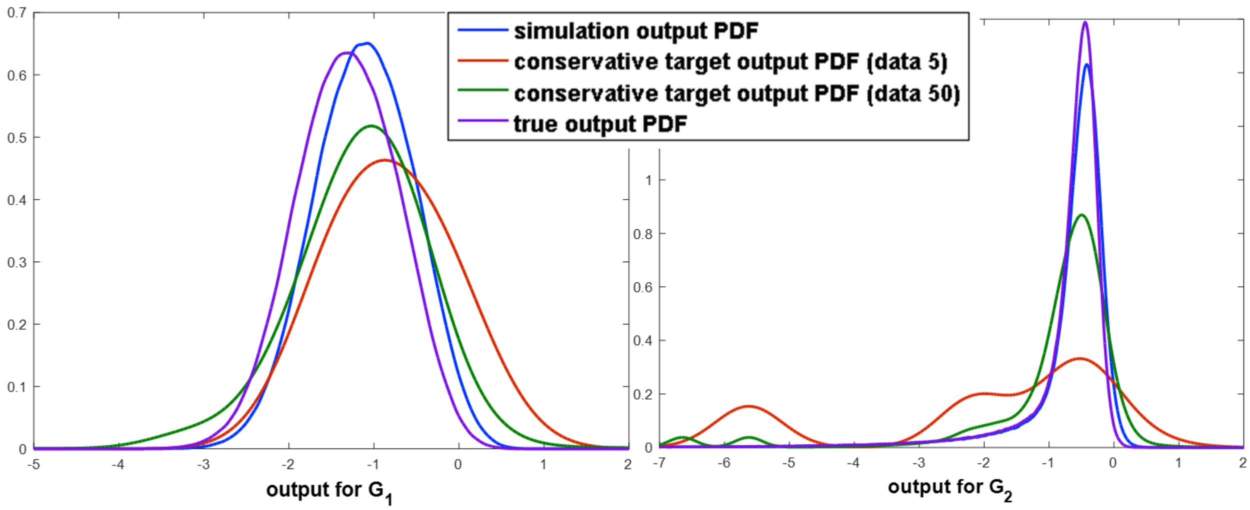


Figure 5.4 Illustration of Confidence-Based Target Output PDF for Small Biased Model

Table 5.6 Confidence-Based Probability of Failure using Validated Simulation Model for Small Biased Case

| | $P_F$ | |
|---|---|---|
| | For $G_1$ | For $G_2$ |
| Biased simulation model | 2.277% | 2.275% |
| Validated simulation model (data 5) | 15.490% | 8.240% |
| Validated simulation model (data 50) | 6.180% | 4.400% |
| True model | 0.803% | 0.571% |

Next, as for the large biased model, the simulation output PDF is significantly biased to the right side of the true output PDF as shown in Figure 5.5. In this situation, the proposed model validation has been carried out at conventional RBDO design, [5.5377, 2.3745]. The target confidence level is 95%. Two cases have been tested assuming (1) five data and (2) 50 data. After carrying out the proposed method, the confidence-based target output PDFs have shifted to the left side and are closer to the true output PDF. Therefore, the model validation optimization will provide a more accurate validated simulation model than the original simulation model. Table 5.7 shows the confidence-based probability of failure using the validated simulation model for the large biased case. It can be clearly seen that the confidence-based probability of failure obtained using the validated simulation model is smaller than the probability of failure of the original simulation model but yet is larger than the true probability of failure. In other words, the validated simulation model could relieve overestimation of the true probability of failure from the original simulation model, which means that the validated simulation model becomes less conservative than the original simulation model and is still reliable.

As discussed above, when the model is significantly biased, the proposed method provides a less conservatively validated simulation model and is still reliable. On the other hand, if the original simulation model is very accurate (*i.e.*, small bias problem), the proposed method can produce an even more conservatively validated simulation model to compensate for the uncertainty induced by insufficient test data. It is questionable whether the model validation is indeed necessary because the proposed model validation did not perform in a desirable way by making a more conservative model for the small biased model. However, unless a sufficient number of experimental tests is available, a user may not be aware of whether the biased model underestimates or overestimates the true probability of failure. Furthermore, it is not easy to determine how much the simulation model is biased in the presence of insufficient data. Thus, the proposed method helps designers build confidence in the design regardless of the type and significance of the bias in the simulation model. Given lack of test data, in order to provide designer confidence in the simulation model, the proposed model validation is essential.

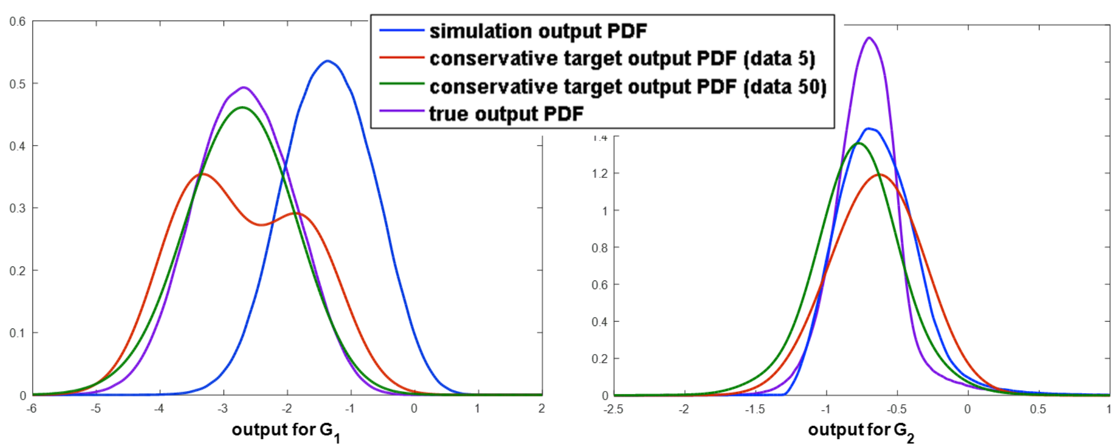


Figure 5.5 Illustration of Confidence-Based Target Output PDF for Large Biased Model

Table 5.7 Confidence-Based Probability of Failure using Validated Simulation Model for Large Biased Case

| | $P_F$ | |
|---|---|---|
| | For $G_1$ | For $G_2$ |
| Biased simulation model | 2.279% | 2.282% |
| Validated simulation model (data 5) | 0.296% | 1.755% |
| Validated simulation model (data 50) | 0.148% | 1.264% |
| True model | 0.001% | 1.376% |

# CHAPTER 6

# PROPOSED RELIABILITY-BASED DESIGN OPTIMIZATION USING CONFIDENCE-BASED MODEL VALIDATION

Conventional RBDO methods have been developed to obtain a reliable design by accounting for only the inherent input variabilities resulting in output variabilities. These methods typically use simulation models to connect input and output variabilities. Thus, the simulation model should be accurate for obtaining accurate RBDO optimum design. For this purpose, the simulation model used for RBDO has to be validated using experimental output data and integrated with the RBDO process. However, we do not have a very large number of experimental output data for the validation. Furthermore, full-scale product testing cannot be carried out at many design configurations. In that sense, the RBDO process should account for the uncertainty of the simulation model for a reliable optimum design. Therefore, this chapter proposes a new RBDO method that incorporates the confidence-based model validation explained in Chapter 4. The proposed RBDO method accounts for the uncertainty induced by insufficient experimental output data as well as the inherent variabilities so that it provides a conservative RBDO optimum design at the target confidence level even for the biased simulation model. The final RBDO optimum design provides the designer confidence that the designed product will satisfy the target probability of failure with a certain probability level – the target confidence level. Section 6.1 explains the formulation of the proposed RBDO using confidence-based model validation compared with the conventional RBDO. Meanwhile, the challenge occurs in the process of RBDO with model validation. The RBDO with model validation may have a convergence issue because the feasible domain changes as the design moves (*i.e.*, a moving-target problem), which will be discussed in Section 6.2. In Section 6.3, a practical RBDO using confidence-based model validation is proposed to resolve an unpredictable moving-target problem for an insufficient experimental output data. In addition, the practical RBDO is numerically demonstrated using a mathematical example.

## 6.1. Formulation of Proposed RBDO using Confidence-Based Model Validation

The mathematical formulation of the RBDO using confidence-based model validation is stated as

$$\begin{aligned} &\text{minimize} \quad \text{Cost}(\mathbf{d}) \\ &\text{subject to} \quad P\left[G_i(\mathbf{x}) + B_i\left(\mathbf{x}; CL^{Target}\right) > 0\right] \le P_{F_i}^{Target},\ i = 1, \cdots, NC \ , \\ &\qquad\qquad \mathbf{d}^L \le \mathbf{d} \le \mathbf{d}^U, \quad \mathbf{d} \in \mathbb{R}^{NDV} \text{ and } \mathbf{x} \in \mathbb{R}^{NRV} \end{aligned} \tag{6-1}$$

where $\mathbf{d} = \mu(\mathbf{x})$ is the design variable vector, which is the mean value of the input random variable vector $\mathbf{x}$; $G_i(\mathbf{x})$ is the biased simulation output for the $i^{th}$ probabilistic constraint; $B_i(\mathbf{x};\ CL^{Target})$ is the confidence-based model bias at the target confidence level for the $i^{th}$ probabilistic constraint; and *NC*, *NDV*, and *NRV* are the number of probabilistic constraints, design variables, and input random variables, respectively. It is noted that the confidence-based model bias is an additional term that the conventional RBDO does not account for. The confidence-based model bias at the given design **d** can be modeled using any flexible distribution. In this study, unknown bias is assumed to follow normal distribution for simplicity. However, in real application other than model bias due to measurement error, bias may not follow normal distribution at a given design. However, it is impossible to obtain the accurate distribution type in the presence of a limited number of test data. In the proposed method, by introducing the additional target value of a target confidence level, we can evaluate the probability of failure at a target confidence level for any distribution type of model bias. For active constraints, the confidence-based model bias correction can be performed in parallel using parallel computing system.

## 6.2. Challenge in RBDO Process with Model Validation

### 6.2.1 Moving-Target Problem

If the true model, the real physics, were available, true limit states for all performance measures could be obtained. Accordingly, the RBDO using the model validation could produce a correct optimum design without any convergence issue by providing the exact probability of failure and design sensitivity with respect to design variables as shown in Figure 6.1. In addition, in Figure 6.1, black dots indicates the trajectory of the true design iteration. However, true limit states are not available when the simulation model involves model bias in real applications. Instead of true limit states, we would have the limit states obtained using a validated simulation model in RBDO using model validation as shown in the top figure of Figure 6.2.

As we have a biased simulation model, which is inherently not perfect, it is noted that the validated simulation model is not the true model, but that it is the best approximation of the true model based on the information (experimental output data) we have at the given design point. Thus, even if we have a very large number of experimental output data, the validated simulation model is not the same as the true model. Thus, the validated simulation model is not able to identify the effect of design change on model bias, and the model bias correction is different at different design points. Hence, during the RBDO process, the feasible domain (solution space) obtained using the validated simulation model changes as the design moves. As a consequence, during the RBDO process, the solution space (feasible domain) obtained using the validated simulation model changes simultaneously when model bias correction is updated as the design moves. Figure 6.2 illustrates the change of the feasible domain as the design moves during the optimization process, and the blue dots indicate the design iteration history in the RBDO process using model validation, which are not the true ones. As a result, the optimum point moves as the feasible domain changes during the RBDO process. Thus, carrying out the model validation during RBDO make it a moving-target problem. Therefore, convergence can become a critical issue and the optimum solution becomes difficult to find.

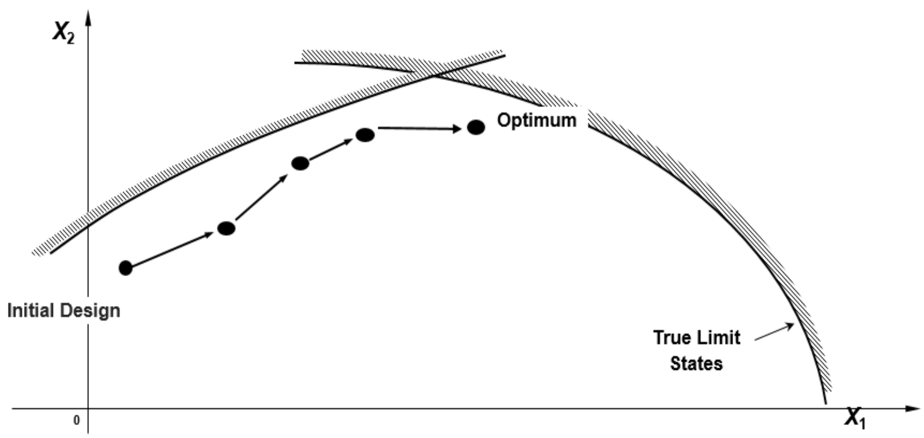


Figure 6.1 True Design Iteration History without Convergence Issue

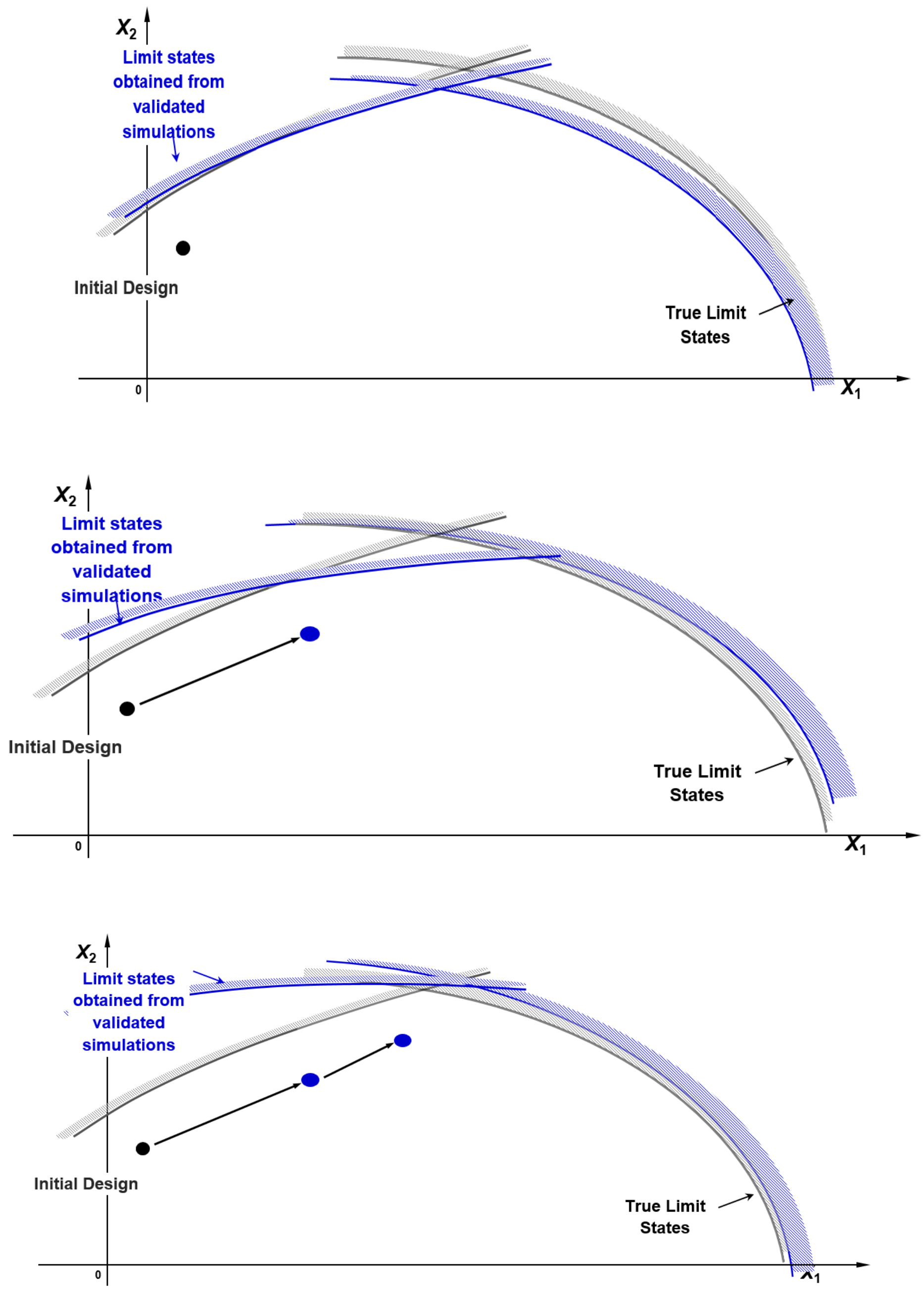


Figure 6.2 Illustration of the Feasible Domain Obtained using the Validated Simulation Model That is Changed as a Design Moves in the RBDO Process using Model Validation.

6.2.2 Problem-Solving Strategy

We address the question: "Is the moving-target problem solvable when the uncertainty induced by the number of experimental output data is negligible?" We want to check whether enough experimental output data will allow us to solve the moving-target problem. The accurate target output PDF, which is very close to the true output PDF, can be obtained with enough experimental output data. If so, the Bayesian analysis in Section 4.3 is not necessary. Then the model validation optimization in Section 4.4 can be carried out using the accurate target output PDF $q^{accurate}(g)$, not the confidence-based target output PDF $q(g;CL^{Target})$ in Eq. (4-14). Furthermore, in Eq. (4-14), $p_F^{coservative}(CL^{Target})$ is replaced with the accurate probability of failure $p_F^{accurate}$. In this case, we have 100% confidence in estimating the true probability of failure as we can evaluate the exact probability of failure. Still, the shape of the validated simulation output PDF may not be the same as that of the true output PDF. As a result, the optimized model bias obtained from the model validation optimization may not be close to true, and the stochastic design sensitivity may not be exactly calculated.

In this section, two algorithms have been investigated: (1) the model validation is carried out at every design iteration and line search using the accurate target output PDF, and (2) the model validation is performed at the initial design using the accurate target output PDF. Then, RBDO is carried out using the same validated simulation model (fixed model bias correction) until the optimization converges. At the RBDO optimum, the simulation model is validated again (*i.e.*, model bias correction is updated), and the probabilistic constraints are re-checked using the newly validated model. This process is repeated until the re-checked probabilistic constraint satisfies the target probability of failure. Thus, multiple RBDO processes could be carried out until all constraints are satisfied. The tested mathematical example is the same as the one described in Section 5.1.1. For efficiency of design optimization, the initial designs of all tests have been launched at the conventional RBDO optimum obtained in Section 5.1.1. As a benchmark, the detailed conventional RBDO history using the true output function in Eq. (5-2) is listed in Table 6.1. Table 6.2 shows the RBDO results using both algorithms 1 and 2. As shown in Table 6.2, it is noted that both algorithms 1 and 2 find the true RBDO optimum. This demonstrates that the moving-target problem can be solved if there is no uncertainty introduced by the limited number of experimental output data. However, algorithm 1 requires a large number of line searches (41), whereas the RBDO using the true output function can find the optimum after 11 line searches even though the total number of design iterations (6) is the same when algorithm 1 is used, as shown in Table 6.2. This indicates that algorithm 1 carries out model validations at 41 different design configurations. In addition, it can be found that algorithm 2 is a more effective process because it requires model validations at only six different design points. A detailed design and constraint history using algorithm 2 is listed in Table 6.3. In Table 6.3, $1^{st}$ indicates the $1^{st}$ intermediate RBDO optimum design, and the $0^{th}$ intermediate RBDO optimum design is the conventional RBDO optimum. Listed constraint values in Table 6.3 are calculated using the newly validated simulation model incorporating experimental output data collected at the intermediate RBDO optimums. It is noted that experimental output data is collected only at intermediate RBDO optimums. It can be seen that cost value in the history of RBDO using model validation when algorithm 2 is used does not decrease monotonically due to the moving target. Yet, in this section, it can be seen that the moving target problem can be solved if there is enough number of data using both algorithms 1 and 2. In addition, it is shown that the algorithm 2 is more efficient than algorithm 1. Hence, algorithm 2 will be more elaborated for RBDO with limited number of test data case in following sections.

Table 6.1 Design and Constraint History using RBDO with True Function as a Benchmark

| Iter. | Cost | Design | | Constraint | | |
|---|---|---|---|---|---|---|
| | | $d_1$ | $d_2$ | $G_1$ | $G_2$ | $G_3$ |
| 0,1* | −1.9748 | 5.1050 | 1.3947 | 1.4694 | 4.5826 | −1.0000 |
| 1,1** | −1.9140 | 5.0802 | 1.5280 | 0.3353 | 1.0411 | −1.0000 |
| 2,1 | −1.8897 | 5.0662 | 1.5819 | 0.0351 | 0.1748 | −1.0000 |
| 3,1 | −1.8850 | 5.0578 | 1.5924 | 0.0065 | 0.0140 | −1.0000 |
| 4,1 | −1.8844 | 5.0575 | 1.5937 | −0.0043 | 0.0043 | −1.0000 |
| 4,2 | −1.8846 | 5.0564 | 1.5934 | 0.0118 | 0.0098 | −1.0000 |
| 4,3 | −1.8838 | 5.0574 | 1.5951 | −0.0064 | −0.0109 | −1.0000 |
| 4,4 | −1.8841 | 5.0572 | 1.5943 | 0.0040 | 0.0038 | −1.0000 |
| 5,1 | −1.8843 | 5.0572 | 1.5940 | −0.0070 | −0.0053 | −1.0000 |
| 6,1 | −1.8848 | 5.0566 | 1.5930 | 0.0007 | −0.0025 | −1.0000 |
| 6,2 | −1.8848 | 5.0569 | 1.5929 | 0.0048 | 0.0058 | −1.0000 |
| 6,3 | −1.8848 | 5.0566 | 1.5930 | 0.0007 | −0.0025 | −1.0000 |
| Opt*** | −1.8848 | 5.0566 | 1.5930 | 0.0007 | −0.0025 | −1.0000 |

* 0,1 is initial design, which is the conventional RBDO optimum design.

** 1,1 means 1$^{st}$ iteration and 1$^{st}$ line search.

*** Opt means optimum.

Table 6.2 Summary of the Result for RBDO using Model Validation Assuming Enough Experimental Output Data

| Case | Cost | Design | | # of design iterations | # of line searches | # of RBDO process | # of validated design points |
|---|---|---|---|---|---|---|---|
| | | $d_1$ | $d_2$ | | | | |
| Algorithm1 | −1.8852 | 5.0570 | 1.5979 | 6 | 41 | 1 | 41 |
| Algorithm2 | −1.8848 | 5.0563 | 1.5928 | - | - | 5 | 6 |
| True | −1.8848 | 5.0566 | 1.5930 | 6 | 11 | 1 | - |

Table 6.3 Design and Constraint History of RBDO using Model Validation for Enough Experimental Output Data (Algorithm 2 is Used)

| Intermediate RBDO optimum | Cost | Design | | Normalized $P_F$ after model validation | | |
|---|---|---|---|---|---|---|
| | | $d_1$ | $d_2$ | $G_1$ | $G_2$ | $G_3$ |
| 0th | −1.9748 | 5.1050 | 1.3947 | 1.4694 | 4.5826 | −1.0000 |
| 1st | −1.8616 | 5.1142 | 1.6457 | −0.3545 | −0.1372 | −1.0000 |
| 2nd | −1.8956 | 5.0559 | 1.5689 | 0.1361 | 0.2309 | −1.0000 |
| 3rd | −1.8850 | 5.0578 | 1.5924 | 0.0065 | 0.0140 | −1.0000 |
| 4th | −1.8801 | 5.0544 | 1.6033 | −0.0513 | −0.1133 | −1.0000 |
| 5th | −1.8848 | 5.0563 | 1.5928 | −0.0024 | −0.0111 | −1.0000 |
| Opt | −1.8848 | 5.0563 | 1.5928 | −0.0024 | −0.0111 | −1.0000 |

## 6.3. Practical RBDO Procedure using Confidence-Based Model Validation for Insufficient Experimental Output Data

Proceeding with RBDO using confidence-model validation (or any model validation) demands experimental output data at various design configurations or within the whole design space. In addition, full-scale product testing cannot be carried out many times at the given design. The greater challenge is that the moving target becomes a more critical issue when insufficient experimental output data is available. Thus, this section proposes a practical RBDO procedure using confidence-based model validation for insufficient experimental output data. In Section 6.3.1, a detailed algorithm for the proposed practical procedure of RBDO using confidence-based model validation is described. In Section 6.3.2, it is demonstrated that the proposed practical RBDO can provide conservative and reliable optimum design with target confidence even for few experimental output data. Furthermore, it is found that the proposed practical RBDO is cost-effective as it requires experimental output data at only a few design configurations.

### 6.3.1. Practical Procedure for RBDO using Confidence-Based Model Validation

In real applications, the moving-target problem is very difficult to solve because the uncertainty due to the insufficient experimental output data changes the feasible domain significantly as the design changes. Thus, a practical RBDO procedure is proposed to resolve the unpredictable and substantial moving-target problem for insufficient experimental output data (Moon et al., 2016; Moon et al., 2017). Furthermore, for an efficient optimization process with minimum testing, DDO and RBDO are sequentially carried out first without confidence-based model validation. The practical procedure is similar to algorithm 2 introduced in Section 6.2.2. Details of the practical RBDO process using confidence-based model validation are as follows.

Step 1: For an efficient optimization process with minimum testing, DDO and RBDO are sequentially carried out first without confidence-based model validation. Based on a reasonably accurate but biased simulation model, we should be able to obtain a conventional RBDO optimum that is not far away from the true RBDO optimum design.
Step 2: At the conventional RBDO optimum, a confidence-based model validation incorporating experimental output data is carried out to obtain the validated simulation model (validated simulation output PDF) with confidence-based model bias correction at the target confidence level $CL^{Target}$.
Step 3: RBDO iterations are carried out from the previous optimum design. During the RBDO process, previously validated simulation model will be used until the convergence of the RBDO. In other words, during the optimization process, no experimental output data is required. In that way, the moving-target issue can be avoided in the middle of the optimization procedure.
Step 4: At the intermediate RBDO optimum design after the optimization converges, the confidence-based model validation is carried out again to obtain the newly validated simulation model by updating the confidence-based model bias and collecting the experimental output data. Then, the confidence-based probability of failure is re-calculated to re-check whether the design satisfies the target probability of failure according to the newly validated simulation model. If the confidence-based probabilities of failure using the newly validated simulation model are less than the target probability of failure, the current design is accepted as a final RBDO design $\mathbf{x}_{opt}^{model\ bias}$. Otherwise, we go to step 3, and additional RBDO processes are repeated from the current intermediate RBDO optimum design. Figure 6.3 depicts the flow chart of the proposed

RBDO scheme using confidence-based model validation for an insufficient experimental output data.

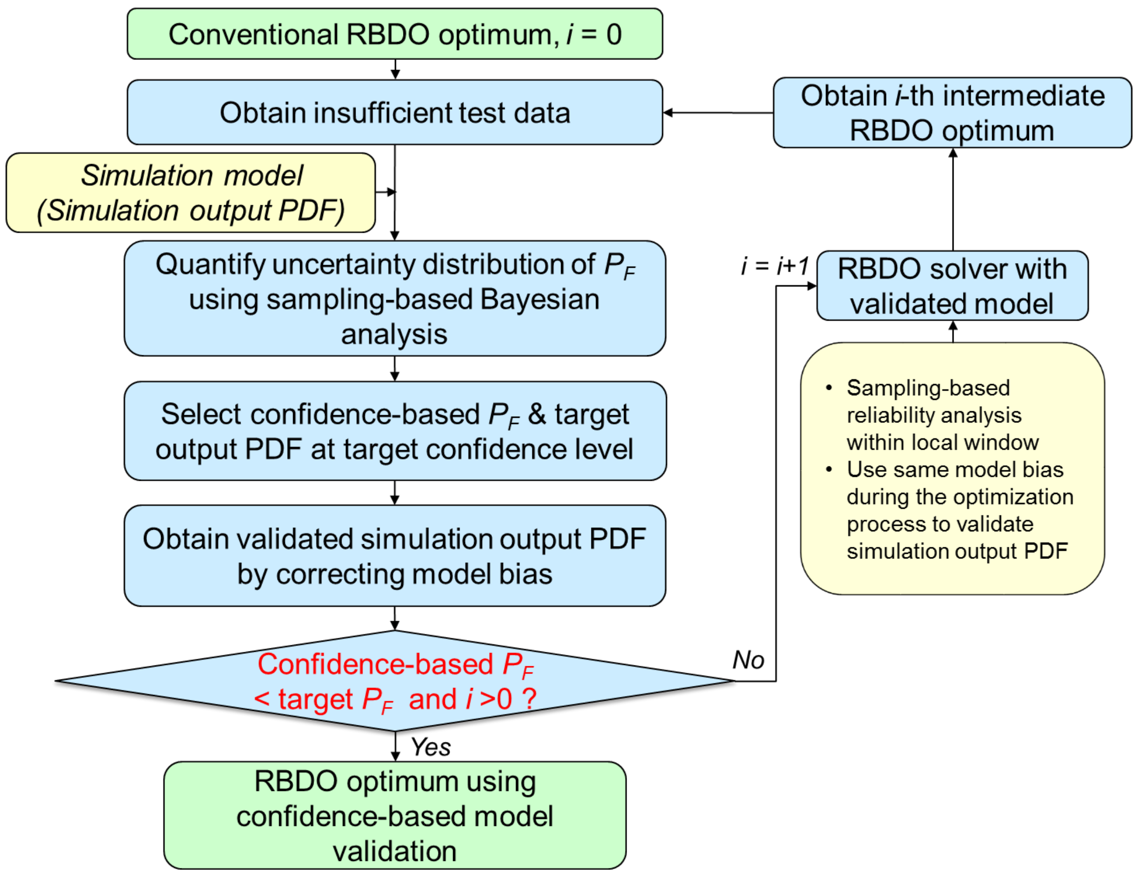


Figure 6.3 Flowchart of Proposed RBDO Scheme using Confidence-Based Model Validation for Insufficient Experimental Output Data

The proposed practical RBDO procedure using confidence-based model validation has two unique features. First, the proposed RBDO provides a conservative design even in the presence of uncertainty due to insufficient experimental output data. Thus, the designer can have confidence in the reliability of the product, which is produced using the conservative design. The confidence originates from the fact that the probability that probability of failure at an RBDO optimum less than the target probability of failure is larger than the target confidence level $CL^{Target}$ as

$$CL^{Target} < P\left[P\left[G\left(\mathbf{x}_{opt}^{model\,bias}\right)+B\left(\mathbf{x}_{opt}^{model\,bias}\right)>0\right]<P_F^{Target}\right]. \tag{6-2}$$

Secondly, the proposed RBDO algorithm is cost-effective in terms of experimental tests. It is anticipated that the conventional RBDO optimum without model validation is not far from the conservative RBDO optimum if the biased simulation model is reasonably accurate. Then, only a few RBDO processes are needed to get to the final RBDO design from the conventional RBDO optimum. That means it only requires experimental output data at a few design configurations (only RBDO optimums). Moreover, as the procedure based on the algorithm 2 in Section 6.2.2, the procedure does not require many confidence-based model validations which means experimental output data is required at a few design configurations. This bolsters the cost-effectiveness of the proposed RBDO algorithm. However, if the quality of the biased simulation model is rather poor to begin with, the conventional RBDO optimum could be far from the conservative optimum. The proposed method may require a large number of validated design points to obtain the conservative optimum design.

### 6.3.2. Numerical Tests

As shown in Section 5, two types of biased simulation models (non-conservative and conservative simulation models) have been tested to carry out confidence-based model validation at the conventional RBDO optimum. In this section, the proposed RBDO procedure using confidence-based model validation in Eq. (6-1) has been applied to two types of biased simulation models. The detailed mathematical description for the non-conservative simulation model and the true model are expressed in Eq. (5-3) and Eq. (5-2), respectively, and the conservative simulation models for the small biased and large biased models are listed in Table 5.4. For all results obtained in this section, the target confidence level is set to 95%. For each biased model, two different cases, (1) five data and (2) ten data, have been tested to represent the insufficient experimental output data. Experimental output data at the conventional RBDO optimum design and the intermediate RBDO optimum designs has been randomly obtained from the true output PDF to calculate the confidence-based probability of failure.

First, the RBDO result for non-conservative simulation will be discussed. Table 6.4 and Table 6.5 show the intermediate RBDO optimum history and the corresponding confidence-based probabilities of failure for the five-data and ten-data cases, respectively. Table 6.6 and Table 6.7 show the randomly collected experimental output data at RBDO optimums for the five-data and ten-data cases, respectively. Due to the moving target, the cost value and confidence-based probability of failure at certain intermediate RBDO optimum designs do not increase (or decrease) monotonically, as shown in both Table 6.6 and Table 6.7. As shown in Table 6.8, practical RBDO optimum designs for both cases are obtained using only a few validated design points where the experimental output data are collected. The five-data case requires five RBDO processes and six validated design points. In the ten-data case, two RBDO processes are carried out, and the experimental output data is provided at three design configurations. As mentioned previously, the practical RBDO procedure saves experimental cost by minimizing the number of validated design points.

Table 6.4 Practical RBDO Optimization History using Non-Conservative Simulation Model for Five-Data Case

| # of RBDO process | Intermediate RBDO optimum | | Cost | Confidence-based $P_F$ using validated simulation model | | |
|---|---|---|---|---|---|---|
| | $d_1$ | $d_2$ | | $G_1$ | $G_2$ | $G_3$ |
| 0th | 5.1050 | 1.3947 | −1.9748 | 26.654% | 13.540% | 0% |
| 1st | 5.4079 | 1.8797 | −1.7703 | 3.350% | 0.466% | 0% |
| 2nd | 5.5862 | 1.8592 | −1.7878 | 0.119% | 5.470% | 0% |
| 3rd | 5.1375 | 1.6045 | −1.8800 | 7.162% | 10.202% | 0% |
| 4th | 5.2025 | 1.8216 | −1.7873 | 2.150% | 5.223% | 0% |
| 5th | 5.1249 | 1.8534 | −1.7721 | 2.239% | 2.077% | 0% |

Table 6.5 Practical RBDO Optimization History using Non-Conservative Simulation Model for Ten-Data Case

| # of RBDO process | Intermediate RBDO optimum | | Cost | Confidence-based $P_F$ using validated simulation model | | |
|---|---|---|---|---|---|---|
| | $d_1$ | $d_2$ | | $G_1$ | $G_2$ | $G_3$ |
| 0th | 5.1050 | 1.3947 | −1.9748 | 5.136% | 26.833% | 0% |
| 1st | 4.9811 | 1.7082 | −1.8335 | 8.124% | 12.393% | 0% |
| 2nd | 5.0099 | 1.9914 | −1.7121 | 1.160% | 0.898% | 0% |

Table 6.6 Randomly Collected Experimental Output Data for Non-Conservative Simulation Model (Five-Data Case)

| Intermediate RBDO optimum | Five experimental output data | |
|---|---|---|
| | $G_1$ | $G_2$ |
| 0th | [−0.0378, −1.4292, −0.2142, −0.9064, −0.1140] | [−2.4262, −0.4494, −0.7760, −0.0516, −2.9991] |
| 1st | [−1.6184, −2.5108, −2.6096, −1.9655, −0.9441] | [−0.4178, −0.5234, −0.7826, −0.5980, −0.4897] |
| 2nd | [−1.9026, −2.6884, −2.6726, −2.6048, −2.2321] | [−0.2748, −0.2889, −0.3653, −0.1817, −0.4441] |
| 3rd | [−0.5890, −1.6790, −0.6981, −1.7457, −0.6907] | [−0.8380, −0.2661, −0.6090, −0.2346, −1.0509] |
| 4th | [−1.3403, −2.2584, −1.6402, −1.0239, −1.9037] | [−0.2902, −0.6271, −0.2787, −0.6033, −0.7414] |
| 5th | [−2.4120, −1.0624, −2.0035, −2.3934, −1.8683] | [−0.5632, −0.3905, −0.5301, −0.8323, −0.6129] |

Table 6.7 Randomly Collected Experimental Output Data for Non-Conservative Simulation Model (Ten-Data Case)

| Intermediate RBDO optimum | Ten experimental output data | |
|---|---|---|
| | $G_1$ | $G_2$ |
| 0th | [−1.1510, −0.5821, −2.1442, −1.2520, −0.5976, −1.3227, −1.1813, −1.9981, −0.6438, −1.5306] | [−0.1300, 0.0863, −0.3453, −0.4378, −0.4961, −0.5410, −0.0721, −0.6692, −0.0784, −0.5094] |
| 1st | [−1.3102, −0.4346, −1.6835, −1.9432, −1.5170, −0.1140, −0.8767, −1.6396, −1.3167, −1.6773] | [−0.3495, −2.1485, −0.6986, −0.5947, −0.7736, −5.0950, −0.9484, −0.2957, −0.3984, −0.5473] |
| 2nd | [−1.3605, −2.4659, −1.8541, −1.2404, −1.0382, −1.7313, −2.5237, −1.1171, −1.4300, −1.4960] | [−0.7843, −0.6619, −0.7204, −0.5002, −1.1533, −0.5082, −0.7389, −0.8567, −0.7513, −0.7675] |

Table 6.8 shows the confidence-based probability of failure and confidence level at the practical RBDO optimum using confidence-based model validation for the two data cases. The confidence level at both practical RBDO optimum designs can be calculated using the CDF value of the probability of failure at the target probability of failure (see Section 4.3.3). The confidence level at both practical RBDO optimum designs is always larger than the target confidence level of 95% because the optimization process is terminated once the confidence-based probability of failure is less than the target probability of failure, 2.275%, as demonstrated in Eq. (6-2).

Table 6.8 Summary of Practical RBDO Optimum using Confidence-Based Model Validation for Insufficient Experimental Output Data

| Case | # of RBDO processes | # of validated design points | Confidence-based $P_F$ | | Confidence level | |
|---|---|---|---|---|---|---|
| | | | $G_1$ | $G_2$ | $G_1$ | $G_2$ |
| 5 data | 5 | 6 | 2.239% | 2.077% | 95.2% | 95.6% |
| 10 data | 2 | 3 | 1.160% | 0.898% | 98.9% | 99.7% |

Table 6.9 RBDO Optimum Summary and True Reliability Analysis at Practical RBDO Optimum Designs for Non-Conservative Simulation Model

| | Optimum design | | Cost | True $P_F$ using true output function | |
|---|---|---|---|---|---|
| | $G_1$ | $G_2$ | | $G_1$ | $G_2$ |
| Conventional RBDO | 5.1050 | 1.3947 | −1.9748 | 5.550% | 12.700% |
| Proposed RBDO (5 data) | 5.1249 | 1.8534 | −1.7721 | 0.395% | 0.174% |
| Proposed RBDO (10 data) | 5.0099 | 1.9914 | −1.7121 | 0.234% | 0.011% |
| True RBDO | 5.0566 | 1.5930 | −1.8848 | 2.277% | 2.269% |

It is found that, at both practical RBDO optimum designs, the confidence-based probability of failure satisfies the target probability of failure of 2.275%. To ensure that the RBDO optimum designs indeed satisfy the target probability of failure, reliability analysis using the true output function has been carried out at practical RBDO optimum designs for both cases. As shown in Table 6.9, at the practical RBDO optimum designs, the true probability of failure is less than the target probability of failure while the conventional RBDO without model validation violates the target value. Therefore, the obtained practical RBDO optimum designs using the proposed method are truly conservative and reliable. However, it can be noted that the cost values at the practical RBDO optimum designs have been increased to −1.7721 (five-data case) and −1.7121 (ten-data case) from the one at the conventional RBDO optimum (−1.9748). This indicates that, to achieve the conservative design with confidence in compensation for the uncertainty due to insufficient test data, the cost values will be increased.

The RBDO optimums using confidence-based model validation for the 95% target confidence level are graphically illustrated in Figure 6.4. The proposed method forces the practical RBDO optimum design to move upward in the direction of increasing cost while achieving more conservativeness of design. On the other hand, the conventional RBDO optimum is located closer to the true limit state function, and thus it eventually violates the target probability of failure. Throughout this example, it is shown that the proposed confidence-based model validation and the practical RBDO procedure can successfully find a conservative RBDO optimum design that satisfies the target probability of failure even in the presence of limited experimental output data.

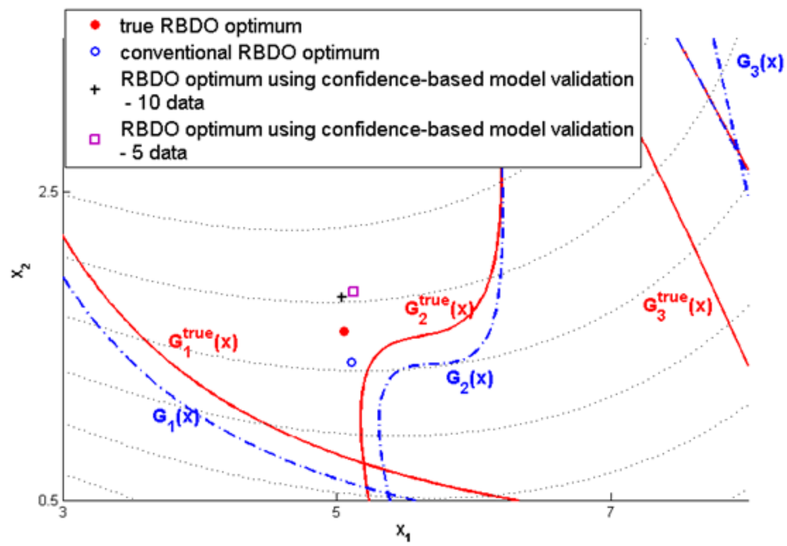


Figure 6.4 Plot of Practical RBDO Optimum using Confidence-Based Model Validation for Non-Conservative Simulation Model

We also have investigated RBDO results when the biased simulation model is conservative so that the conventional RBDO design without model validation is reliable readily. As mentioned at the beginning of this section, for a conservative simulation model, two cases have been tested: (1) a small biased model, and (2) a large biased model. We are curious about whether or not the final RBDO optimum design with model validation can be less conservative than the conventional RBDO design and still satisfy the target probability of failure. First, the RBDO results for the small biased model are discussed. Table 6.10 and Table 6.11 show the intermediate RBDO optimum history and confidence-based probability of failure for the five-data case and the ten-data case, respectively. The experimental output data used in the intermediate RBDO optimum designs for the five-data case and the ten-data case are expressed in Table 6.12 and Table 6.13, respectively.

Table 6.10 Practical RBDO Optimization History using Small Biased Conservative Simulation Model for Five-Data Case

| # of RBDO process | Intermediate RBDO optimum | | Cost | Confidence-based $P_F$ using validated simulation model | | |
|---|---|---|---|---|---|---|
| | $d_1$ | $d_2$ | | $G_1$ | $G_2$ | $G_3$ |
| 0th | 5.1035 | 1.7491 | −1.8163 | 15.486% | 8.243 % | 0% |
| 1st | 5.3733 | 2.0688 | −1.6932 | 1.204% | 4.858% | 0% |
| 2nd | 5.1309 | 2.0167 | −1.7044 | 1.951% | 2.723% | 0% |
| 3rd | 5.0835 | 2.0025 | −1.7090 | 2.678% | 6.943% | 0% |
| 4th | 5.0158 | 2.0772 | −1.6767 | 1.065% | 0.117% | 0% |

Table 6.11 Practical RBDO Optimization History using Small Biased Conservative Simulation Model for Ten-Data Case

| # of RBDO process | Intermediate RBDO optimum | | Cost | Confidence-based $P_F$ using validated simulation model | | |
|---|---|---|---|---|---|---|
| | $d_1$ | $d_2$ | | $G_1$ | $G_2$ | $G_3$ |
| 0th | 5.1035 | 1.7491 | −1.8163 | 9.495% | 5.071 % | 0% |
| 1st | 5.3012 | 1.9662 | −1.6932 | 5.513% | 0.258% | 0% |
| 2nd | 5.5846 | 2.0159 | −1.7044 | 2.394% | 9.236% | 0% |
| 3rd | 5.4532 | 2.1073 | −1.7090 | 0.544% | 3.579% | 0% |
| 4th | 5.1984 | 1.9591 | −1.6767 | 0.265% | 0.874% | 0% |

Table 6.12 Randomly Collected Experimental Output Data for Small Biased Conservative Simulation Model (Five-Data Case)

| Intermediate RBDO optimum | Five experimental output data | |
|---|---|---|
| | $G_1$ | $G_2$ |
| 0th | [−0.9177, −1.4563, −0.0345, −0.5472, −1.1357] | [−0.5082, −0.4535, −5.6262, −2.2081, −0.8607] |
| 1st | [−2.0136, −1.2870, −2.1423, −2.2788, −2.3255] | [−0.6930, −0.4374, −0.4603, −0.2623, −1.1971] |
| 2nd | [−2.5097, −2.0830, −1.0282, −1.2696, −1.4219] | [−0.4221, −0.7682, −0.9220, −0.4286, −0.3833] |
| 3rd | [−1.4506, −1.2960, −1.1429, −1.1582, −0.8082] | [−0.6604, −0.4387, −0.2109, −0.6800, −0.8879] |
| 4th | [−2.0825, −1.9727, −1.2861, −2.3064, −2.7941] | [−0.7641, −0.7529, −0.9006, −0.9762, −1.1803] |

Table 6.13 Randomly Collected Experimental Output Data for Small Biased Conservative Simulation Model (Ten-Data Case)

| Intermediate RBDO optimum | Ten experimental output data | |
|---|---|---|
| | $G_1$ | $G_2$ |
| 0th | [−2.2122, −0.1968, −1.4412, −1.7196, −0.2557, −1.9938, −0.9931, −1.3406, −1.1578, −0.8870] | [−0.8477, −3.0290, −0.5097, −0.3907, −2.4758, −0.6259, −0.2526, −0.3785, −0.5176, −0.2935] |
| 1st | [−1.9863, −2.7222, −2.3337, −0.5593, −2.1589, −0.6403, −2.2950, −3.3496, −2.5029, −1.6981] | [−0.5460, −1.1360, −0.7345, −1.7192, −0.6122, −1.1501, −0.5678, −0.7434, −0.7488, −0.6748] |
| 2nd | [−1.2341, −1.8933, −2.4484, −2.6914, −1.0387, −3.4111, −2.8837, −3.5692, −1.8048, −2.3217] | [−0.2775, −0.2275, −0.2376, −0.6469, −0.2766, −0.1595, −0.1865, −0.5070, −0.3490, −0.5384] |
| 3rd | [−2.0593, −1.7815, −2.1279, −1.9700, −1.3348, −1.9166, −2.1224, −2.7818, −2.7351, −2.9298] | [−0.3533, −0.4837, −0.7372, −0.2890, −0.4314, −0.3855, −0.2529, −0.6574, −0.8634, −0.9855] |
| 4th | [−2.2152, −1.6362, −1.8290, −1.4246, −1.8618, −1.4189, −1.7773, −2.5101, −2.5630, −2.2779] | [−0.6515, −0.5497, −0.4333, −0.4659, −0.7673, −0.6479, −0.4991, −0.6242, −1.0057, −0.7204] |

Confidence-based probability of failure satisfies the target probability of failure, 2.275%, after the four RBDO processes for both data cases. Experimental output data was required at only five design configurations to obtain the final RBDO optimum design. To check whether the final RBDO optimum design truly satisfies the target probability of failure, true reliability analysis using the true output function has been carried out at the final RBDO optimum designs, as shown in Table 6.14. It is found that the true probabilities of failure at the final RBDO optimum designs for both data cases satisfy the target probability of failure and provide conservative design. It can be seen that the true probabilities of failure at the proposed RBDO optimums are lower than those obtained at the conventional RBDO optimum. This, therefore, indicates that the proposed RBDO provides a more reliable design to consider the uncertainty due to insufficient test data.

Accordingly, the cost value at the proposed RBDO optimums using five data and ten data has been increased compared to the cost value at conventional RBDO design. The proposed RBDO optimums using confidence-based model validation have been illustrated in Figure 6.5. It can be noted that the conventional RBDO is very close to the true RBDO optimum, which means the original simulation model is very accurate. However, we do not know how accurate the simulation model is and how close the conventional RBDO optimum design is to the true RBDO optimum in advance. As shown in Figure 6.5, the proposed RBDO optimums are far away from the true limit states—further than the conventional RBDO optimum. In other words, the proposed RBDO yields a more conservative design than the conventional RBDO. Thus, it is highlighted that the proposed RBDO could make a more reliable design than the conventional RBDO design when the simulation model is originally very accurate (*i.e.*, small biased model). In order to build confidence in the product designed with lacking experimental output data, the proposed RBDO using confidence-based model validation could yield a more conservative design than the conventional RBDO design.

Table 6.14 RBDO Optimum Summary and True Reliability Analysis at Practical RBDO Optimum Designs for Small Biased Conservative Simulation Model

| | Optimum design | | Cost | True $P_F$ using true output function | |
|---|---|---|---|---|---|
| | $G_1$ | $G_2$ | | $G_1$ | $G_2$ |
| Conventional RBDO | 5.1035 | 1.7491 | −1.8163 | 0.803% | 0.571% |
| Proposed RBDO (5 data) | 5.0158 | 2.0772 | −1.6767 | 0.129% | 0.006% |
| Proposed RBDO (10 data) | 5.1984 | 1.9591 | −1.7300 | 0.152% | 0.110% |
| True RBDO | 5.0566 | 1.5930 | −1.8848 | 2.277% | 2.269% |

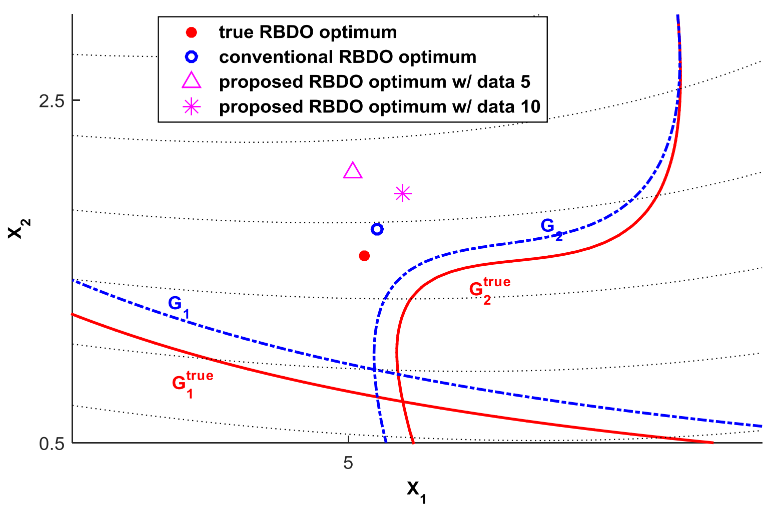


Figure 6.5 Plot of Practical RBDO Optimum using Confidence-Based Model Validation for Small Biased Conservative Simulation Model

Secondly, the RBDO results for the large biased model are discussed. Table 6.15 and Table 6.16 list the intermediate RBDO optimum design history and the confidence-based probability of failure using five data and ten data, respectively. Experimental output data at the intermediate RBDO optimum designs has been randomly drawn from the true output PDF, as shown in Table 6.17 for the five-data case and Table 6.18 for the ten-data case. Notice that, even though the $0^{th}$ intermediate RBDO optimum design (conventional RBDO design) already satisfies the target probability of failure for both data cases, the confidence-based model validation is carried out, followed by the RBDO iterations. As explained in Section 6.3.1, at the conventional RBDO optimum design, the confidence-based model validation is necessarily carried out even though the design satisfies the target probability of failure because we could obtain a better and reliable optimum design. As shown in Table 6.15 and Table 6.16, final RBDO optimum designs are obtained after five RBDO processes for the five-data case and after two RBDO processes for the ten-data case. Experimental output data was collected at six design points for the five-data case and three design points for the ten-data case. It is noted that the number of RBDO processes required to satisfy the target probability of failure is not uniquely determined for every problem, but rather depends on how good the experimental output data collected at the given design are.

Table 6.15 Practical RBDO Optimization History using Large Biased Conservative Simulation Model for Five-Data Case

| # of RBDO process | Intermediate RBDO optimum | | Cost | Confidence-based $P_F$ using validated simulation model | | |
|---|---|---|---|---|---|---|
| | $d_1$ | $d_2$ | | $G_1$ | $G_2$ | $G_3$ |
| 0th | 5.5377 | 2.3745 | −1.5892 | 0.235% | 0.915% | 0% |
| 1st | 5.3761 | 2.0785 | −1.6895 | 0.443% | 2.445% | 0% |
| 2nd | 5.0556 | 1.8834 | −1.7582 | 0.551% | 2.458% | 0% |
| 3rd | 4.8009 | 1.7098 | −1.8340 | 16.601% | 11.224% | 0% |
| 4th | 4.7458 | 2.3783 | −1.5503 | 2.788% | 0.210% | 0% |
| 5th | 5.0512 | 2.2504 | −1.6082 | 0.897% | 0.030% | 0% |

Table 6.16 Practical RBDO Optimization History using Large Biased Conservative Simulation Model for Ten-Data Case

| # of RBDO process | Intermediate RBDO optimum | | Cost | Confidence-based $P_F$ using validated simulation model | | |
|---|---|---|---|---|---|---|
| | $d_1$ | $d_2$ | | $G_1$ | $G_2$ | $G_3$ |
| 0th | 5.5377 | 2.3745 | −1.5892 | 0.232% | 1.603% | 0% |
| 1st | 5.3123 | 2.0143 | −1.6762 | 0.781% | 4.202% | 0% |
| 2nd | 5.0797 | 2.0120 | −1.7050 | 1.321% | 0.909% | 0% |

Table 6.17 Randomly Collected Experimental Output Data for Large Biased Conservative Simulation Model (Five-Data Case)

| Intermediate RBDO optimum | Five experimental output data | |
|---|---|---|
| | $G_1$ | $G_2$ |
| 0th | [−3.3197, −2.2801, −1.9570, −3.3137, −3.8047] | [−1.1037, −0.7163, −0.6349, −0.8417, −0.5484] |
| 1st | [−1.9622, −2.6826, −1.4754, −3.0181, −1.8441] | [−0.7222, −0.7548, −0.4691, −0.7795, −0.5660] |
| 2nd | [−1.8661, −1.6221, −1.1792, −1.9949, −1.3853] | [−0.5772, −0.7603, −0.6656, −0.9293, −0.5974] |
| 3rd | [−0.7282, −0.4090, −1.5982, −0.0867, −0.7415] | [−1.2194, −3.0073, −0.5059, −5.9754, −1.0628] |
| 4th | [−2.6470, −2.7288, −0.9589, −2.0105, −1.9609] | [−1.4881, −1.4400, −2.4320, −1.0063, −1.5863] |
| 5th | [−1.6148, −2.2207, −2.7987, −1.9818, −1.2520] | [−0.9772, −0.9661, −0.7568, −0.7307, −0.9164] |

Table 6.18 Randomly Collected Experimental Output Data for Large Biased Conservative Simulation Model (Ten-Data Case)

| Intermediate RBDO optimum | Ten experimental output data | |
|---|---|---|
| | $G_1$ | $G_2$ |
| 0th | [−2.0101, −2.3145, −2.6729, −3.1660, −2.9781, −3.3364, −2.2865, −1.7495, −2.7081, −3.7362] | [−0.6823, −0.6730, −0.5755, −0.8095, −0.4079, −0.9141, −0.8692, −0.4732, −0.8181, −0.9545] |
| 1st | [−2.3715, −2.7760, −1.9716, −1.2196, −2.2557, −2.2234, −1.4541, −2.6870, −1.5031, −2.0254] | [−0.7833, −0.8598, −0.6610, −0.6651, −0.3616, −0.9591, −0.3480, −0.4728, −0.4152, −0.6768] |
| 2nd | [−2.7760, −1.1744, −2.2308, −2.1686, −0.8978, −2.2394, −2.2758, −1.2262, −1.0223, −1.6620] | [−1.2636, −0.6514, −0.8591, −0.5896, −1.1660, −0.9604, −0.8515, −0.6046, −0.8871, −0.6867] |

To ensure that the proposed RBDO optimum designs truly satisfy the target probability of failure, true reliability analysis using the true output function has been performed at the final RBDO optimum designs, as listed in Table 6.19. The true probability of failure at the proposed RBDO optimums for both data cases is less than the target probability of failure, and they are conservative. For the $G_1$ constraint, the proposed RBDO is much less conservative than the conventional RBDO. For the $G_2$ constraint, the true probability of failure at the proposed RBDO optimums is smaller than the one at the conventional RBDO optimum. It is worth nothing that the proposed RBDO optimum is less conservative than the conventional RBDO optimum and the cost value decreases from −1.5892 to −1.6080 for the five-data case and to −1.7050 for the ten-data case. It is found that when we have more data, as in the ten-data case, the proposed RBDO is able to decrease cost value more significantly. The final RBDO optimums using confidence-based model validation for the large biased model are illustrated in Figure 6.6. It is evident that the conventional RBDO optimum is very far from the true RBDO optimum, which confirms that original simulation model is significantly biased. The proposed RBDO optimums for both data cases are closer to the true RBDO optimum compared to the conventional RBDO optimum, which leads to reliable yet less conservative design. Therefore, it is concluded that the proposed RBDO method can provide a cost-effective and still reliable design when the simulation model is significantly biased.

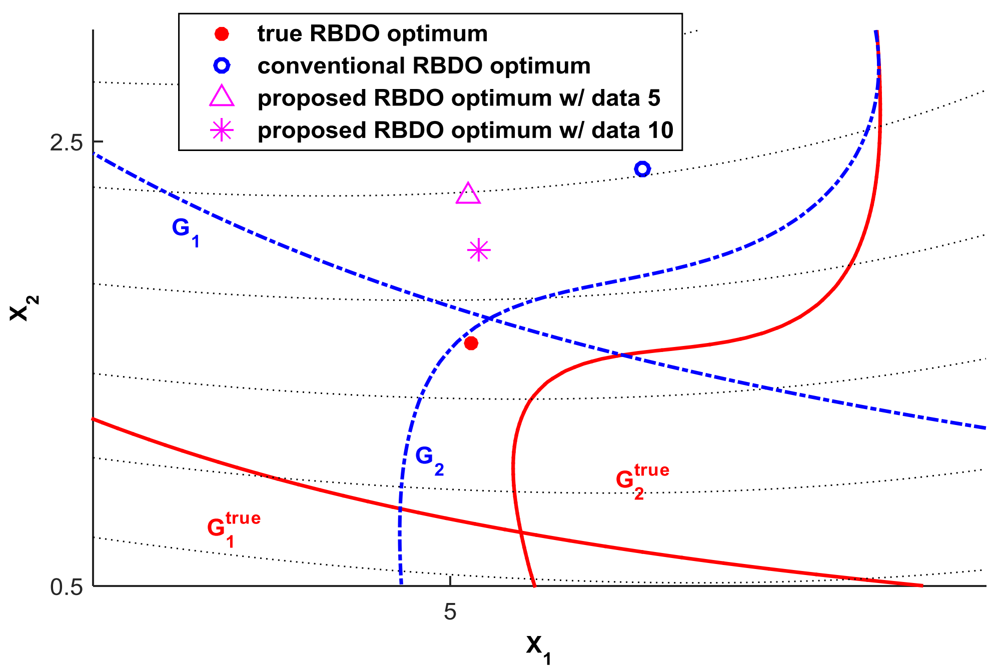


Figure 6.6 Plot of Practical RBDO Optimum using Confidence-Based Model Validation for Large Biased Conservative Simulation Model

Table 6.19 RBDO Optimum Summary and True Reliability Analysis at Practical RBDO Optimum Designs for Large Biased Conservative Simulation Model

| | Optimum design | | Cost | True $P_F$ using true output function | |
|---|---|---|---|---|---|
| | $G_1$ | $G_2$ | | $G_1$ | $G_2$ |
| Conventional RBDO | 5.5377 | 2.3745 | −1.5892 | 0.001% | 1.376% |
| Proposed RBDO (5 data) | 5.0512 | 2.2504 | −1.6082 | 0.029% | 0.007% |
| Proposed RBDO (10 data) | 5.0797 | 2.0120 | −1.7050 | 0.162% | 0.020% |
| True RBDO | 5.0566 | 1.5930 | −1.8848 | 2.277% | 2.269% |

# CHAPTER 7

# CONFIDENCE-BASED RELIABILITY ASSESSMENT CONSIDERING BOTH PARAMETER UNCERTAINTY AND MODEL BIAS FOR INSUFFICIENT INPUT AND EXPERIMENTAL OUTPUT DATA

Previous sections assume that true input distribution are known and thus handle only limited experimental output data when simulation model is biased. However, in real applications, true input distribution models, which require large number of input data, are not available due to high cost in experimental or coupon testing. The uncertainty of input distribution model due to the limited number of input data is called parameter uncertainty. In this section, we present a new methodology of confidence-based reliability assessment for more practical situation in which parameter uncertainty, model bias and the uncertainty due to insufficient experimental output data exist. To combine both uncertainties caused by limited input/output data and model bias, a hierarchical Bayesian model is formulated to quantify the uncertainty of reliability. Since this section focuses on reliability assessment, not RBDO, numerical results are represented using the reliability (probability of success) instead of the probability of failure (1−reliability).

Section 7.1 explains how to quantify the uncertainty induced by limited input data. Section 7.2 describes the hierarchical Bayesian model and explains the quantification of uncertainty of reliability considering both limited number of input data and output data. Section 7.3 and Section 7.4 present numerical tests to verify the proposed confidence-based reliability assessment using two engineering examples: 9-D cantilever tube-shaped beam and 11-D vehicle side impact problem, respectively.

## 7.1. Quantification of Uncertainty Induced by Limited Number of Input Data

In the presence of limited number of input data, input distribution model becomes uncertain. In the meantime, input distribution model can be defined as the function of input distribution type, $\zeta$, and input distribution parameter, $\boldsymbol{\psi}$. Thus, input distribution type and parameters follow certain probability distribution, not being a specific type or constant values, in the presence of the limited number of input data. Using Bayesian approach, the probability distributions of input distribution type and distribution parameters can be obtained given limited number of input data (Cho et al., 2016).

Input distribution parameter consists of input mean $\mu_i$, and input variance $\sigma_i^2$ as $\boldsymbol{\psi_i} = [\mu_i, \sigma_i^2]$. Input variance, $\sigma_i^2$ , for $i^{\text{th}}$ independent random variable $X_i$ given corresponding data $\mathbf{x}_i^e$, follows inverse-gamma distribution as

$$\sigma_i^2 \middle| \mathbf{x}_i^e \sim \mathrm{IG}\left(\frac{nd-1}{2}, \frac{(nd-1)s_i^2}{2}\right), \quad (7\text{-}1)$$

where *nd* is the number of input data and $s_i^2$ is the sample variance. Input mean $\mu_i$ follows normal distribution given input variance and input data as

$$\mu_i \middle| \sigma_i^2, \mathbf{x}_i^e \sim \mathrm{N}\left(\bar{\mathbf{x}}_i, \frac{\sigma_i^2}{nd}\right), \quad (7\text{-}2)$$

where $\bar{\mathbf{x}}_i$ is the mean of input data. Once probabilities of distribution parameters are obtained, the probability of input distribution type can be evaluated as (Cho et al., 2016)

$$P\left(\zeta \middle| \boldsymbol{\psi}, \mathbf{x}^e\right) \propto P\left(\mathbf{x}^e \middle| \zeta, \boldsymbol{\psi}\right) P\left(\zeta \middle| \boldsymbol{\psi}\right), \quad (7\text{-}3)$$

where $P\left(\mathbf{x}^{e}\middle|\zeta,\boldsymbol{\psi}\right)$ is the likelihood function and $P\left(\zeta\middle|\boldsymbol{\psi}\right)$ is the probability distribution of input distribution type, given distribution parameters, which is constant assuming that all candidate distribution types are equally probable before having the input data. Since it is not easy to cover all input distribution types in the evaluation of Eq. (7-3), seven marginal distribution types are considered as candidate distribution types (Normal, Lognormal, Weibull, Gumbel, Gamma, Extreme, and Extreme Type II). Once the candidates of input distribution model is obtained, the candidates of biased simulation output distribution for each candidate of input distribution model can be generated using (biased) simulation model.

## 7.2. Quantification of Uncertainty Distribution of Reliability Considering Both Limited Number of Input and Output Data

In the presence of uncertain input distribution models induced by limited number of input data, many possible candidates of biased simulation output distribution exist as explained in Section 7.1. Thus, one-level Bayesian model that is proposed Section 4 is not appropriate; hierarchical Bayesian model is proposed in this section. Using hierarchical Bayesian analysis, uncertainty distribution of reliability can be obtained considering limited number of experimental output data under uncertain input distribution models.

In Section 7.2.1, further investigation of kernel function, which is used in AKDE for modeling output PDF, is carried out. Section 7.2.2 explains the proposed hierarchical Bayesian analysis to obtain the uncertainty distribution of reliability accounting for both uncertainties due to limited input/output data. Section 7.2.3 describes how to assess confidence-based reliability and discusses confidence level.

### 7.2.1. Investigation of Kernel Function in AKDE Used to Model Output PDF

As for modeling of target output PDF, AKDE is still used. Further investigation of kernel function, which is used in AKDE, is carried out in this section. In Section 4, as for one-level Bayesian model considering only limited number of output data, Gaussian kernel – the most popular kernel – was chosen. However, even though Gaussian kernel is popular due to its convenient mathematical properties such as infinitely differentiable everywhere, it is found that Gaussian kernel has infinite support size (see Figure 7.1) which leads to a significant computational disadvantage. Epanechnikov kernel is optimal in the sense of minimizing a mean square error (Epanechnikov, 1969); but, its first derivative is not continuous as shown in Figure 7.1. On the other hand, both biweight and triweight kernels have smooth property as shown in Figure 7.1 and have distinct computational advantage due to finite support. In this section, triweight kernel is chosen because it is smoother and the more recently developed than biweight kernel. Figure 7.2 depicts the effect of each kernel on fitting output PDF given insufficient data. It is noticed that the shape of density function using Epanechnikov has multiple non-smooth points while triweight yields smoother density function.

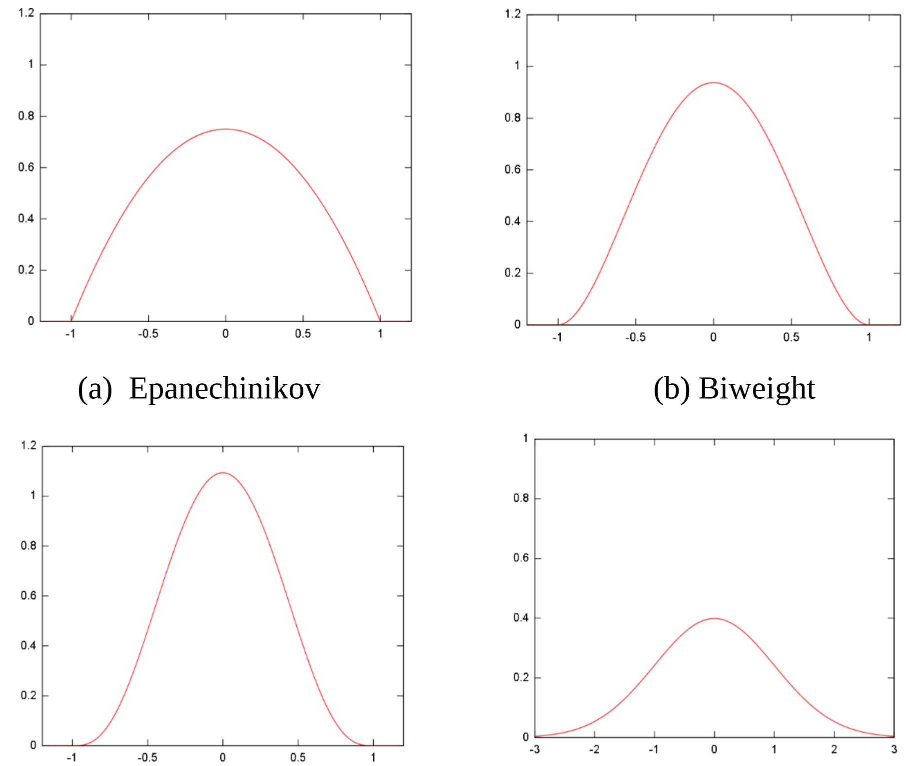

(a) Epanechinikov (b) Biweight

(c) Triweight (d) Gaussian

Figure 7.1 Shape of Different Kernel Functions

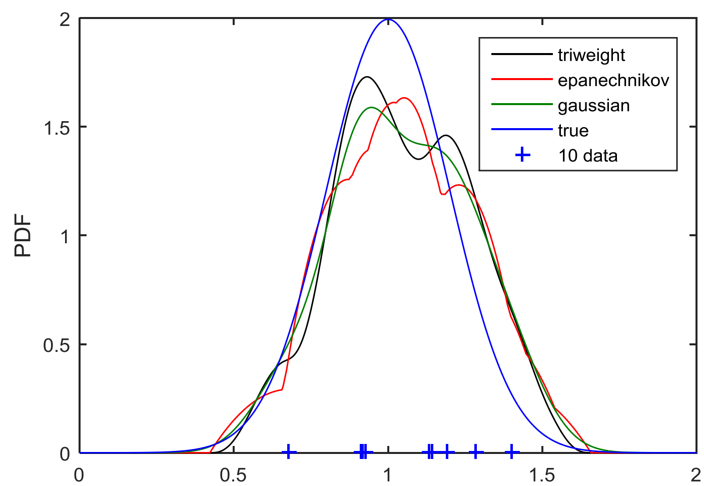


Figure 7.2 Kernel Density Estimation using Different Kernel Function Given Insufficient Data

7.2.2. Quantification of Uncertainty Distribution of Reliability

A hierarchical Bayesian model is formulated to combine uncertainties induced by input/output test data. The joint PDF of bandwidth, input distribution type and input distribution parameters given input/output test data, $P\left(h_0, \zeta, \boldsymbol{\psi} \mid \mathbf{y}^e, \mathbf{x}^e\right)$, can be derived by

$$\begin{aligned} P\left(h_0, \zeta, \boldsymbol{\psi} \mid \mathbf{y}^e, \mathbf{x}^e\right) &\propto L\left(\mathbf{y}^e \middle| h_0, \zeta, \boldsymbol{\psi}, \mathbf{x}^e\right) P\left(h_0, \zeta, \boldsymbol{\psi} \middle| \mathbf{x}^e\right) \\ &\propto L\left(\mathbf{y}^e \middle| h_0, \zeta, \boldsymbol{\psi}, \mathbf{x}^e\right) P\left(h_0 \middle| \zeta, \boldsymbol{\psi}, \mathbf{x}^e\right) P\left(\zeta, \boldsymbol{\psi} \middle| \mathbf{x}^e\right) \end{aligned}, \quad (7\text{-}4)$$

where $L\left(\mathbf{y}^e \middle| h_0, \zeta, \boldsymbol{\psi}, \mathbf{x}^e\right)$ is the likelihood function, which can be evaluated using AKDE (See Eq. (4-3)) and $P\left(h_0 \middle| \zeta, \boldsymbol{\psi}, \mathbf{x}^e\right)$ is the prior distribution of bandwidth given input distribution type $\zeta$ and input distribution parameter $\boldsymbol{\psi}$. Here, distribution parameters of prior distribution, $\zeta$ and $\boldsymbol{\psi}$, are defined as hyper parameters. $P\left(\zeta, \boldsymbol{\psi} \middle| \mathbf{x}^e\right)$ is hyper prior (distribution of hyper parameters) for $\zeta$ and $\boldsymbol{\psi}$, which can be obtained as the product of the probability of input distribution parameters, $P\left(\zeta \middle| \boldsymbol{\psi}, \mathbf{x}^e\right)$, and the probability of input distribution type, $P\left(\boldsymbol{\psi} \middle| \mathbf{x}^e\right)$. $P\left(\zeta \middle| \boldsymbol{\psi}, \mathbf{x}^e\right)$ can be obtained as the product of Eqs. (7-1) and (7-2), and $P\left(\boldsymbol{\psi} \middle| \mathbf{x}^e\right)$ is same as Eq. (7-3). It is noted that the hierarchical Bayesian model in Eq. (7-4) additionally includes the hyper prior term, which represents uncertain input distribution models, whereas single level Bayesian model in Eq. (4-7) does not.

With regard to prior distribution of bandwidth $P\left(h_0 \middle| \zeta, \boldsymbol{\psi}, \mathbf{x}^e\right)$ in Eq. (7-4), further improvement has been carried out, compared to the prior distribution used in Eq. (4-6), as

$$\begin{aligned} &P\left(h_0 \middle| \zeta, \boldsymbol{\psi}, \mathbf{x}^e\right) \sim \text{Gamma}\left(14, \frac{a}{14}\right), \\ &\quad \text{where } \; a = c_0(K) n_p^{-1/5} \sigma_s^{random}\left(\zeta, \boldsymbol{\psi}, \mathbf{x}^e\right) \end{aligned}, \quad (7\text{-}5)$$

where prior sample size $n_p$ is equal to the number of experimental output data, $K$ is type of kernel function, and $\sigma_s^{random}\left(\zeta, \boldsymbol{\psi}, \mathbf{x}^e\right)$ is the randomly-selected sample standard deviation (sample size is equal to the number of experimental output data) of biased simulation output distribution given input distribution model. First, it is worth noting that prior sample size properly reflects limited number of output data; whereas, in Eq. (4-6), prior sample size $n_p$ was arbitrary, which is problem-dependent. Second, the mean of prior distribution (optimal bandwidth using normal reference rule-of-thumb), $a$, is derived using triweight kernel, not Gaussian kernel and thus $c_0(K)$ in Eq. (7-5) is 3.169 as shown in Table 7.1, which is larger than one obtained using Gaussian kernel (Henderson & Parmeter, 2012). As a consequence, the estimated density function with triweight kernel tends to be wider and the reliability estimation using triweight kernel becomes more conservative than the one using Gaussian kernel. Lastly, instead of using the standard deviation of simulation output distribution, sample standard deviation with $n_p$ sample size is randomly chosen from the simulation output distribution. As a result, mean of prior distribution for bandwidth can be adaptively adjusted depending on number of output data.

Table 7.1 Normal Reference Rule-of-Thumb Constants for Second Order Kernels

| Type of kernel, $K$ | $C_0$ in Eq. (7-5) |
|---|---|
| Uniform | 1.8431 |
| Epanechinikov | 2.3449 |
| Gaussian | 1.0592 |
| Biweight | 2.7779 |
| Triweight | 3.1690 |

After the joint PDF of bandwidth, input distribution type, and input distribution parameters are obtained, the CDF of reliability given limited number of input/output test data can be formulated as

$$F_{Re}\left(Re\,|\,\mathbf{y}^e,\mathbf{x}^e\right) = \int_0^{Re}\int_{\Omega_{h_0}}\int_{\Omega_\zeta}\int_{\Omega_\psi} f\left(\rho\,|\,h_0,\zeta,\boldsymbol{\psi},\mathbf{y}^e,\mathbf{x}^e\right)P\left(h_0,\zeta,\boldsymbol{\psi}\,|\,\mathbf{y}^e,\mathbf{x}^e\right)d\boldsymbol{\psi}\,d\zeta\,dh_0\,d\rho, \tag{7-6}$$

where $f\left(\rho\,|\,h_0,\zeta,\boldsymbol{\psi},\mathbf{y}^e,\mathbf{x}^e\right)$ is the conditional PDF of reliability, which becomes Dirac delta measure because reliability can be uniquely evaluated once the bandwidth and input distribution model given input/output data are determined. Meanwhile, the integration in Eq. (7-6) cannot be analytically obtained so that it is numerically evaluated using MCS integration as

$$\begin{aligned} F_{Re}\left(Re\,|\,\mathbf{y}^e,\mathbf{x}^e\right) &\cong \frac{1}{nMCS_h}\int_0^{Re}\sum_{i=1}^{nMCS_h} f\left(\rho\,|\,h_0^{(i)},\zeta^{(i)},\boldsymbol{\psi}^{(i)},\mathbf{y}^e,\mathbf{x}^e\right)d\rho \\ &= \frac{1}{nMCS_h}\int_0^{Re}\sum_{i=1}^{nMCS_h}\delta\left[\rho - Re\left(h_0^{(i)},\zeta^{(i)},\boldsymbol{\psi}^{(i)}\,|\,\mathbf{y}^e,\mathbf{x}^e\right)\right]d\rho \\ &= \frac{1}{nMCS_h}\sum_{i=1}^{nMCS_h} I_{\left[0,Re\left(h_0^{(i)},\zeta^{(i)},\boldsymbol{\psi}^{(i)}|\mathbf{y}^e,\mathbf{x}^e\right)\right]}\left(Re\right) \end{aligned} \tag{7-7}$$

$$\text{where}\quad I_{\left[0,Re\left(h_0^{(i)},\zeta^{(i)},\boldsymbol{\psi}^{(i)}|\mathbf{y}^e,\mathbf{x}^e\right)\right]}\left(Re\right) = \begin{cases} 1 & \text{if } 0 \le Re \le Re\left(h_0^{(i)},\zeta^{(i)},\boldsymbol{\psi}^{(i)}\,|\,\mathbf{y}^e,\mathbf{x}^e\right) \\ 0 & \text{if } Re > Re\left(h_0^{(i)},\zeta^{(i)},\boldsymbol{\psi}^{(i)}\,|\,\mathbf{y}^e,\mathbf{x}^e\right) \end{cases}.$$

Here, $nMCS_h$ is the number of MCS sample in the hierarchical Bayesian model. $h_0^{(i)},\zeta^{(i)},\boldsymbol{\psi}^{(i)}$ are $i^{\text{th}}$ realization of bandwidth, input distribution type and input distribution parameter, respectively. First, the realization of $\psi$ can be generated from Eqs. (7-1) and (7-2). Afterwards, the realization of $\zeta$ is obtained in accordance with $P\left(\zeta|\boldsymbol{\psi},\mathbf{x}^e\right)$. Finally, the realization of $h_0$ needs to be generated using the MCMC sampler in accordance with

Eq. (7-4). The Metropolis-Hasting algorithm has been used to obtain the random realization of $h_0$. At each MCMC sample, the output PDF and corresponding reliability can be uniquely determined using AKDE.

### 7.2.3. Confidence-Based Reliability and Confidence Level

The proposed method suggests to use a conservatively selected reliability value based on the complementary CDF (CCDF), which is defined as 1–CDF, of reliability. In the CCDF, higher percentile indicates more conservative estimation of reliability. This is why the percentile is referred to as the confidence level. Similar to the confidence-based model validation in Section 4.3.3, users can select target confidence level $CL^{target}$. The reliability at the target confidence level is the confidence-based reliability as shown in Figure 7.3. The corresponding output PDF that produces confidence-based reliability is the confidence-based target output PDF. Once the confidence-based target output PDF is selected, the biased simulation model output PDF can be validated against it.

The validation process to obtain validated simulation model considering both limited number of input/output test data is left as future research. In the following sections 7.3 and 7.4, the proposed confidence-based reliability assessment considering both uncertainties induced by limited input/output test data is demonstrated using engineering examples.

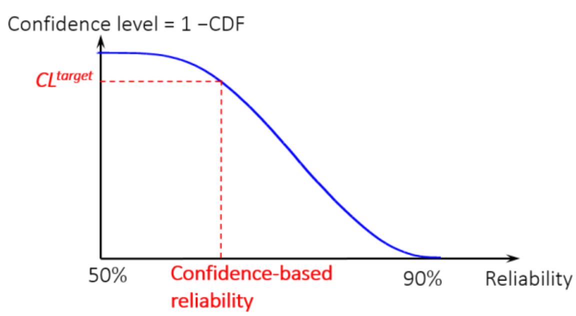


Figure 7.3 Confidence-Based Reliability

## 7.3. Numerical Test using 9-D Cantilever Tube Shape Beam

In this section, 9-D cantilever tube-shaped beam shown in Figure 7.4 is considered to demonstrate the proposed confidence-based reliability assessment (Arora, 2004). There are nine input random variables as shown in Table 7.2. Two constraints are considered as

Constraint 1: maximum stress at the fixed support point A ($\sigma_{max}$) – yield strength ($\sigma_Y$) ≤ 0

Constraint 2: torsion ($T$) – critical buckling torsion ($T_{cr}$) ≤ 0

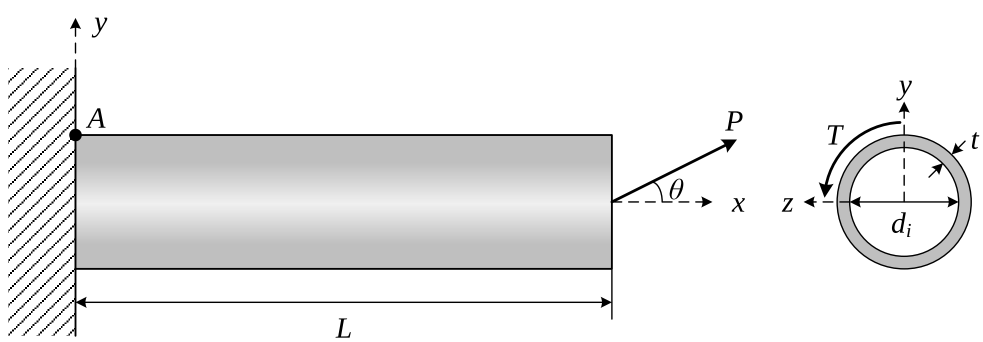


Figure 7.4 Cantilever Tube-Shaped Beam

In this example, it is assumed that true input distributions for only three input variables (inner diameter, length and thickness) are known because the variability of geometry parameter can be easily identified. In contrast, only limited number of data is given for the rest of six variables, which are either material properties or loading parameters.

Table 7.2 Input Random Variable Information for 9-D Cantilever Tube-Shaped Beam

| Description | | True input distribution | | | Remark |
|---|---|---|---|---|---|
| | | Type | Mean | STD | |
| $d_i$ | Inner diameter (mm) | Normal | 189.8126 | 10 | True input distribution is known |
| $t$ | Thickness (mm) | Normal | 1.6611 | 0.08 | True input distribution is known |
| $L$ | Length (mm) | Normal | 500 | 10 | True input distribution is known |
| $P$ | Force (N) | Normal | 50,000 | 5,000 | Only limited number of data is given |
| $T$ | Torsion (N-mm) | Normal | 10,000,000 | 1,000,000 | Only limited number of data is given |
| $\theta$ | Angle (°) | Normal | 0 | 10 | Only limited number of data is given |
| $E$ | Young's modulus (MPa) | Normal | 200,000 | 10,000 | Only limited number of data is given |
| $v$ | Poisson's ratio | Log Normal | 0.26 | 0.026 | Only limited number of data is given |
| $\sigma_Y$ | Yield strength (Mpa) | Normal | 220 | 15.4 | Only limited number of data is given |

To verify the proposed method, two models are considered. First, as a true model, analytical expressions for maximum stress, $\sigma_{max}$, and critical buckling torsion, $T_{cr}$, are treated as true physical output, which represent real physics. Then, true constraints $G_i^{true}(\mathbf{x})$ can be summarized as

$$G_1^{true}(\mathbf{x}) = \frac{\sigma_{max}}{\sigma_y} - 1 = \frac{\sqrt{\sigma_x^2 + 3\tau_{xz}^2}}{\sigma_y} - 1 \le 0$$

$$where \ \sigma_x = \frac{P\cos\theta}{A} + \frac{P\sin\theta L}{I}\frac{d_0}{2} \ and \ \tau_{xz} = \frac{Td_o}{4I} \ . \qquad (7\text{-}8)$$

$$G_2^{true}(\mathbf{x}) = 1 - \frac{T_{cr}}{T} \le 0 \le 0 \ \ where \ \ T_{cr} = \frac{\pi d_o^3 E}{3\left(1-\nu^2\right)^{0.75}}\left(\frac{t}{d_o}\right)^{2.5}$$

Here, $A$ is cross sectional area defined as $A=\pi(d_0 - t)t$, $I$ is the section modulus defined as $I = \pi/64(d_0^4 - (d_0 - 2t)^4)$, and $d_o$ is the outer diameter defined as $d_o=d_i+2t$. We can generate limited number of physical output test data using Eq. (7-8) as the outcome of physical testing. Secondly, biased constraints $G_i(\mathbf{x})$ is formulated by subtracting bias (assumed unknown) $B_i(\mathbf{x})$ to the true (assumed unknown) constraint $G_i^{true}(\mathbf{x})$ as $G_i(\mathbf{x}) = G_i^{true}(\mathbf{x}) - B_i(\mathbf{x})$. The unknown biases for two constraints are mathematically constructed as

$$B_1 = \frac{\sqrt{0.01\sigma_x^2 + 0.036\tau_{xz}^2 + 0.37\left(P\cos\theta / \mathrm{A}\right)^2 + 5}}{\sigma_y}$$

$$B_2 = \frac{\pi E}{T}\left(\frac{d_o^{0.5}}{6\left(1-\nu\right)^{0.7}} - \frac{1}{5\left(1-\nu^2\right)^{1.5}}\right) \ . \qquad (7\text{-}9)$$

It is noted that only biased constraint $G_i(\mathbf{x})$ is used as the simulation model to demonstrate the proposed method assuming we do not know true constraint and bias. In this example, analytical function of the biased constraint is directly used to evaluate output response at the MCS samples in the sampling-based reliability analysis. To check the error of biased simulation model, non-normalized output mean value for biased constraints $G_1$ (maximum stress) and $G_2$ (critical buckling torsion) are compared with those obtained using true model in Eq. (7-8). As shown in Table 7.3, the error level is around 20% for $G_1$ and 15% for $G_2$, which indicates that the biased simulation model is fairly inaccurate. This biased simulation model is used to demonstrate the proposed confidence-based reliability assessment given lack of input/output test data. For comparison, two experimental situations are studied in each of following Section 7.3.1 and 7.3.2.

Table 7.3 Accuracy of Biased Simulation Model for 9-D Cantilever Tube-Shaped Beam

| | Non-normalized output mean | |
|---|---|---|
| | $G_1$ | $G_2$ |
| Biased simulation model $(a)$ | 167.31 | 12,615,870 |
| True model $(b)$ | 210.14 | 10,958,273 |
| Error $\left(\frac{b-a}{b} \times 100\right)$ | 20.38% | −15.13% |

### 7.3.1. Data Case 1: Limited Number of Input and Output Test Data

In this section, limited number of test data is considered and applied to the proposed confidence-based reliability assessment. To generate limited number of input test data, 30 data for each of six input variables, which are material properties and loads are randomly drawn from its true input distribution in Table 7.2. Figure 7.5 depicts 30 input data for each of six variables and their true input distributions. Figure 7.6 describes how 20 output test data are distributed, which are randomly generated from the true output distribution for each constraint. As for both constraints, 20 data each are not biased since they are well distributed. More data are densely located around at the mean value and few data are collected at the tail part.

Before applying the proposed confidence-based reliability assessment, simulation based-reliability assessment is carried out. First, a best-fit input distribution model is obtained, which is approximated by maximum likelihood estimation given input data. After that, the best-fit input distribution is fed into the biased simulation model to obtain biased output distribution. Once the output distribution is available, the corresponding reliability can be evaluated.

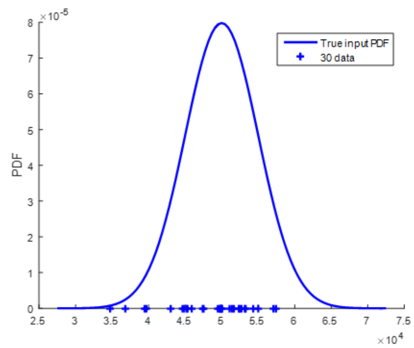


(a) Force

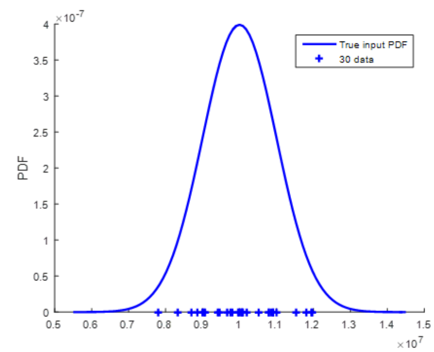


(b) Torsion

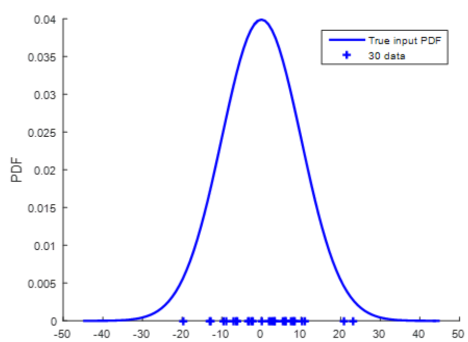


(c) Angle

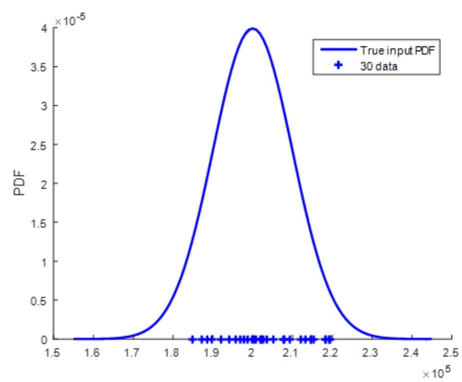


(d) Young’s modulus

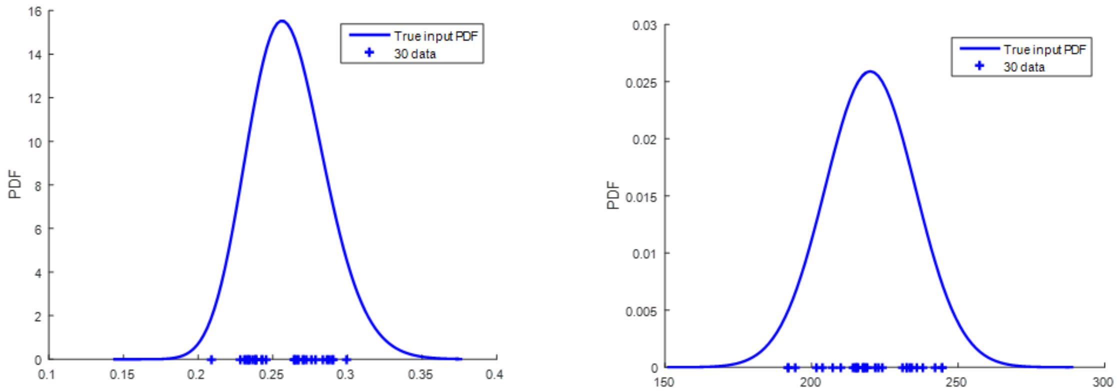


(e) Poisson's ratio (f) Yield strength

Figure 7.5 30 Input Data Randomly Drawn from True Input Distribution

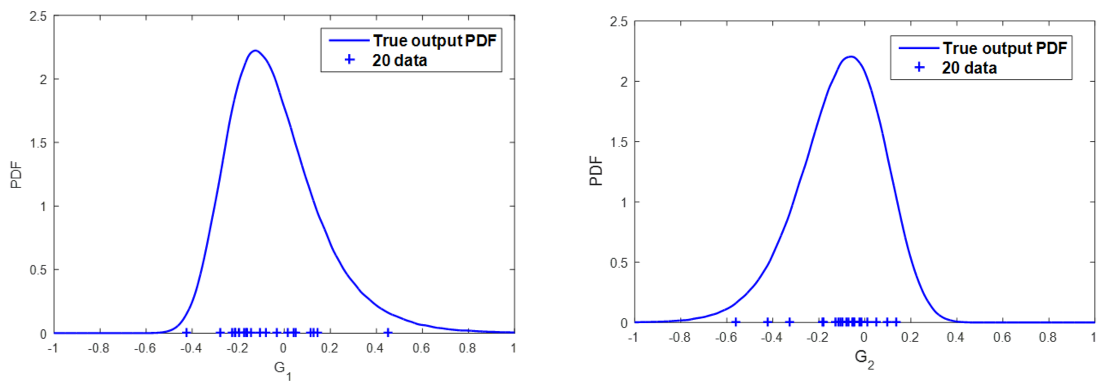


(a) Constraint 1 (b) Constraint 2

Figure 7.6 20 Output Test Data Randomly Drawn from True Output Distribution

Given 30 input data and biased model, simulation-based reliability is evaluated as 88.86% for $G_1$ and 93.48% for $G_2$. On the other hand, the true reliability is only 63.91% for constraint 1 and 69.97% for constraint 2. Figure 7.7 illustrates the comparison of output PDF between the true model and biased simulation model. It is noted that biased simulation output PDF is shifted to left to the true one, which indicates that the biased simulation model overestimates the true reliability. Hence, if the biased simulation output PDF with best-fit input distribution is used, the simulation result could falsely predict the current design is reliable.

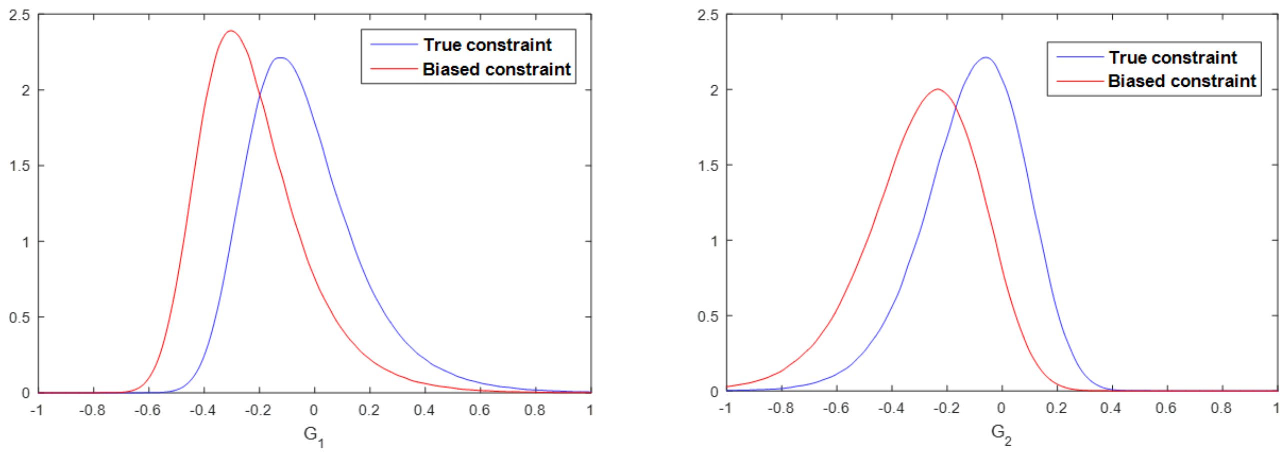


Figure 7.7 Comparison of True Output PDF and Biased Simulation Output PDF (Left: Constraint 1 and Right: Constraint 2)

Given 30 input data/20 output data shown in Figures 7.5 and 7.6 and the biased simulation model, the proposed confidence-based reliability assessment produces the uncertainty distribution (CCDF) of reliability as shown in Figure 7.8. To draw the CCDF of reliability, $nMCS_h$ in Eq. (7-7) are set to 1000. Thus, 1000 possible reliabilities are obtained. At 90% target confidence level, confidence-based reliability is selected as 61.19% for $G_1$ and 63.52% for $G_2$, which are lower than the true reliabilities (63.91% for $G_1$ and 69.97% for $G_2$). This implies that the proposed confidence-based method provides conservative reliability estimation. In addition, the proposed method is compared with the output best-fit method. In the output best-fit method, reliability is calculated by fitting experimental output data to AKDE, without incorporating simulation model. Table 7.4 compares reliabilities obtained using the proposed method, the output best-fit method, and the simulation-based method which uses best-fit input distribution model and the biased simulation model. It is found that both the output best-fit method and the simulation-based method overestimate reliability compared to the true reliability. Therefore, it is emphasized that using either only simulation model or only physical test data does not provide confidence in the estimation of reliability. On the other hand, the proposed confidence-based method can predict reliability with confidence and thus it can be right guidance to design product when it is applied to the RBDO process.

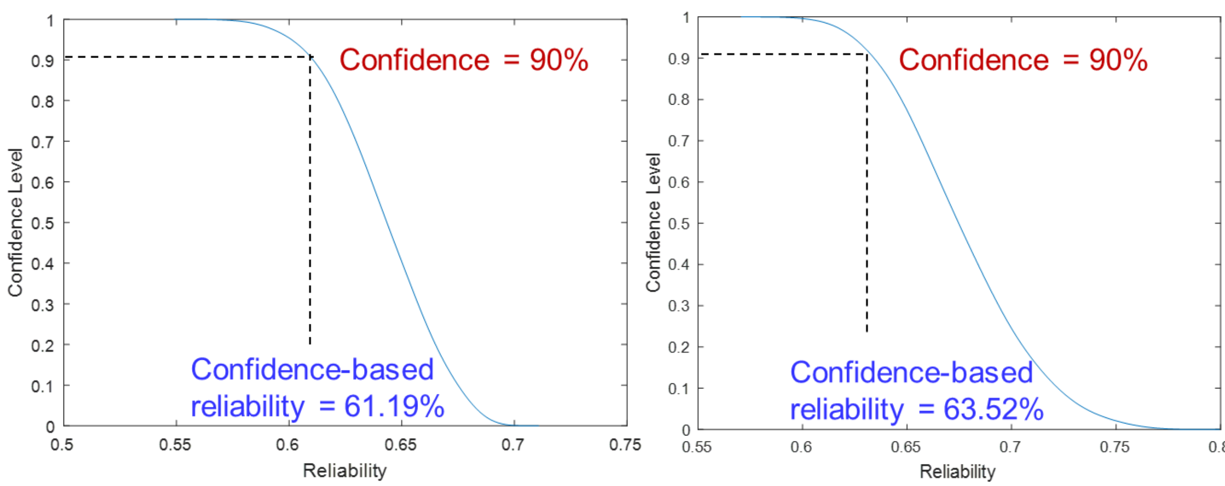


Figure 7.8 CCDF of Reliability and Confidence Level Given 30 Input/20 Output Data (Left: Constraint 1 and Right: Constraint 2)

Table 7.4 Comparison of Reliability under Different Methods for 30 Input/20 Output Data

| Reliability | Constraints | |
|---|---|---|
| | $G_1$ | $G_2$ |
| Confidence-based method | 61.19% | 63.52% |
| Output best-fit method | 67.36% | 76.39% |
| Simulation-based method | 88.86% | 93.48% |
| True | 63.91% | 69.97% |

### 7.3.2. Data Case 2: Small Number of Input/Output Test Data

Compared to data set in Section 7.3.1, the numbers of input and output test data are decreased to ten and five, respectively. This case is closer to practical application than the data case 1. To generate the small number of input data, only ten data for each of six variables is randomly drawn from the true input distribution in Table 7.2, which are plotted as blue cross as shown in Figure 7.9. With such a small amount of data, the collected ten data do not well represent the true input distribution compared to the previous 20 input data. For instance, most of ten data for force variable shown in Figure 7.9 (a) are from the right tail of the true input distribution and thus they are biased.

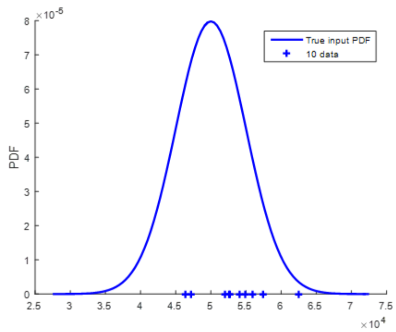


(a) Force

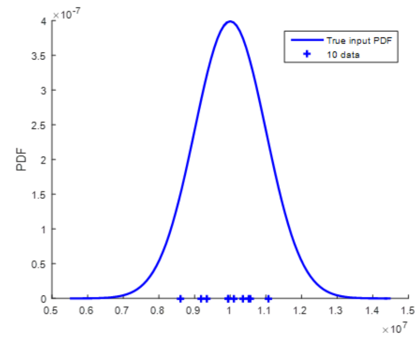


(b) Torsion

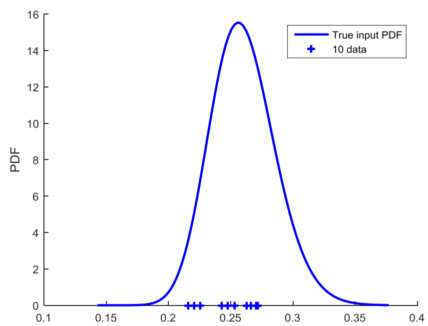


(c) Angle

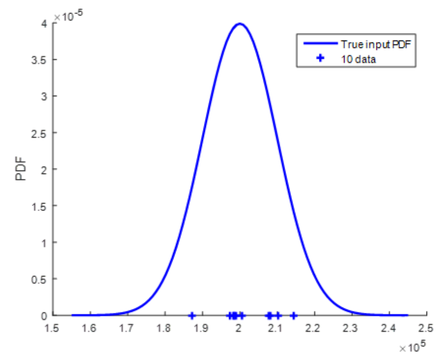


(d) Young’s modulus

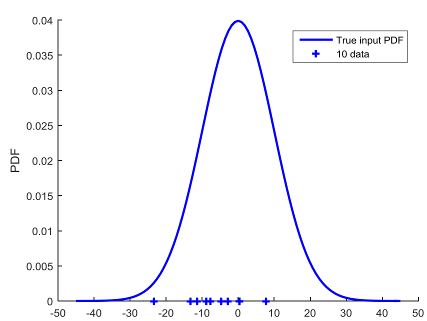


(e) Poisson’s ratio

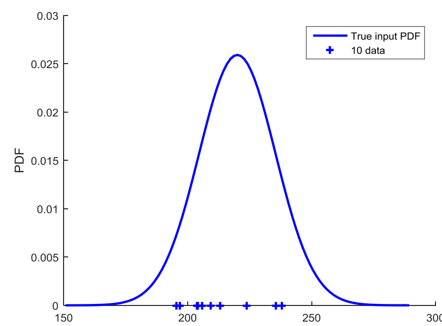


(f) Yield strength

Figure 7.9 Ten Input Data Randomly Drawn from True Input Distribution

To generate small number of output test data, only five test data are randomly drawn from the true output distribution for each constraint. It is noted that the five data for constraint 2 are quite biased since all five data comes from the left tail of the true output distribution. In particular, one of them is drawn from the left tail end of the true output distribution. As a result, it is anticipated that this biased data can lead to gross overestimation of reliability.

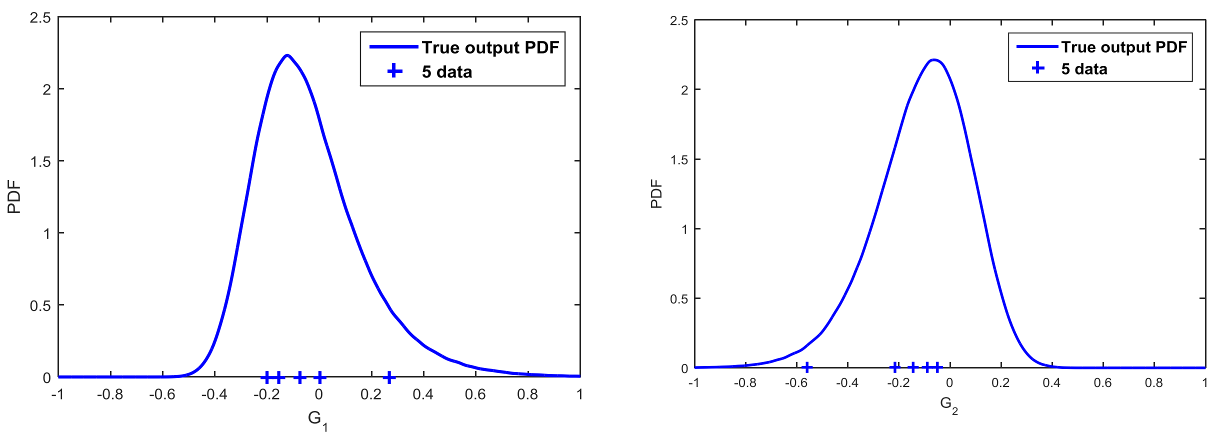


(a) Constraint 1 (b) Constraint 2

Figure 7.10 Five Output Test Data Randomly Drawn from True Output Distribution

Given ten input data and biased model, biased simulation output distribution can be obtained as shown in Figure 7.11. The corresponding simulation-based reliability can be evaluated as 93.04% for $G_1$ and 96.06% for $G_2$, which grossly overestimates the true reliabilities (63.91% for $G_1$ and 69.97% for $G_2$). On the other hand, the proposed method generate 1000 possible reliabilities ($nMCS_h$ in Eq. (7-7) are set to 1000) and construct the CCDF of reliability as shown in Figure 7.12. At 90% target confidence level, the confidence-based reliabilities are 52.81% for $G_1$ and 65.13% for $G_2$. It is highlighted that the proposed confidence-based reliability is less (*i.e.*, more conservative) than true reliability. In addition, Table 7.5 summarizes the result of the proposed confidence method and compares it with existing reliability estimation methods (output best-fit method and simulation-based method). It is noted that output best-fit method provides the reliabilities of 67.65% for $G_1$ and 95.03% for $G_2$, which are overestimating true reliability. In particular, as for constraint 2, the output best-fit reliability is very high, which could lead to a wrong decision to design product in the RBDO process. This may be due to the biased data illustrated in Figure 7.10. Also, simulation-based reliabilities overestimate reliability with well over than 90% reliabilities. Therefore, it is concluded that both output best-fit method and simulation-based method cannot induce right decision for very small number of data. Whereas, the proposed method yields conservative reliability estimation even with small number of data.

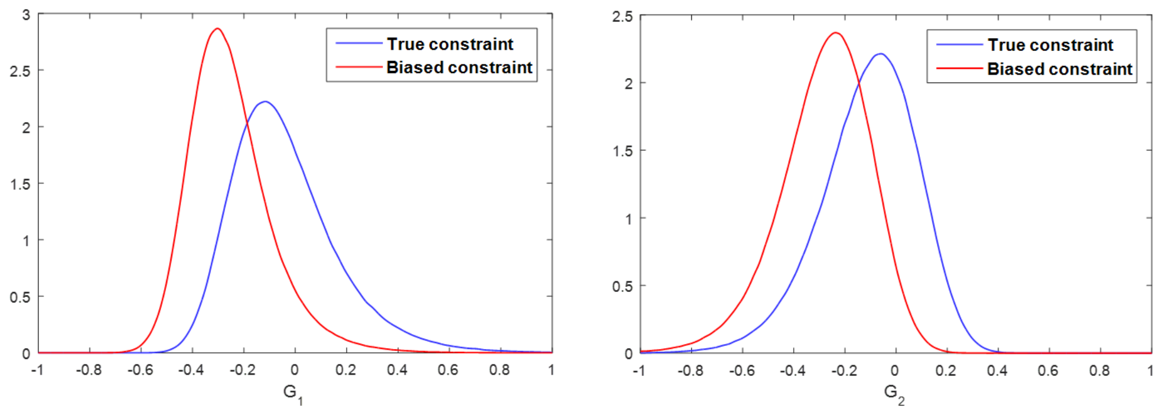


Figure 7.11 Comparison of True Output PDF and Biased Simulation Output PDF (Left: Constraint 1 and Right: Constraint 2)

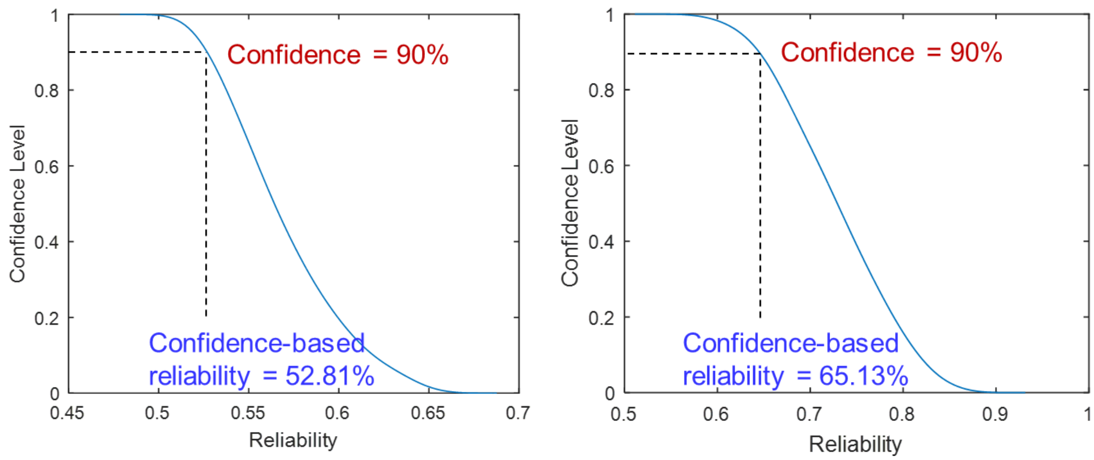


Figure 7.12 CCDF of Reliability and Confidence Level Given Ten Input/Five Output Data (Left: Constraint 1 and Right: Constraint 2)

Table 7.5 Comparison of Reliability under Different Methods for Ten Input/Five Output Data

| Reliability | Constraints | |
|---|---|---|
| | $G_1$ | $G_2$ |
| Confidence-based method | 52.81% | 65.13% |
| Output best-fit method | 67.65% | 95.03% |
| Simulation-based method | 93.04% | 96.06% |
| True | 63.91% | 69.97% |

7.3.3. Verification of Confidence Level

In this section, it is checked whether the proposed confidence-based reliability satisfies the target confidence level. In Section 5.1.2, the confidence level was demonstrated in the developed confidence-based model validation considering only limited number of physical output test data. This section demonstrates the confidence level used in the proposed confidence-based reliability estimation that accounts for both insufficient input/output test data. However, it is not easy to theoretically prove that the confidence-based reliability is conservative. For this reason, the confidence level is numerically demonstrated by repeating 100 times of confidence-based reliability assessment with independently generated 100 sets of input/output test data. Each set includes 30 input/20 output data which are randomly drawn from the true input distribution for each of six variables described in Table 7.2 and the true output distribution for two constraints, respectively. It is noted that this 100 repeated tests have been carried out on the HPC system—Excalibur (30-50 nodes in parallel; each node has 32 cores and 128 GB memory)—at the U.S. ARL because 100 trials require heavy computational time. One confidence-based reliability assessment for 20 input/10 output data takes around 66 hours using 30 cores and 128 GB memory. Thus, carrying out 100 trials would not be easily achievable as it would take around 275 days in order to complete it. On the other hand, using the ARL HPC, we have been able to successfully finish 100 trials within two weeks.

Figures 7.13 and 7.14 show the histograms of confidence-based reliabilities and reliabilities obtained using output best-fit method for 100 trials, respectively. It can be noticed that, using the proposed confidence-based method, 89 trials for constraint 1 and 95 trials for constrain 2 among 100 trials with different data sets are conservatively estimating the true reliability. This implies that the proposed method satisfies 90% of target confidence level. On the other hand, the output best-fit method does not provide enough confidence level because only 65 trials for constraint 1 and 67 trials for constraint

2 are conservative reliability estimations. Table 7.6 compares the reliabilities between confidence-based method and best-fit method. The mean value, standard deviation, maximum, and minimum value of 100 confidence-based reliabilities at 90% target confidence level are summarized. Those values can be compared with the mean value, standard deviation, maximum and minimum values of 100 output best-fit reliabilities. It is worth noting that when using the best-fit method, maximum value (84.31% for constraint 1 and 92.01% for constraint 2) is much higher than the one for confidence-based method (70.74% for constraint 1 and 78.54% for constraint 2). Therefore, this indicates that output best-fit method can significantly overestimate reliability for certain data sets.

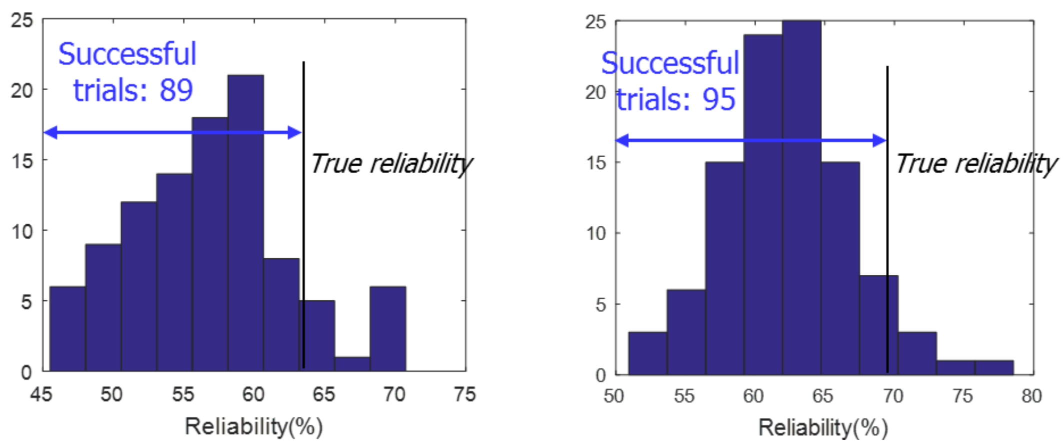


Figure 7.13 Histogram of Confidence-Based Reliabilities Obtained by 100 Repeated Tests (Left: Constraint 1 and Right: Constraint 2)

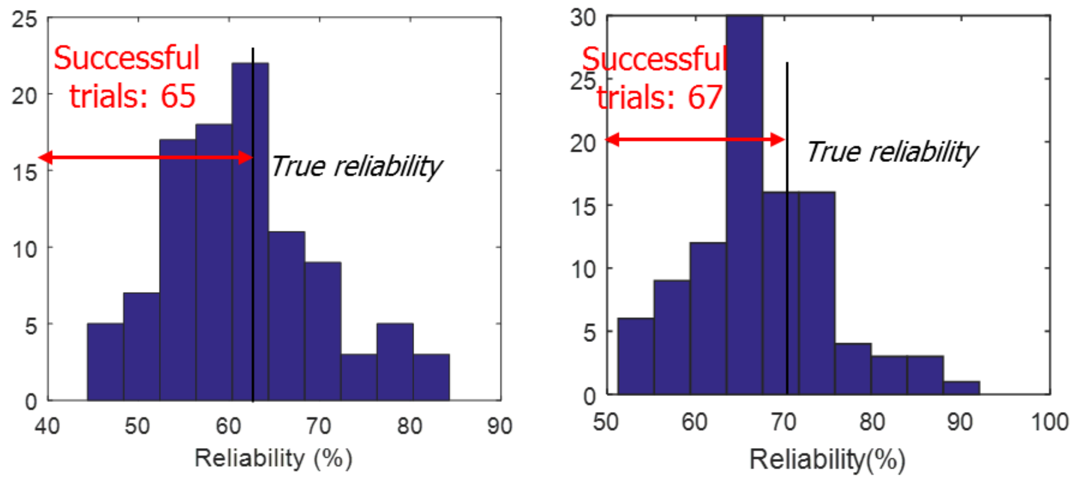


Figure 7.14 Histogram of Output Best-Fit Reliabilities Obtained by 100 Repeated Tests (Left: Constraint 1 and Right: Constraint 2)

Table 7.6 Statistical Summary of the Results for 100 Trials of Confidence-Based Method and Output Best-Fit Method

| | Confidence-based method at 90% target confidence level | | Output Best-fit method | |
|---|---|---|---|---|
| | Constraint 1 | Constraint 2 | Constraint 1 | Constraint 2 |
| Mean | 56.76% | 62.31% | 61.59% | 67.36% |
| Standard deviation | 5.65% | 4.79% | 8.46% | 7.71% |
| Maximum | 70.74% | 78.54% | 84.31% | 92.01% |
| Minimum | 45.52% | 50.93% | 44.37% | 51.25% |
| True reliability | 63.91% | 69.97% | 63.91% | 69.97% |
| # of successful trial | 89 | 95 | 65 | 67 |

## 7.4. Numerical Test using 11-D Vehicle Side Impact Problem

In this section, the proposed confidence-based reliability assessment is demonstrated using 11-D vehicle side impact problem (Gu et al., 2001; Youn, Choi, Yang & Gu, 2004). Table 7.7 shows the true input distributions of 11 input random variables. To represent a practical situation, it is assumed that we only know true input distributions for $X_1$~$X_7$ which are thicknesses of steel plates. On the other hand, only limited numbers of data are available for material properties ($X_8$~$X_9$) and crash experiment properties ($X_{10}$~$X_{11}$).

Table 7.7 Summary of Input Variable Information for 11-D Vehicle Side Impact Problem

| | Description | True input distribution | | | Remark |
| --- | --- | --- | --- | --- | --- |
| | | Type | Mean | STD | |
| $X_1$ | B-pillar inner | Normal | 0.5 | 0.015 | True input distribution models are known |
| $X_2$ | B-pillar reinforce | | 1.3 | 0.039 | |
| $X_3$ | Floor side inner | | 0.5 | 0.015 | |
| $X_4$ | Cross member | | 1.3 | 0.039 | |
| $X_5$ | Door beam | | 1.1 | 0.033 | |
| $X_6$ | Door belt line | | 1.5 | 0.045 | |
| $X_7$ | Roof rail | | 0.5 | 0.015 | |
| $X_8$ | Mat. B-pillar inner | Log Normal | 0.345 | 0.0242 | Only ten limited number of data is given |
| $X_9$ | Mat. Floor side inner | | 0.192 | 0.0134 | |
| $X_{10}$ | Barrier height | Normal | 0 | 10 | |
| $X_{11}$ | Barrier hitting | | 0 | 10 | |

Out of ten constraints related to internal and regulated side impact requirements given in the reference paper (Youn, Choi, Yang & Gu, 2004), only three active constraints are used in this example as:

Constraint 1: lower rib deflection – 32mm ≤ 0

Constraint 2: pubic symphysis force – 4.0kN ≤ 0

Constraint 3: velocity of front door at B-pillar – 15.7mm/ms ≤ 0

Biased constraint $G_i(\mathbf{x})$ is formulated by subtracting bias $B_i(\mathbf{x})$ from true output model $G_i^{true}(\mathbf{x})$ as $G_i(\mathbf{x}) = G_i^{true}(\mathbf{x}) - B_i(\mathbf{x})$. The true output models (*i.e.*, true physical output) are defined as

$$\begin{aligned} G_1^{true}(\mathbf{x}) &= 14.36 + \left(-9.9x_2 - 12.9x_1x_8 + 0.1107x_3x_{10}\right) \\ G_2^{true}(\mathbf{x}) &= 0.72 + \begin{pmatrix} -0.5x_4 - 0.19x_2x_3 - 0.0122x_4x_{10} \\ +0.009325x_6x_{10} + 0.000191x_{11}^2 \end{pmatrix} \\ G_3^{true}(\mathbf{x}) &= 1.35 + \begin{pmatrix} -0.489x_3x_7 - 0.843x_5x_6 + 0.0432x_9x_{10} \\ -0.0556x_9x_{11} - 0.000786x_{11}^2 \end{pmatrix} \end{aligned} \quad (7\text{-}10)$$

and biases for three constraints (included in the simulation model) are given by

$$\begin{aligned} B_1(\mathbf{x}) &= 1.67x_1^{2.3} + 2.6x_2 - 0.017x_8x_{10}^2 \\ B_2(\mathbf{x}) &= 0.16x_4^{2.4} \\ B_3(\mathbf{x}) &= 0.79\left(2x_6 - x_5\right) - 0.00013x_{10}^2x_{11} \end{aligned} . \quad (7\text{-}11)$$

To obtain the error level of the biased simulation model, the biased simulation model outputs have been compared with those obtained using the true model in Eq. (7-10). As shown in Table 7.8, the error is around 10% of true model. In this 11-D vehicle side impact problem, instead of using actual function of biased constraints, DKG surrogate models (Song et al., 2013a; Zhao et al., 2011) have been generated using the biased constraints as CAE simulations at the design of experiment (DoE) points.

Table 7.8 Accuracy of Biased Simulation Model for 11-D Vehicle Side Impact Problem

| | Deterministic Output | | |
|---|---|---|---|
| | $G_1$ | $G_2$ | $G_3$ |
| Biased simulation model $(a)$ | 27.700 | 3.643 | 13.822 |
| True model $(b)$ | 30.834 | 3.944 | 15.323 |
| Error $\left(\frac{b-a}{b} \times 100\right)$ | 10.16% | 7.63% | 9.80% |

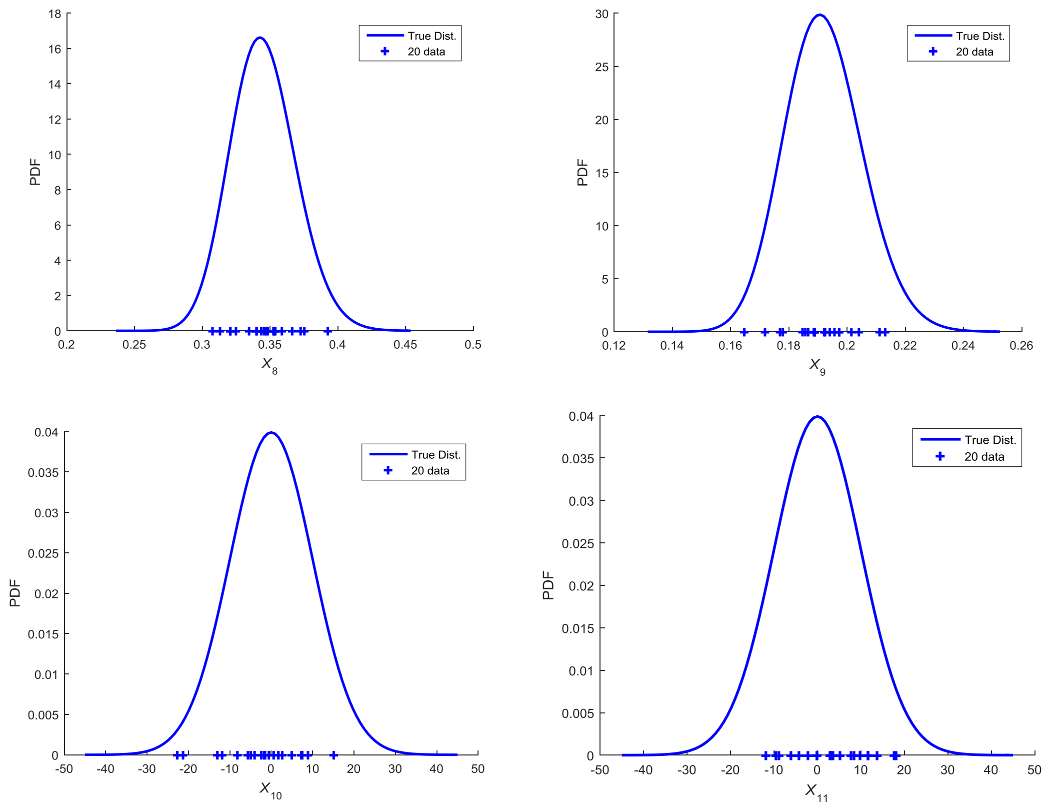


Figure 7.15 20 Input Data Randomly Drawn From True Input Distribution for Each of Four Variables ($X_8$~$X_{11}$)

Similar to 9-D cantilever tube-shaped beam example in the Section 7.3, two different numbers of data cases – 1) 20 input/ten output data and 2) ten input/five output data – are studied. In Case 1, 20 limited number of data for each of four variables ($X_8$~$X_{11}$) are randomly drawn from true input distribution to mimic testing as shown in Figure 7.15. In addition, ten output data, which are randomly generated from true output distribution to mimic physical testing, are used for each constraint. Figure 7.16 shows how ten data are distributed.

Using the proposed confidence-based method, the CCDF of reliability is obtained as shown in Figure 7.17. Total 1000 MCS samples are generated to construct the CCDF of reliability. At 90% target confidence level, the confidence-based reliabilities are evaluated as 74.66% for $G_1$, 66.40% for $G_2$ and 70.98% for $G_3$. In addition, for the purpose of comparison, two other methods have been carried out: the simulation-based method and the output best-fit method. Hence, the simulation model is not used for the output best-fit method. Table 7.9 lists confidence-based reliability, output best-fit reliability and simulation-based reliability. It can be found that both the simulation-based reliability and output best-fit reliability overestimate the true reliability. On the other hand, the confidence-based reliability is conservative compared to the true reliability. In particular, both simulation-based reliability and output best-fit reliability for $G_2$ and $G_3$ are very close to 100% which could mislead to wrong decision on product design. However, the developed method can prevent the wrong decision by providing conservative estimation of the reliability.

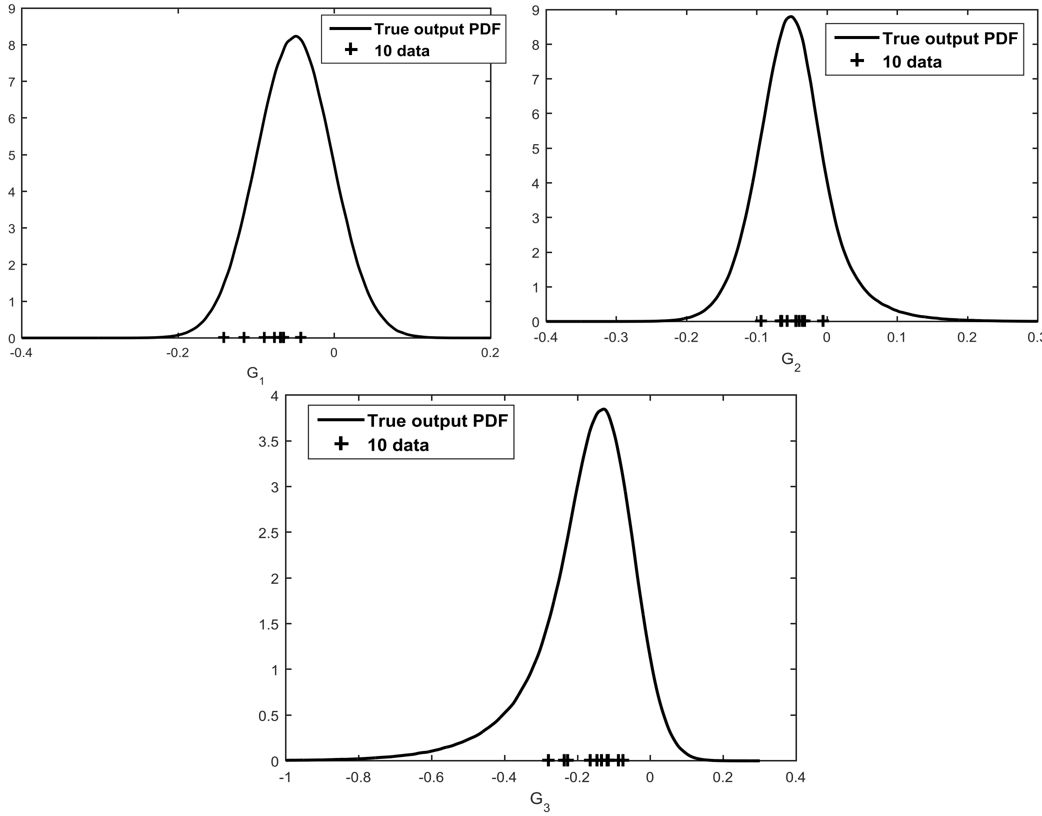


Figure 7.16 Ten Output Data Randomly Drawn From True Output Distribution (Top-Left: Constraint 1, Top-Right: Constraint 2, and Bottom: Constraint 3)

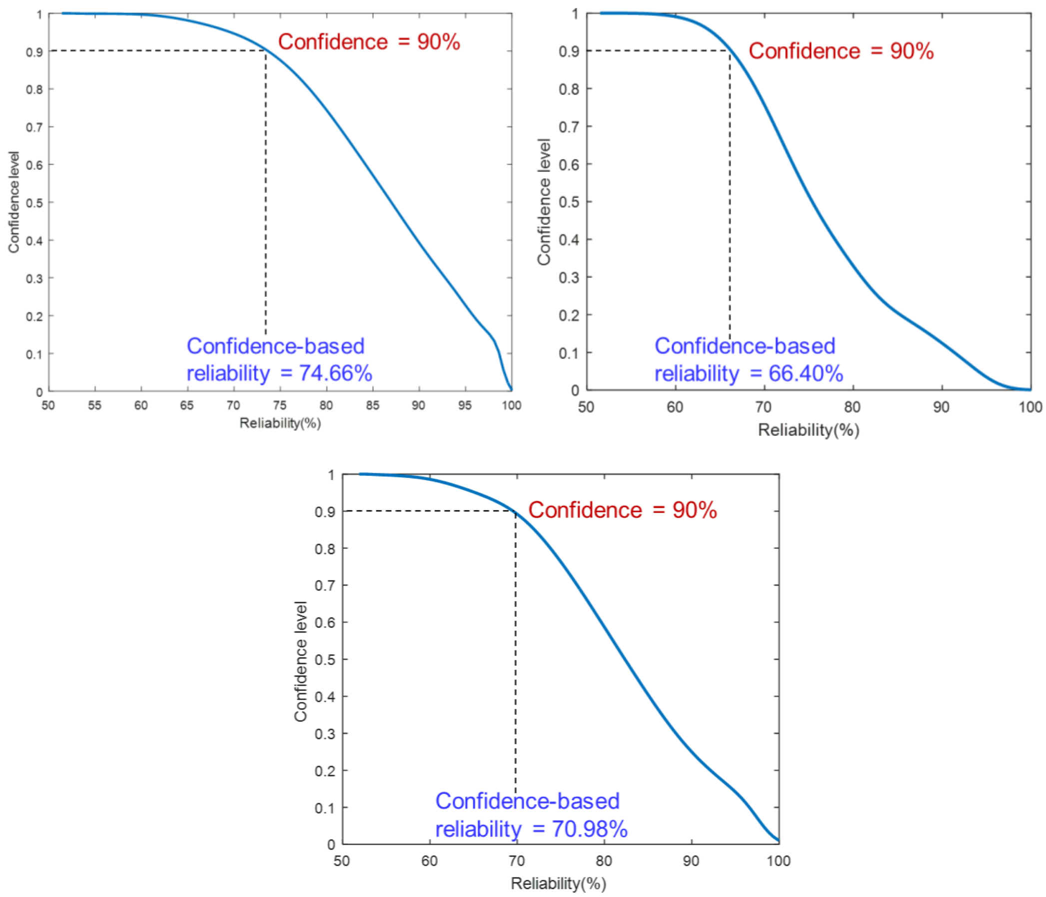


Figure 7.17 CCDF of Reliability and Confidence-Based Reliability Given 20 Input/Ten Output Data (Top-Left: Constraint 1, Top-Right: Constraint 2, and Bottom: Constraint 3)

Table 7.9 Comparison of Different Methods in the Estimation of Reliability Given 20 Input/Ten Output Data

| Reliability | Constraints | | |
|---|---|---|---|
| | $G_1$ | $G_2$ | $G_3$ |
| Confidence-based method | 74.66% | 66.40% | 70.98% |
| Output best-fit method | 100.00% | 96.25% | 99.98% |
| Simulation-based method | 98.56% | 100.00% | 99.68% |
| True | 85.46% | 84.88% | 95.55% |

In Case 2 of experimental situation, numbers of input data for $X_8$~$X_{11}$ are decreased to ten, which are randomly drawn from true input distribution as shown in Figure 7.18. Also, only five output data for each constraint are considered, which are plotted in Figure 7.19. Using the proposed confidence-based reliability assessment, the CCDF of reliability can be obtained as shown in Figure 7.20. At the 90% target confidence level, confidence-based reliability is obtained as 61.20% for $G_1$, 62.05% for $G_2$, and 59.00% for $G_3$, which significantly underestimate true reliabilities. It is worth noting that the confidence-based reliability for smaller number of data is more conservative than the one (74.66% for $G_1$, 66.40% for $G_2$ and 70.98% for $G_3$) for Case 1 (20 input/ten output data). Because the numbers of data are smaller, the uncertainty becomes larger. As a result, it is found that the possible range of reliability (*i.e.*, the support size of CCDF of reliability) become wider than that of reliability for Case 1, which can be observed from the horizontal axes in Figures 7.17 and 7.20 . Table 7.10 shows that both output best-fit method and simulation-based method significantly overestimate the reliability; while the proposed confidence-based method conservatively estimates the reliability.

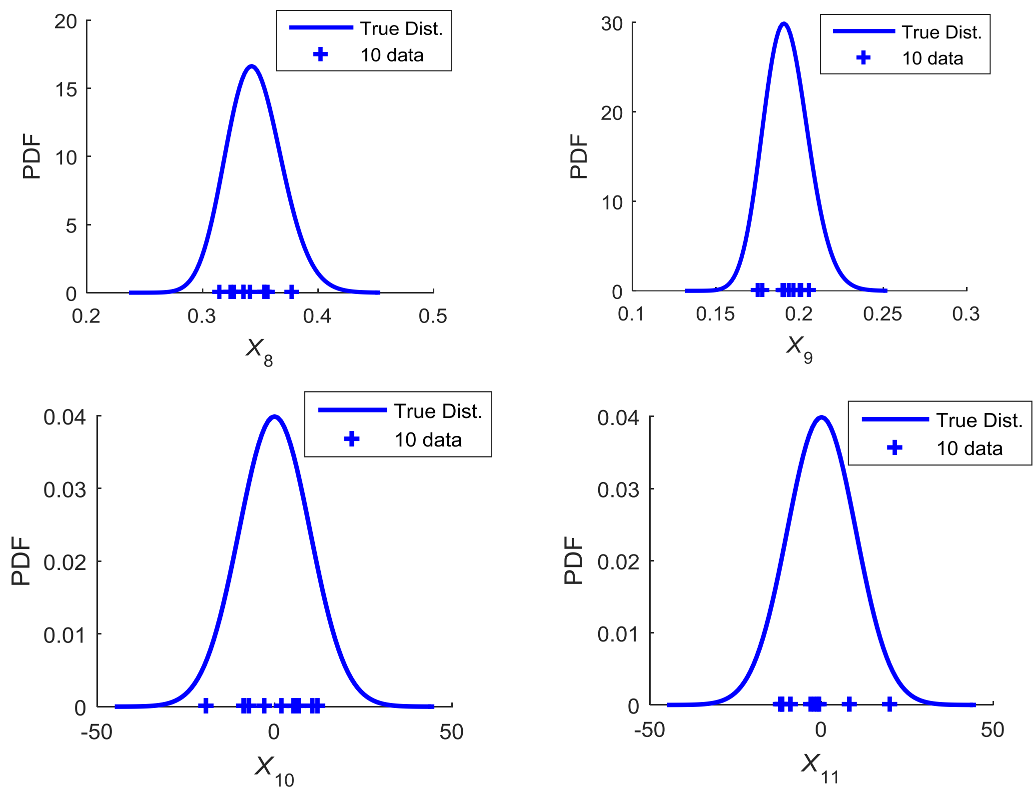


Figure 7.18 Ten Input Data Randomly Drawn From True Input Distribution for Each of Four Variable ($X_8$~$X_{11}$)

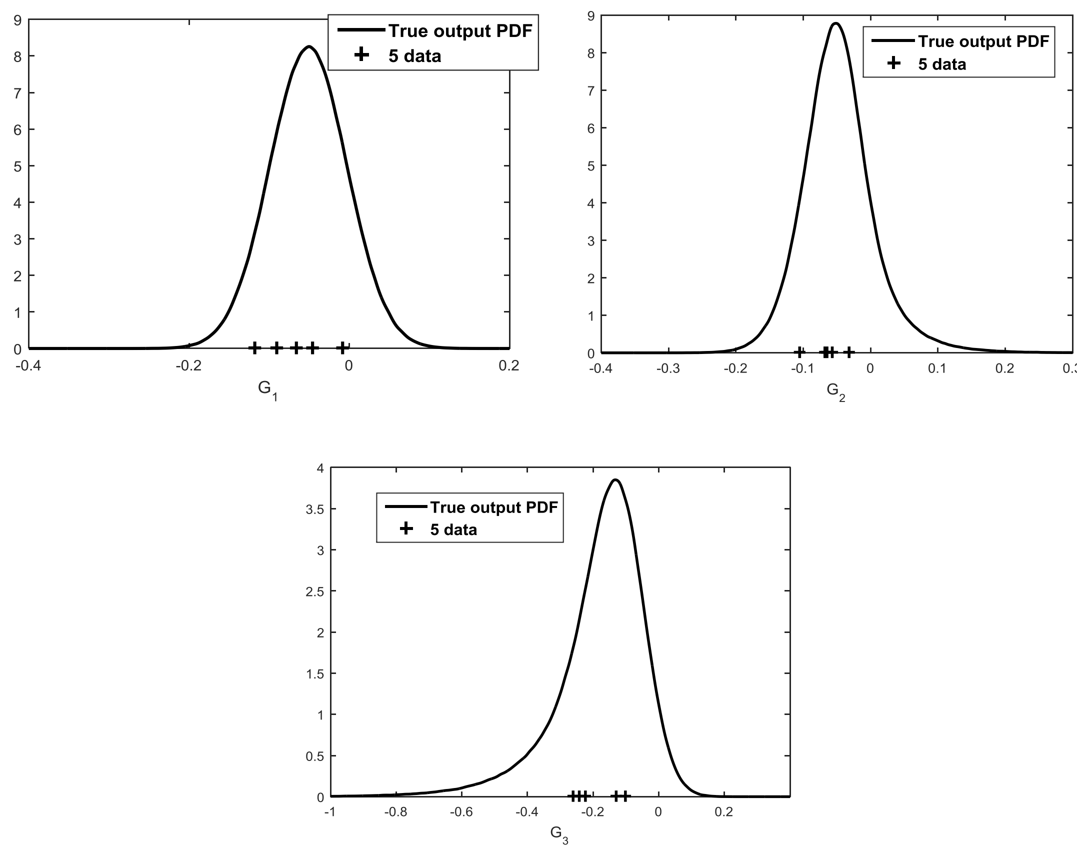


Figure 7.19 Five Output Data Randomly Drawn From True Output Distribution (Top-Left: Constraint 1, Top-Right: Constraint 2, and Bottom: Constraint 3)

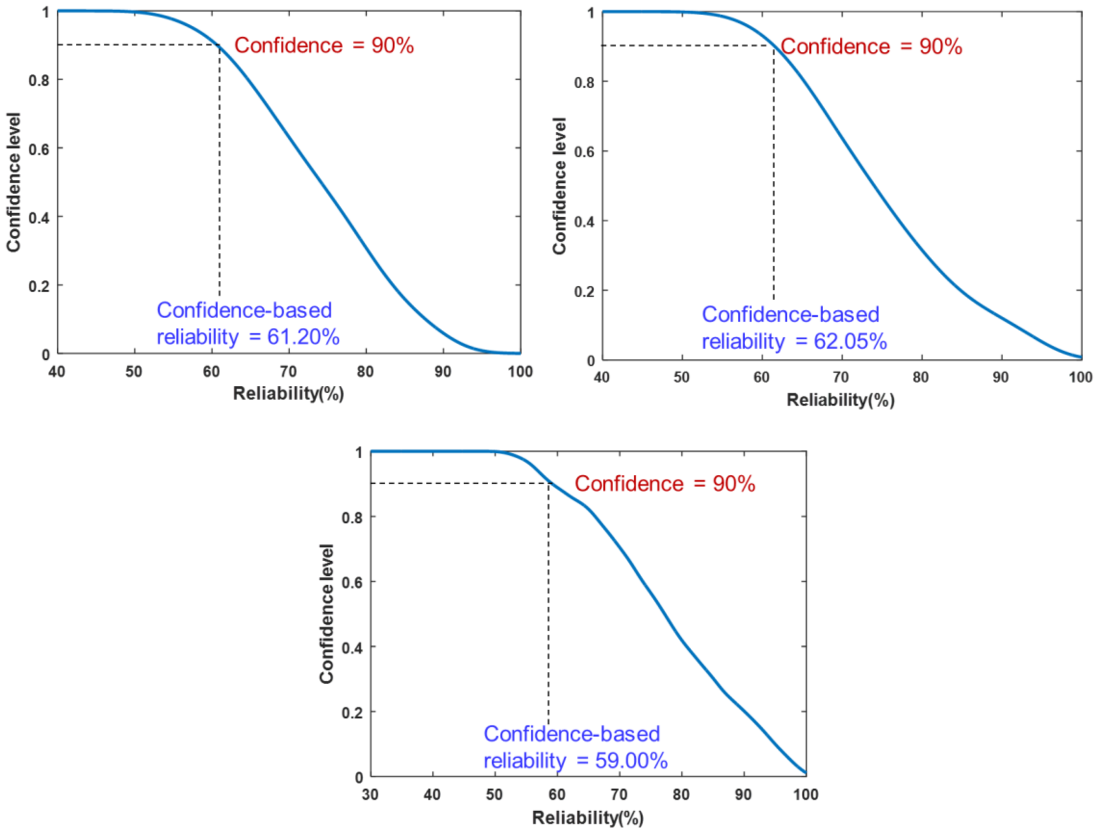


Figure 7.20 CCDF of Reliability and Confidence-Based Reliability Distribution (Top-Left: Constraint 1, Top-Right: Constraint 2, and Bottom: Constraint 3)

Table 7.10 Comparison of Different Methods in the Estimation of Reliability Given Ten Input/Five Output Data

| Reliability | Constraints | | |
|---|---|---|---|
| | $G_1$ | $G_2$ | $G_3$ |
| Confidence-based method | 61.20% | 62.05% | 59.00% |
| Output best-fit method | 91.19% | 99.93% | 99.61% |
| Simulation-based method | 99.50% | 99.93% | 99.96% |
| True | 85.46% | 84.88% | 95.55% |

In this 11-D vehicle side impact problem, we asked the same question whether the proposed method truly satisfies target confidence level. Therefore, 100 times of confidence-based reliability assessment have been carried out with independenlty drawn 100 sets of input/output test data. Each set contains ten input test data and five output test data, which are randomly drawn from true input and output distributions, respectively. A comparison study between two methods, the proposed confidence-based method and output best-fit method, has been carried out. In the proposed method, target confidence level is set to 90%. Figure 7.21 and Figure 7.22 illustrate the histograms of confidence-based reliability and output best-fit reliability for 100 trials, respectively. Based on the histograms obtained for both methods, we can calculate how many trials conservatively estimate (less than) true reliability among 100 trials. The confidence-based method satisfies target confidence level of 90% − 100% for $G_1$, $G_2$ and $G_3$, whereas output best-fit method does not provide enough confidence − 63% for $G_1$, 50% for $G_2$ and 54% for $G_3$. In addition, it can be noticed that the right-tail of histogram for output best-fit method in Figure 7.22 is heavier than one for the confidence-based method in Figure 7.21. This indicates that many data sets yield almost 100% reliability estimation when using output best-fit method. Thus, it is demonstrated that by utilizing either only physical test data or simulation model, we cannot build enough confidence in the estimation of reliability. In contrast, the proposed method can prevent the dangerous overestimation of reliability. In conclusion, by using both physical test data and simulation model, the proposed method can save cost and provide conservative reliability estimation. On the other hand, the confidence-based method seemed to yield too conservative estimation of the reliability, which needs to be further investigated.

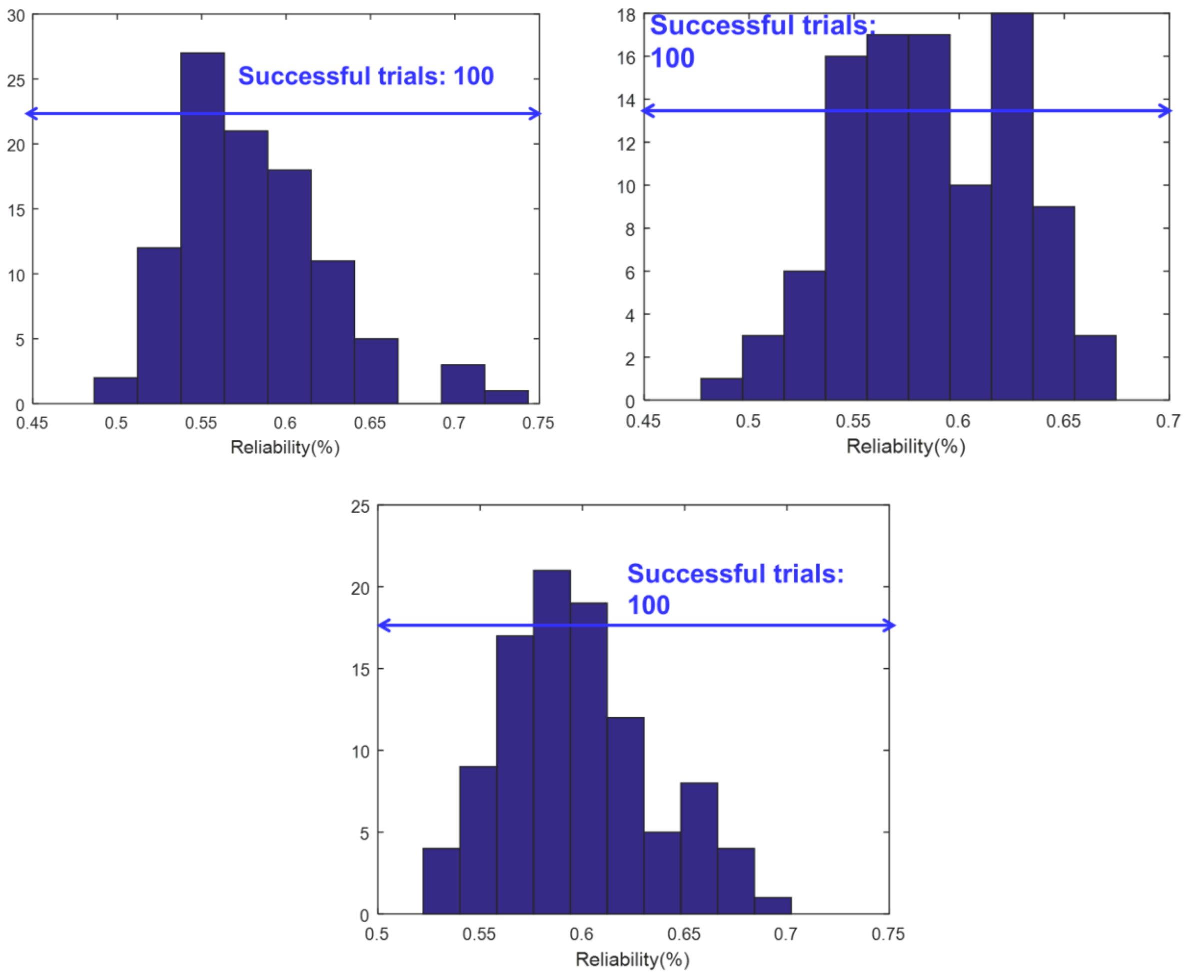


Figure 7.21 Histogram of Confidence-Based Reliabilities Obtained by 100 Repeated Tests (Top-Left: Constraint 1, Top-Right: Constraint 2 and Bottom: Constraint 3)

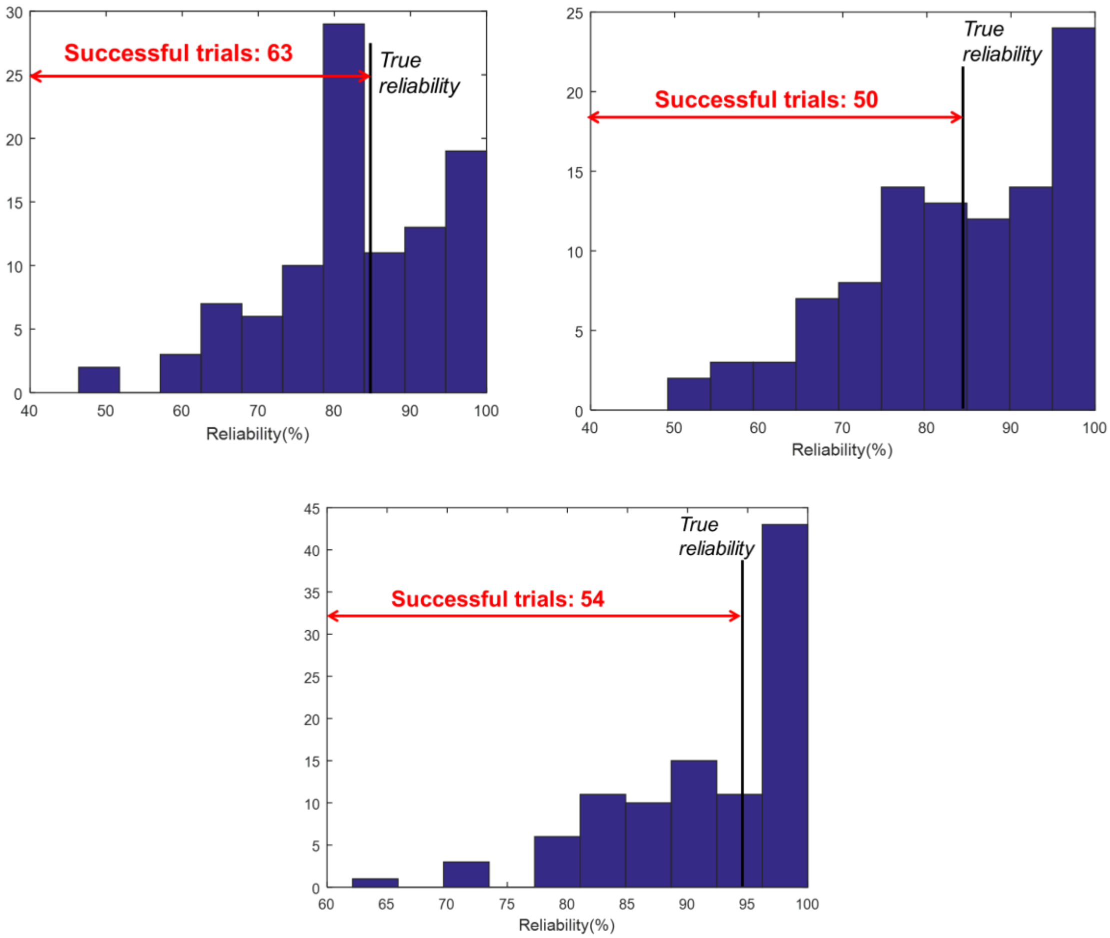


Figure 7.22 Histogram of Output Best-Fit Reliabilities Obtained by 100 Repeated Tests (Top-Left: Constraint 1, Top-Right: Constraint 2 and Bottom: Constraint 3)

# CHAPTER 8

# CONCLUSIONS AND FUTURE WORK

In this study, we have developed confidence-based model validation for reliability estimation when experimental output data is insufficient. The proposed confidence-based model validation takes the uncertainty induced by insufficient experimental output data as well as inherent input variability into consideration to conservatively estimate the probability of failure. The distribution (CDF) of probability of failure, which is an outcome of the uncertainty induced by insufficient experimental output data, has been quantified using the sampling-based Bayesian analysis. After that, the probability of failure and target output PDF are selected at the user-specified target confidence level. Then, the validated simulation model can be obtained using model bias correction by matching the simulation output PDF with the confidence-based target output PDF. Furthermore, it has been demonstrated that the validated simulation model using the proposed confidence-based model validation satisfies the target confidence level and converges to the true model as the experimental output data size increases.

Next, the developed confidence-based model validation has been integrated into the sampling-based RBDO process, which assures a reliable and conservative optimum design with certain probability (target confidence level). To handle the uncertainty, the RBDO constraint has been conservatively estimated at a target confidence level to achieve the conservativeness of the RBDO optimum design. Furthermore, the moving-target problem that occurs in the RBDO process with model validation has been discussed. It has been numerically demonstrated that, when enough experimental output data is given, the moving-target problem can be solved. To resolve the moving-target problem for insufficient experimental output data, a practical RBDO procedure using confidence-based model validation has been proposed. It has been demonstrated that the practical RBDO procedure can provide a conservative and reliable optimum design by using experimental output data at only a few design configurations. Therefore, the effectiveness and efficiency of the practical RBDO procedure using confidence-based model validation has been verified. The practical RBDO has been applied to two types of biased models: (1) non-conservative and (2) conservative simulation models, respectively. For the non-conservative simulation model, the conventional RBDO optimum does not satisfy the target probability of failure, which leads to unreliable design. However, the proposed RBDO can make a conservative and reliable design. As for the conservative simulation model, two different amounts of bias have been tested: (1) a small biased model and (2) a significantly biased model. For the conventional RBDO optimum design using a small biased model, the proposed RBDO provides a more conservative and reliable design than the conventional RBDO as the uncertainty is induced by insufficient experimental output data. On the other hand, when the simulation model is significantly biased, the proposed RBDO makes a less conservative and better reliable optimum design than the conventional RBDO design. In all cases, the proposed RBDO using confidence-based model validation aims to provide the designer with confidence that the design produced would be reliable even with insufficient experimental output data.

Aforementioned confidence-based model validation and its integration with RBDO using confidence-based validation assume that input variability is precisely known (*i.e.*, no parameter uncertainty), which may not be real practical situation. Thus, new confidence-based reliability assessment that accounts for input parameter uncertainty as well as model bias when limited number of input/output is given has been developed. When a small amount of input data is available due to a limited number of coupon tests, the true input distribution model cannot be accurately obtained. Thus, there exists the uncertainty due to limited number of input data, the uncertainty due to limited number of experimental output data, as well as the biased simulation model. To combine all uncertainties due to limited number of input/output data and model bias, hierarchical

Bayesian analysis is carried out to obtain the uncertainty distribution (CCDF) of reliability that can provide confidence level of reliability. Thus, the proposed confidence-based reliability method provides the conservative reliability estimation at the target confidence level that engineers set. It is numerically demonstrated that the proposed method satisfies the target confidence level that the true reliability is larger than the estimated reliability. The proposed method can be applied to many practical engineering problems because their experimental situation necessitates reliability assessment with confidence.

In the future, the developed confidence-based reliability method needs to be tested using various industry applications. Second, output PDF modeling method can be further improved because AKDE that is chosen in this study has a limitation. Since there exists only one unknown parameter, bandwidth, the obtained confidence-based target PDF is highly dominated by bandwidth. In addition, the proposed reliability assessment method can be further extended to obtain validated simulation model by correcting model bias. Then, the obtained model bias can provide useful information that how much simulation model is biased to engineers.

# REFERENCES


AIAA. (1998). Guide for the verification and validation of computational fluid dynamics simulations. *Am. Institute of Aeronautics and Astronautics*.

Arendt, P. D., Apley, D. W. & Chen, W. (2012a). Quantification of model uncertainty: Calibration, model discrepancy, and identifiability. *Journal of Mechanical Design, 134*(10), 100908.

Arendt, P. D., Apley, D. W., Chen, W., Lamb, D. & Gorsich, D. (2012b). Improving identifiability in model calibration using multiple responses. *Journal of Mechanical Design, 134*(10), 100909.

Arora, J. (2004). *Introduction to optimum design*: Academic Press.

ASME. (2006). Guidelines for the verification and validation in computational solid mechanics. *American Society of Mechanical Engineers*(ASME Standard V&V 10-2006).

Chen, W., Xiong, Y., Tsui, K.-L. & Wang, S. (2006). *Some metrics and a Bayesian procedure for validating predictive models in engineering design.* Paper presented at the ASME 2006 International Design Engineering Technical Conferences and Computers and Information in Engineering Conference.

Chiralaksanakul, A. & Mahadevan, S. (2005). First-order approximation methods in reliability-based design optimization. *Journal of Mechanical Design, 127*(5), 851-857.

Cho, H. (2014). Efficient variable screening method and confidence-based method for reliability-based design optimization.

Cho, H., Choi, K., Gaul, N. J., Lee, I., Lamb, D. & Gorsich, D. (2016). Conservative reliability-based design optimization method with insufficient input data. *Structural and Multidisciplinary Optimization*, 1-22.

Choi, J., An, D. & Won, J. (2010). Bayesian approach for structural reliability analysis and optimization using the Kriging Dimension Reduction Method. *Journal of Mechanical Design, 132*(5), 051003.

DoD. (1994). DoD Driective No. 5000.59: Modeling and simulation (M&S) Management.

Drignei, D., Mourelatos, Z. P., Kokkolaras, M., Pandey, V. & Koscik, G. (2012a). A variable-size local domain approach for increased design confidence in simulation-based optimization. *Structural and Multidisciplinary Optimization, 46*(1), 83-92.

Drignei, D., Mourelatos, Z. P., Pandey, V. & Kokkolaras, M. (2012b). Concurrent design optimization and calibration-based validation using local domains sized by bootstrapping. *Journal of Mechanical Design, 134*(10), 100910.

Epanechnikov, V. A. (1969). Non-parametric estimation of a multivariate probability density. *Theory of Probability & Its Applications, 14*(1), 153-158.

Ferson, S., Oberkampf, W. L. & Ginzburg, L. (2008). Model validation and predictive capability for the thermal challenge problem. *Computer Methods in Applied Mechanics and Engineering*, *197*(29), 2408-2430.

Gu, L., Yang, R., Tho, C., Makowskit, M., Faruquet, O. & Y. Li, Y. L. (2001). Optimisation and robustness for crashworthiness of side impact. *International Journal of Vehicle Design, 26*(4), 348-360.

Gunawan, S. & Papalambros, P. Y. (2006). A bayesian approach to reliability-based optimization with incomplete information. *Journal of Mechanical Design*, *128*(4), 909-918.

Haldar, A. & Mahadevan, S. (2000). *Probability, reliability, and statistical methods in engineering design* (Vol. 1): Wiley New York.

Hasofer, A. M. & Lind, N. C. (1974). Exact and invariant second-moment code format(for reliability analysis in multivariate problems). *American Society of Civil Engineers, Engineering Mechanics Division, Journal*, *100*, 111-121.

Henderson, D. J. & Parmeter, C. F. (2012). Normal reference bandwidths for the general order, multivariate kernel density derivative estimator. *Statistics & Probability Letters*, *82*(12), 2198-2205.

Higdon, D., Nakhleh, C., Gattiker, J. & Williams, B. (2008). A Bayesian calibration approach to the thermal problem. *Computer Methods in Applied Mechanics and Engineering, 197*(29), 2431-2441.

Hohenbichler, M. & Rackwitz, R. (1988). Improvement of second-order reliability estimates by importance sampling. *Journal of Engineering Mechanics, 114*(12), 2195-2199.

IEEE. (1984). IEEE Standard Dictionary of Electrical and Electronics Terms, ; The Institute of Electrical and Electronics Engineers. *Inc.: New York.*

IEEE. (1990). IEEE standard glossary of software engineering terminology. *IEEE Std, 610121990*(121990), 3.

Jiang, Z., Chen, W., Fu, Y. & Yang, R.-J. (2013). Reliability-based design optimization with model bias and data uncertainty. *SAE International Journal of Materials and Manufacturing, 6*(2013-01-1384), 502-516.

Kennedy, M. C. & O'Hagan, A. (2001). Bayesian calibration of computer models. *Journal of the Royal Statistical Society: Series B (Statistical Methodology), 63*(3), 425-464.

Klir, G. J. & Folger, T. A. (1988). Fuzzy sets, uncertainty, and information.

Kullback, S. & Leibler, R. A. (1951). On information and sufficiency. *The annals of mathematical statistics, 22*(1), 79-86.

Lee, I., Choi, K., Du, L. & Gorsich, D. (2008). Dimension reduction method for reliability-based robust design optimization. *Computers & Structures, 86*(13), 1550-1562.

Lee, I., Choi, K. & Gorsich, D. (2010). System reliability-based design optimization using the MPP-based dimension reduction method. *Structural and Multidisciplinary Optimization, 41*(6), 823-839.

Lee, I., Choi, K. & Zhao, L. (2011a). Sampling-based RBDO using the stochastic sensitivity analysis and Dynamic Kriging method. *Structural and Multidisciplinary Optimization, 44*(3), 299-317.

Lee, I., Choi, K. K., Noh, Y., Zhao, L. & Gorsich, D. (2011b). Sampling-based stochastic sensitivity analysis using score functions for RBDO problems with correlated random variables. *Journal of Mechanical Design, 133*(2), 021003.

Loeppky, J., Bingham, D. & Welch, W. (2006). Computer model calibration or tuning in practice. *Technometrics, submitted for publication*.

Martins, J. R., Sturdza, P. & Alonso, J. J. (2003). The complex-step derivative approximation. *ACM Transactions on Mathematical Software (TOMS), 29*(3), 245-262.

Moon, M.-Y., Choi, K., Cho, H., Gaul, N., Lamb, D. & Gorsich, D. (2015). *Development of a Conservative Model Validation Approach for Reliable Analysis.* Paper presented at the ASME 2015 International Design Engineering Technical Conferences and Computers and Information in Engineering Conference.

Moon, M.-Y., Choi, K., Cho, H., Gaul, N., Lamb, D. & Gorsich, D. (2016). *Reliability-Based Design Optimization Using Confidence-Based Model Validation for Insufficient Experimental Data.* Paper presented at the ASME 2016 International Design Engineering Technical Conferences and Computers and Information in Engineering Conference.

Moon, M.-Y., Choi, K. K., Cho, H., Gaul, N., Lamb, D. & Gorsich, D. (2017). Reliability-based design optimization using confidence-based model validation for insufficient experimental data. *Journal of Mechanical Design, 139*(3), 031404-031404-031410. doi: 10.1115/1.4035679

Nikulin, M. S. (2001). Hellinger distance. *Encyclopedia of Mathematics*.

Noh, Y., Choi, K., Lee, I., Gorsich, D. & Lamb, D. (2011a). Reliability-based design optimization with confidence level under input model uncertainty due to limited test data. *Structural and Multidisciplinary Optimization, 43*(4), 443-458.

Noh, Y., Choi, K. K., Lee, I., Gorsich, D. & Lamb, D. (2011b). Reliability-based design optimization with confidence level for non-Gaussian distributions using bootstrap method. *Journal of Mechanical Design, 133*(9), 091001.

Oberkampf, W. L. & Barone, M. F. (2006). Measures of agreement between computation and experiment: validation metrics. *Journal of Computational Physics, 217*(1), 5-36.

Oberkampf, W. L., Helton, J. C. & Sentz, K. (2001). *Mathematical representation of uncertainty*. Paper presented at the AIAA Non-Deterministic Approaches Forum.

Oberkampf, W. L. & Roy, C. J. (2010). *Verification and validation in scientific computing*: Cambridge University Press.

Pan, H., Xi, Z. & Yang, R.-J. (2016). Model uncertainty approximation using a copula-based approach for reliability based design optimization. *Structural and Multidisciplinary Optimization*, 1-14.

Pearson, K. (1916). Mathematical contributions to the theory of evolution. XIX. Second supplement to a memoir on skew variation. *Philosophical Transactions of the Royal Society of London. Series A, Containing Papers of a Mathematical or Physical Character, 216*, 429-457.

Picheny, V., Kim, N. H. & Haftka, R. T. (2010). Application of bootstrap method in conservative estimation of reliability with limited samples. *Structural and Multidisciplinary Optimization, 41*(2), 205-217.

Rahman, S. (2009). Stochastic sensitivity analysis by dimensional decomposition and score functions. *Probabilistic Engineering Mechanics, 24*(3), 278-287.

Rahman, S. & Wei, D. (2006). A univariate approximation at most probable point for higher-order reliability analysis. *International journal of solids and structures, 43*(9), 2820-2839.

Rahman, S. & Wei, D. (2008). Design sensitivity and reliability-based structural optimization by univariate decomposition. *Structural and Multidisciplinary Optimization, 35*(3), 245-261.

Rubinstein, R. Y. & Kroese, D. (1981). Simulation and the Monte Carlo Method. John Wiley&Sons. *Inc. Publication*.

Rubinstein, R. Y. & Shapiro, A. (1993). *Discrete event systems: Sensitivity analysis and stochastic optimization by the score function method*: John Wiley & Sons Inc.

Sen, O., Davis, S., Jacobs, G. & Udaykumar, H. (2015). Evaluation of convergence behavior of metamodeling techniques for bridging scales in multi-scale multimaterial simulation. *Journal of Computational Physics, 294*, 585-604.

Shi, L., Yang, R. & Zhu, P. (2012). A method for selecting surrogate models in crashworthiness optimization. *Structural and Multidisciplinary Optimization, 46*(2), 159-170.

Silverman, B. W. (1986). *Density estimation for statistics and data analysis* (Vol. 26): CRC press.

Song, H., Choi, K. & Lamb, D. (2013a). *A study on improving the accuracy of kriging models by using correlation model/mean structure selection and penalized log-likelihood function.* Paper presented at the 10th World Congress on Structural and Multidisciplinary Optimization. Florida, Orlando.

Song, H., Choi, K. K., Lee, I., Zhao, L. & Lamb, D. (2013b). Adaptive virtual support vector machine for reliability analysis of high-dimensional problems. *Structural and Multidisciplinary Optimization, 47*(4), 479-491.

Tu, J., Choi, K. K. & Park, Y. H. (1999). A new study on reliability-based design optimization. *Journal of Mechanical Design, 121*(4), 557-564.

Tu, J., Choi, K. K. & Park, Y. H. (2001). Design potential method for robust system parameter design. *AIAA journal, 39*(4), 667-677.

Volpi, S., Diez, M., Gaul, N. J., Song, H., Iemma, U., Choi, K., Campana, E.F. & Stern, F. (2015). Development and validation of a dynamic metamodel based on stochastic radial basis functions and uncertainty quantification. *Structural and Multidisciplinary Optimization, 51*(2), 347-368.

Xi, Z., Fu, Y. & Yang, R. (2013). Model bias characterization in the design space under uncertainty. *International Journal of Performability Engineering, 9*(4), 433-444.

Xiong, Y., Chen, W., Tsui, K.-L. & Apley, D. W. (2009). A better understanding of model updating strategies in validating engineering models. *Computer Methods in Applied Mechanics and Engineering, 198*(15), 1327-1337.

Youn, B. D., Choi, K., Yang, R.-J. & Gu, L. (2004). Reliability-based design optimization for crashworthiness of vehicle side impact. *Structural and Multidisciplinary Optimization, 26*(3), 272-283.

Youn, B. D., Jung, B. C., Xi, Z., Kim, S. B. & Lee, W. (2011). A hierarchical framework for statistical model calibration in engineering product development. *Computer Methods in Applied Mechanics and Engineering*, *200*(13), 1421-1431.

Youn, B. D. & Wang, P. (2008). Bayesian reliability-based design optimization using eigenvector dimension reduction (EDR) method. *Structural and Multidisciplinary Optimization*, *36*(2), 107-123.

Zhao, L. (2011). *Reliability-based design optimization using surrogate model with assessment of confidence level.* The University of Iowa.

Zhao, L., Choi, K. & Lee, I. (2011). Metamodeling method using dynamic kriging for design optimization. *AIAA journal*, *49*(9), 2034-2046.